

# *Reverberation Chambers: Overview and Applications*

*Christopher L. Holloway*

*John Ladbury, Galen Koepke, Dave Hill, Kate Remley, William Young*

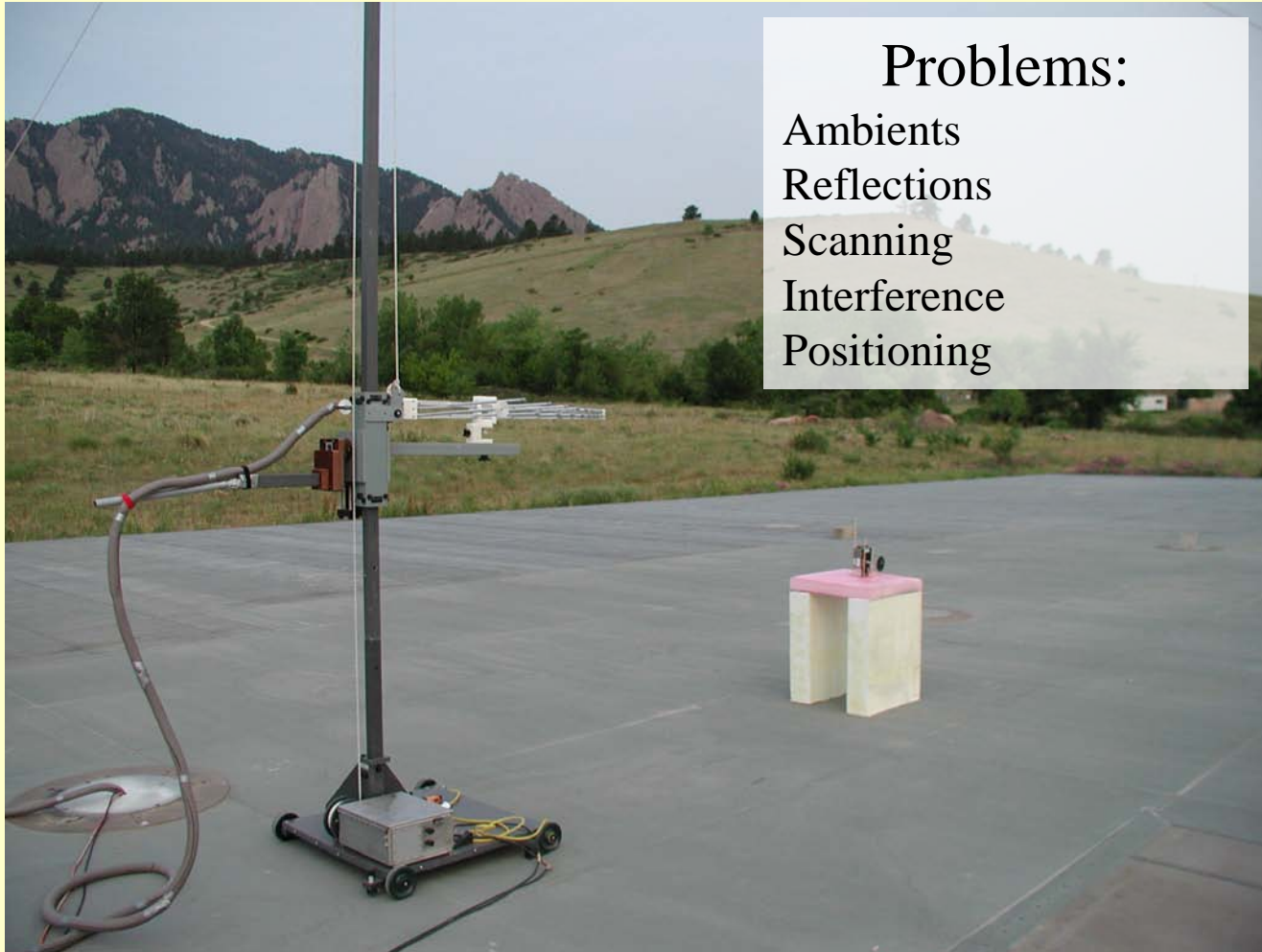
*National Institute of Standards and Technology*

*Electromagnetics Division*

*Boulder, Colorado*

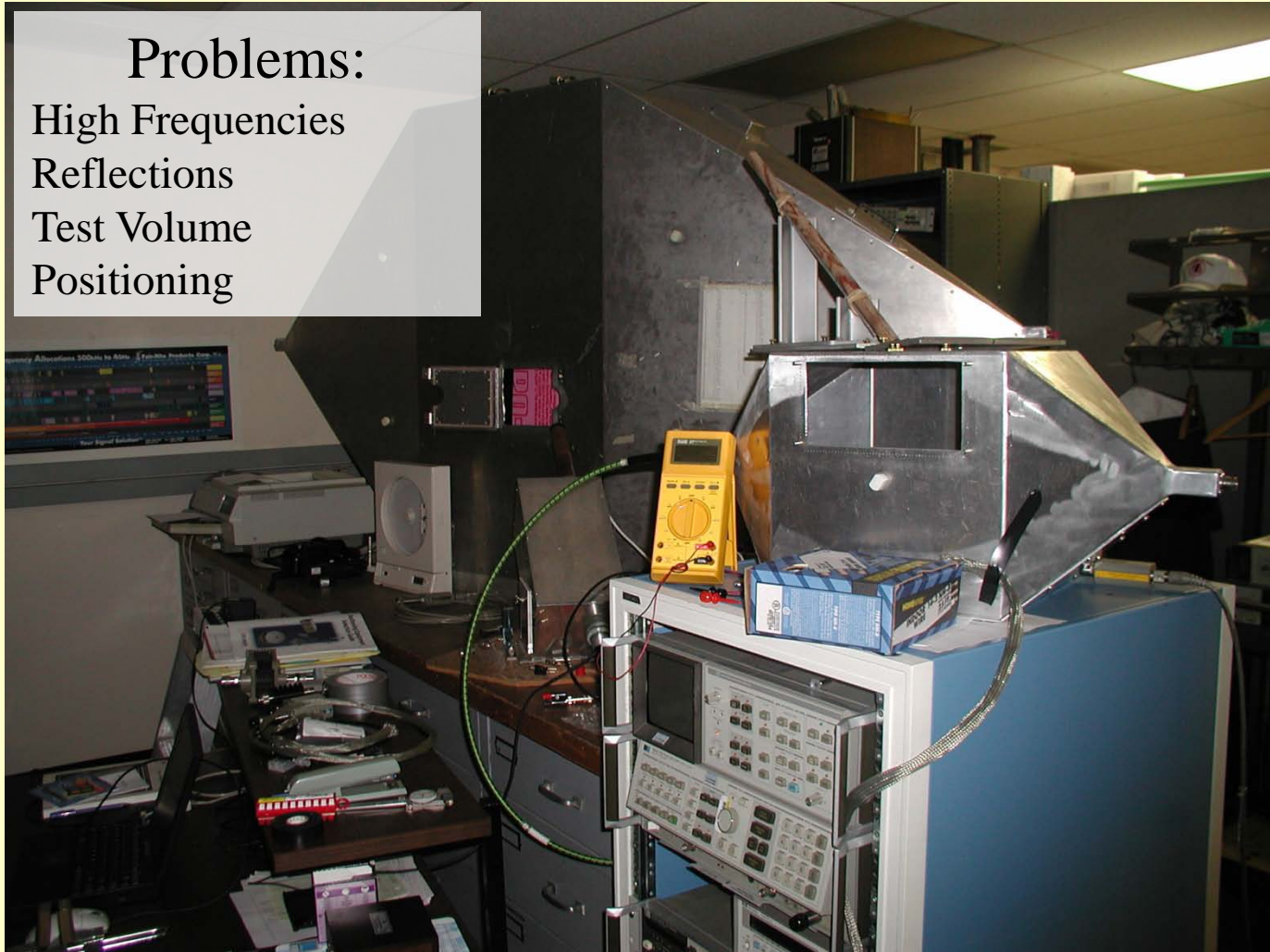
*303-497-6184, email: [holloway@boulder.nist.gov](mailto:holloway@boulder.nist.gov)*

# OPEN AREA TEST SITES (OATS)



# TEM

Problems:  
High Frequencies  
Reflections  
Test Volume  
Positioning





# GTEM



Problems:  
Test Volume  
Uniformity Along Cell  
Positioning

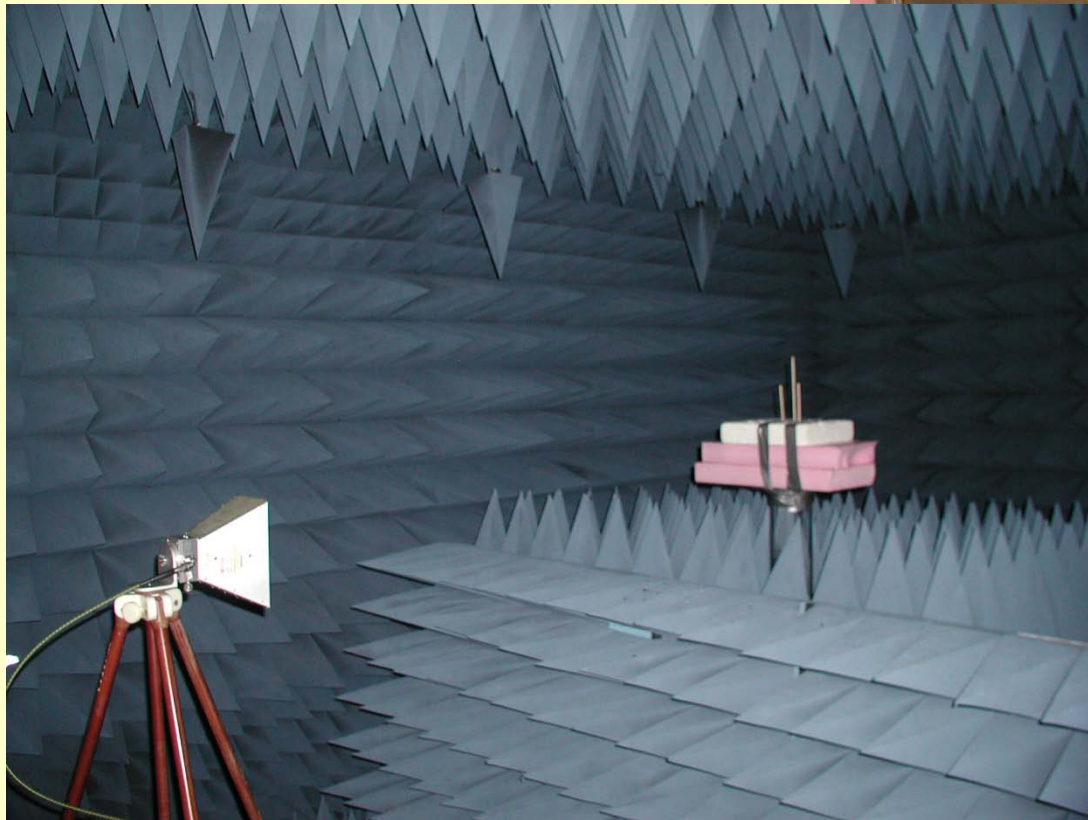
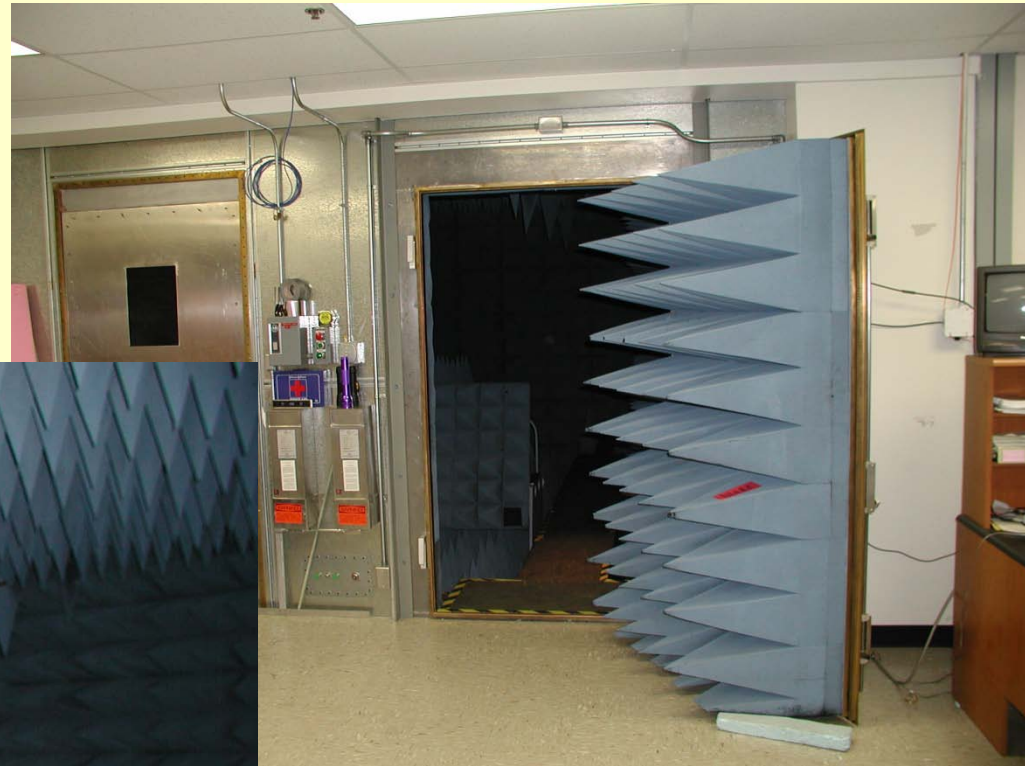




# ANECHOIC CHAMBER

## Problems:

Low Frequencies  
Reflections  
Positioning



# REVERBERATION CHAMBER

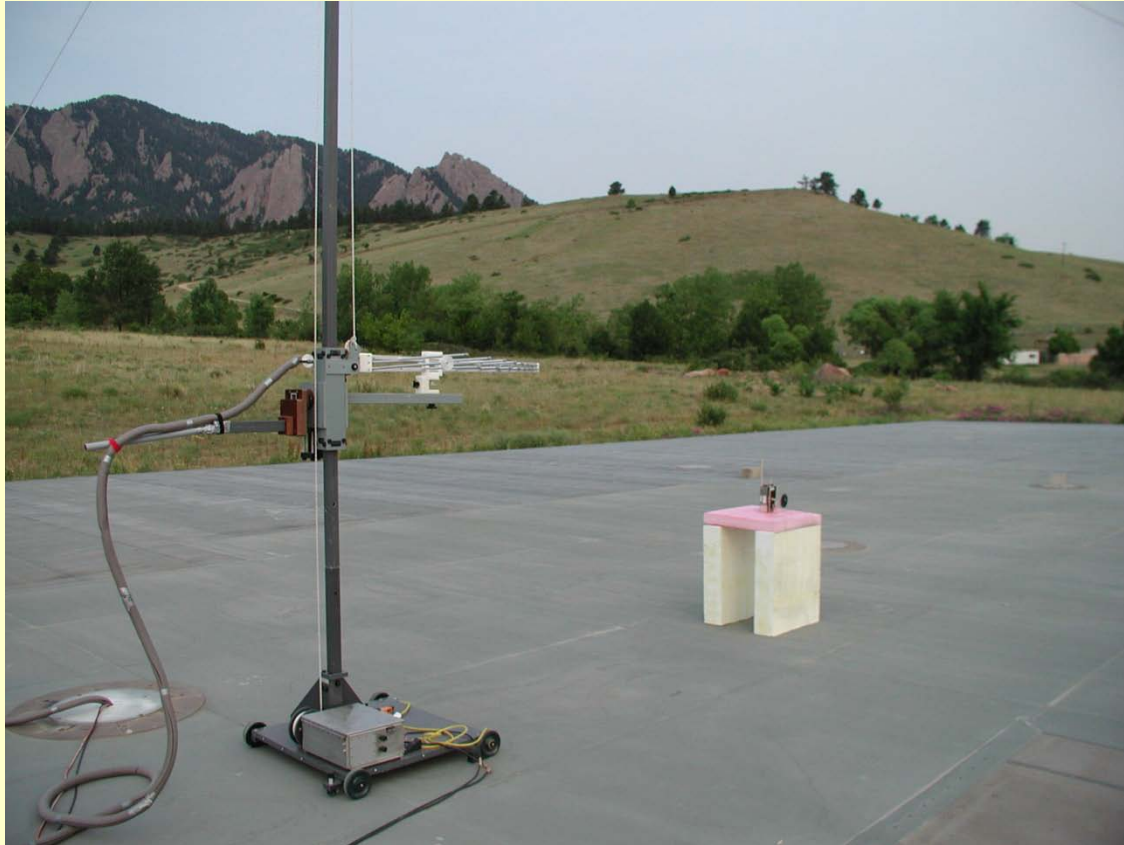


**Why use reverberation chambers?**

**1) Relatively inexpensive**

**2) Relatively fast**

# The Classical OATS Measurements



**The classic emissions test and standard limits (i.e, testing a product above a ground plane at a specified antenna separation and height) have their origins in interference problems with TV reception.**



# Emissions Test Standard Problem

One problem with the emissions test standard is that it is based on an interference paradigm (interference to terrestrial broadcast TV) that is, in general, no longer valid nor realistic today. *In a recent report, the FCC indicated that 85 % of US households receive their TV service from either cable, direct broadcast satellite (DBS), or other multichannel video programming distribution service, and that only a small fraction of US households receive their TV via direct terrestrial broadcast.*

**Coupling to TV antennas designed to receive terrestrial broadcast may no longer be an issue.**

# EM/EMC Environment Today

- In recent years, a proliferation of communication devices that are subject to interference have been introduced into the marketplace.
- Today, cell phones and pagers are used in confined offices containing personal computers (PCs). Many different products containing microprocessors (e.g., TVs, VCRs, PCs, microwave ovens, cell phones, etc.) may be operating in the same room.
- Different electronic products may also be operating within metallic enclosures (e.g., cars and airplanes). The walls, ceiling, and floor of an office, a room, a car, or an airplane may or may not be highly conducting.
- Hence, emissions from electric devices in these types of enclosures will likely be quite different from emissions at an OATS. In fact, the environment may more likely behave as either a reverberation chamber or a free space environment.

# Where Should We Test?

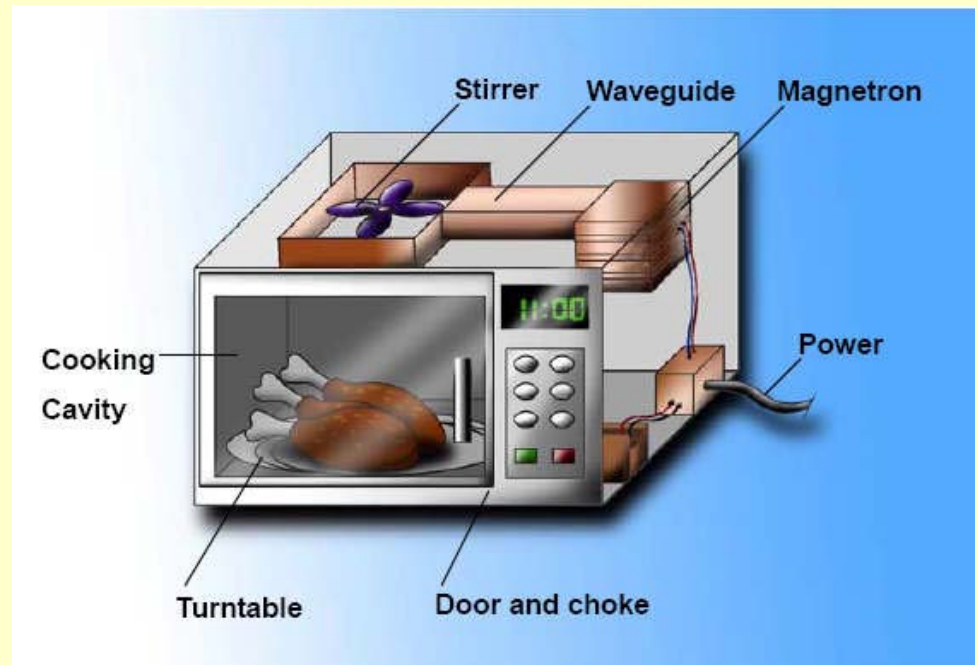
- Thus, would it not be better to perform tests more appropriate to today's electromagnetic environment?
- Tests should be Shielded, Repeatable, Simple, Inexpensive, Fast, Thorough, ...



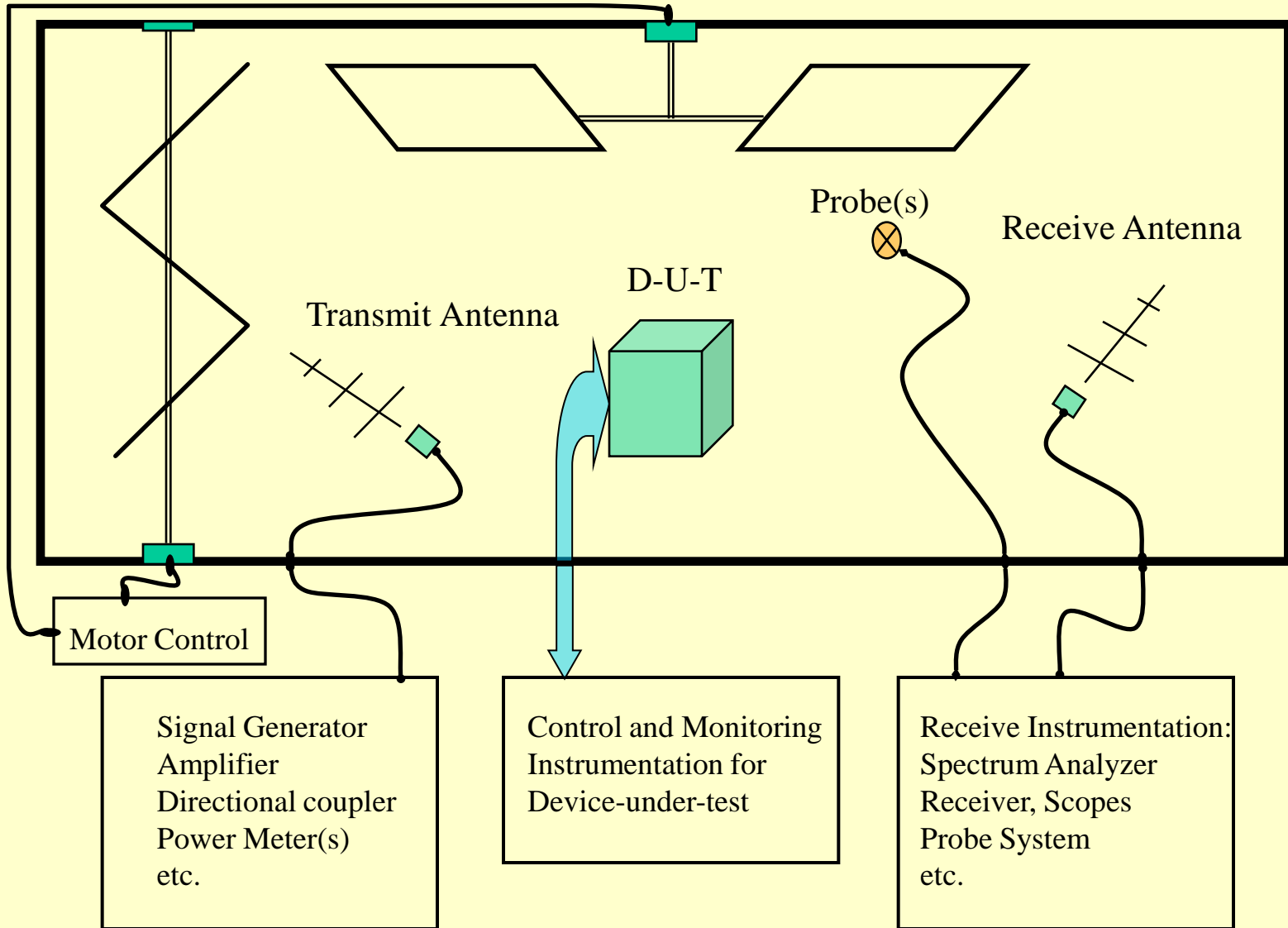


# Commercial Solutions...

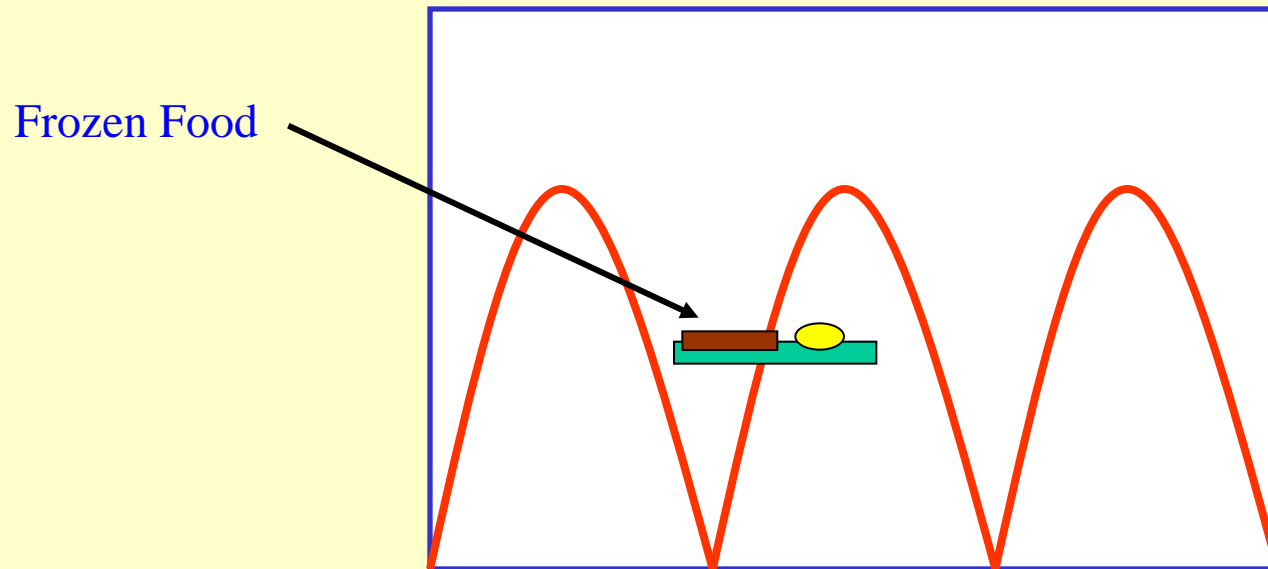
- Stirrer
- Turntable



# *Reverberation Chamber*



# Fields in a Metal Box (A Shielded Room)



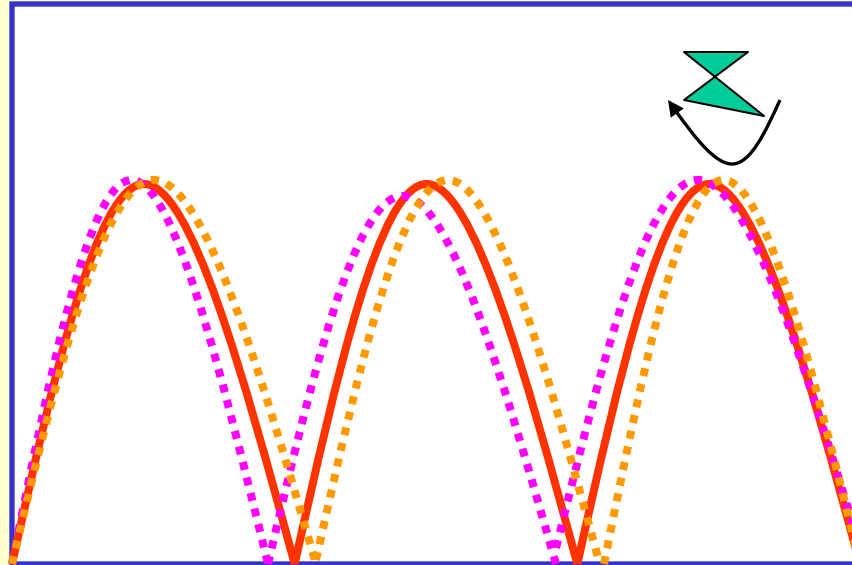
- In a metal box, the fields have well defined modal field distributions.

Locations in the chamber with very high field values

Locations in the chamber with very low field values



# Fields in a Metal Box with Small Scatterer

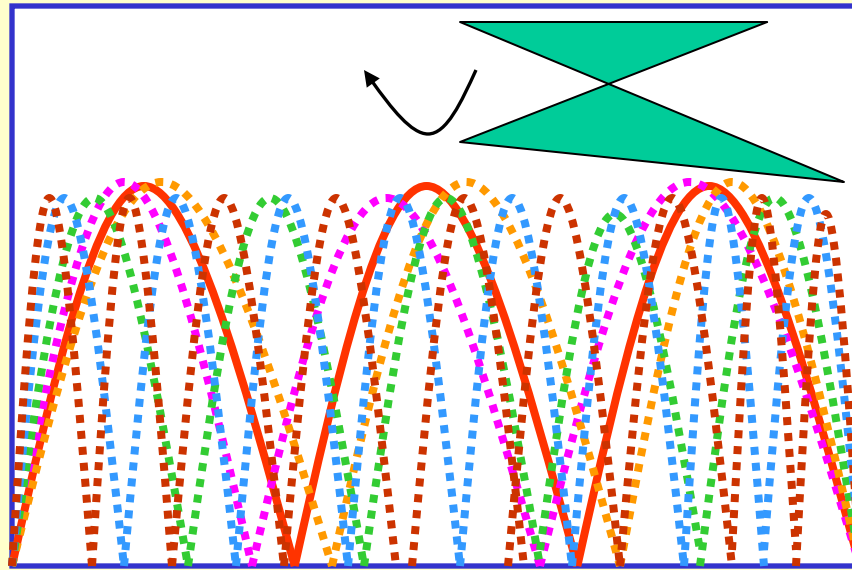


In a metal box, the fields have well defined modal field distributions.

Small changes in locations where very high field values occur

Small changes in locations where very low field values occur

# Fields in a Metal Box with Large Scatterer (Paddle)



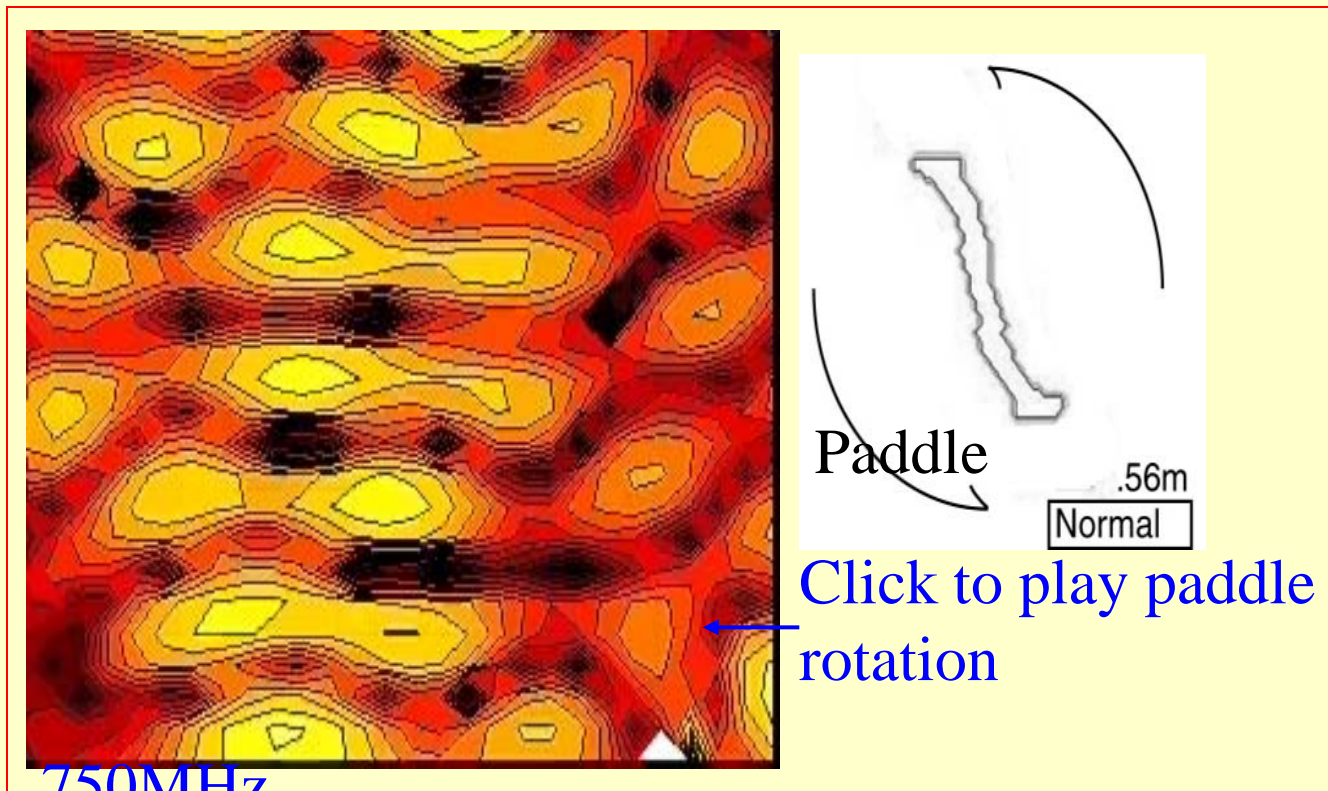
Large changes in locations where very high field values occur

Large changes in locations where very low field values occur

In fact, after one fan rotation, all locations in the chamber will have the same maxima and minima fields.

# Stirring Method

TIME DOMAIN



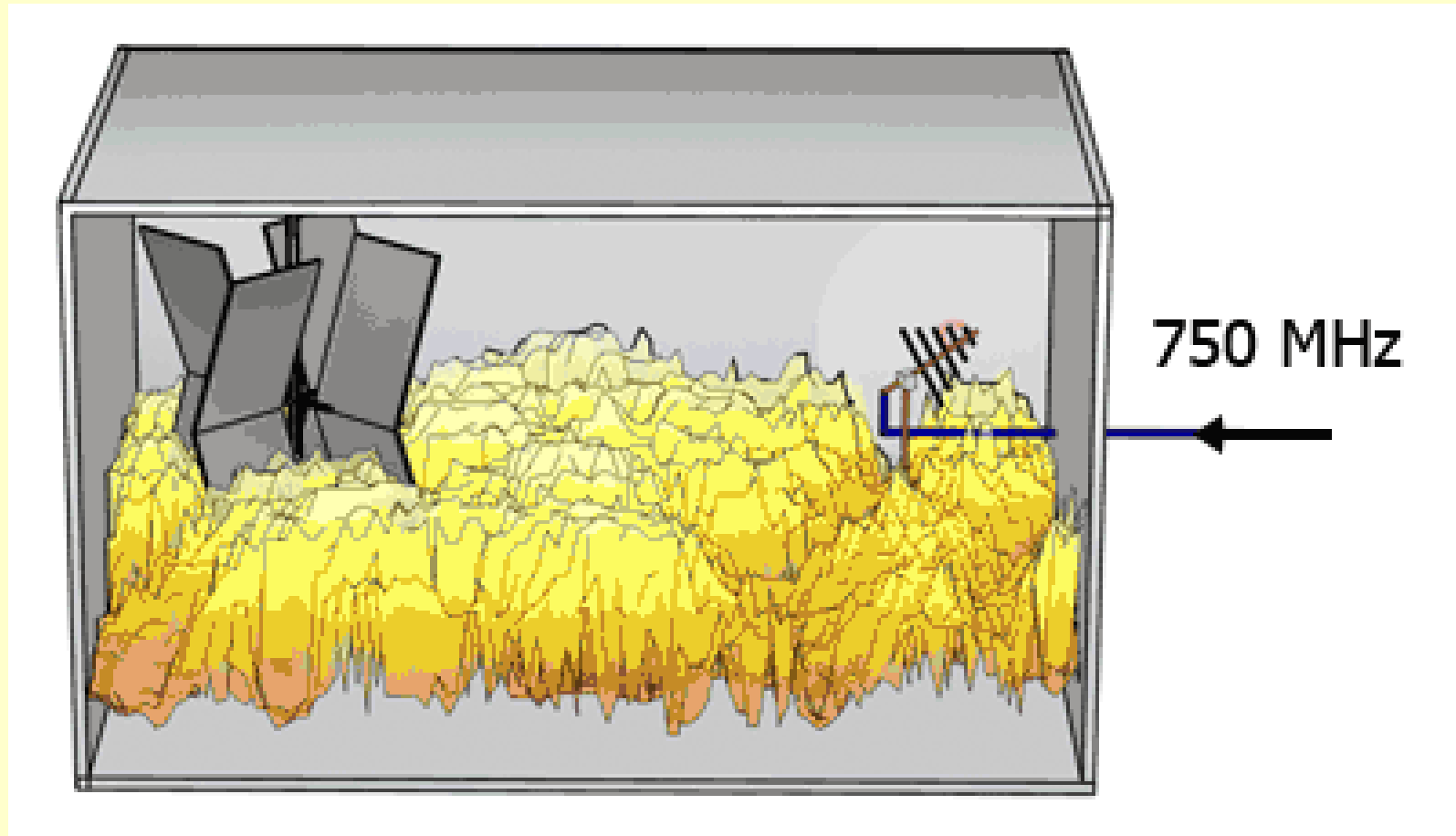
The complex block contains two main visual elements. On the left is a large, detailed NMR spectrum with a color scale from red to yellow, showing complex, irregular patterns. On the right is a schematic diagram of a paddle stirrer. The paddle is a vertical, slightly curved shape with a serrated edge. A curved arrow indicates its rotation. A scale bar below the paddle is labeled ".56m" and "Normal". A blue arrow points from the text "Click to play paddle rotation" to the paddle schematic. A large black arrow points from the right side of the red-bordered box towards the right edge of the slide.

750MHz

Click to play paddle rotation



# Field Variations with Rotating Stirrer



# *Reverberation Chamber: All Shape and Sizes*



Small Chamber



Large Chamber



Moving walls

# NASA: Glenn Research Center (Sandusky, OH)



# *Reverberation Chamber with Moving Wall*



# *Original Applications*

- *Radiated Immunity*
  - components
  - large systems
- *Radiated Emissions*
- *Shielding*
  - cables
  - connectors
  - materials
- *Antenna efficiency*
- *Calibrate rf probes*
- *RF/MW Spectrograph*
  - absorption properties
- *Material heating*
- *Biological effects*
- *Conductivity and material properties*

# *Wireless Applications*

- **Radiated power of mobile phones**
- **Gain obtained by using diversity antennas in fading environments**
- **Antenna efficiency measurements**
- **Measurements on multiple-input multiple-output (MIMO) systems**
- **Emulated channel testing in Rayleigh multipath environments**
- **Emulated channel testing in Rician multipath environments**
- **Measurements of receiver sensitivity of mobile terminals**
- **Investigating biological effects of cell-phone base-station RF exposure**



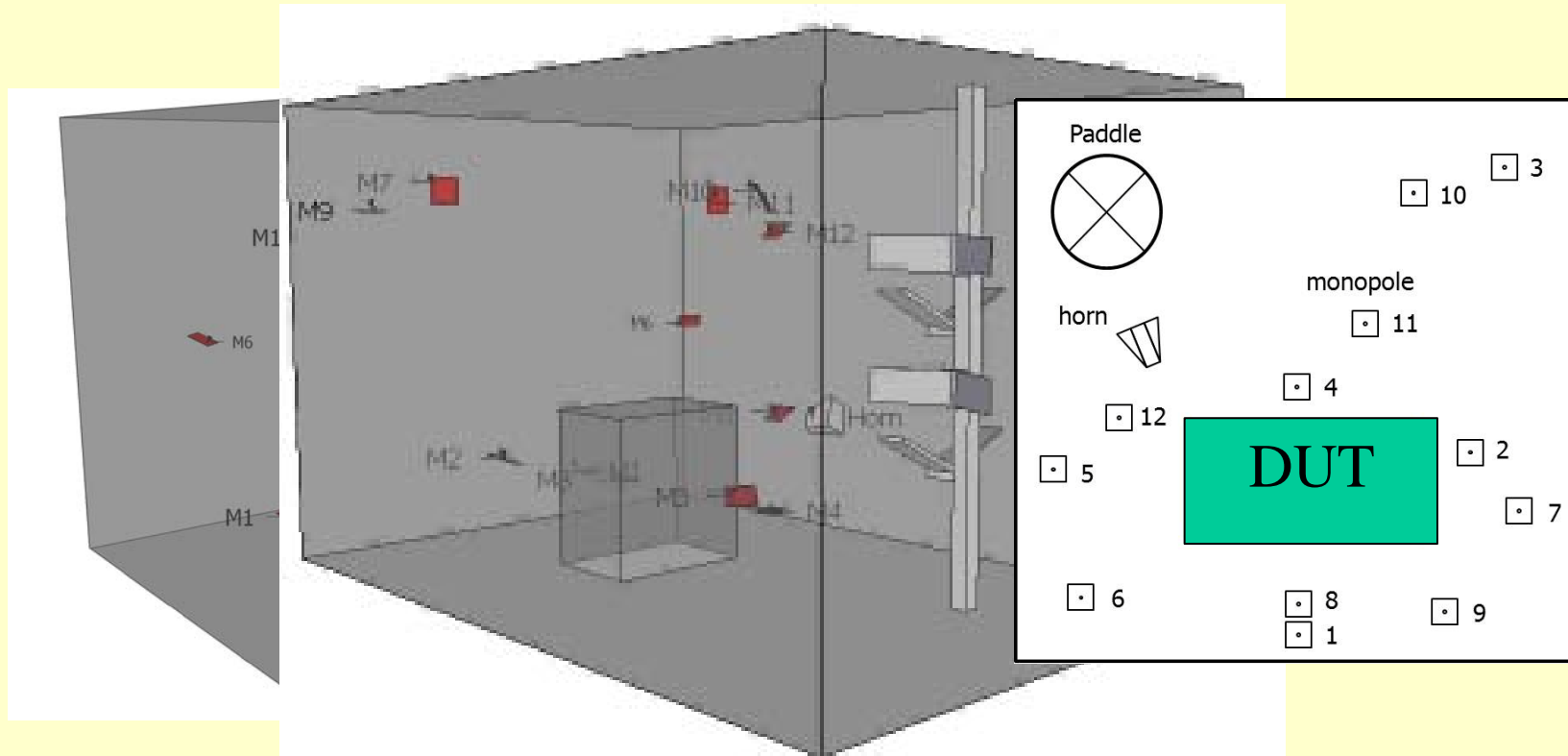
# *Sampling Considerations*

## *Techniques to Generate Samples*

- ***Mechanical techniques***
  - Paddle(s) or Tuner(s)
    - stepped (tuned)
    - continuous (stirred)
  - Device-under-test and antenna position
  - Moving walls (conductive fabric, etc.)
- ***Electrical techniques*** (*immunity tests*)
  - Frequency stirring
    - stepped or swept
    - random (noise modulation)
- ***Hybrid techniques***

# Metric for a “Well” Performing Chamber

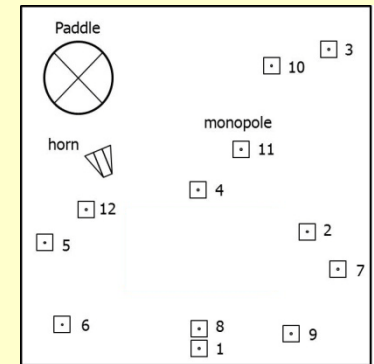
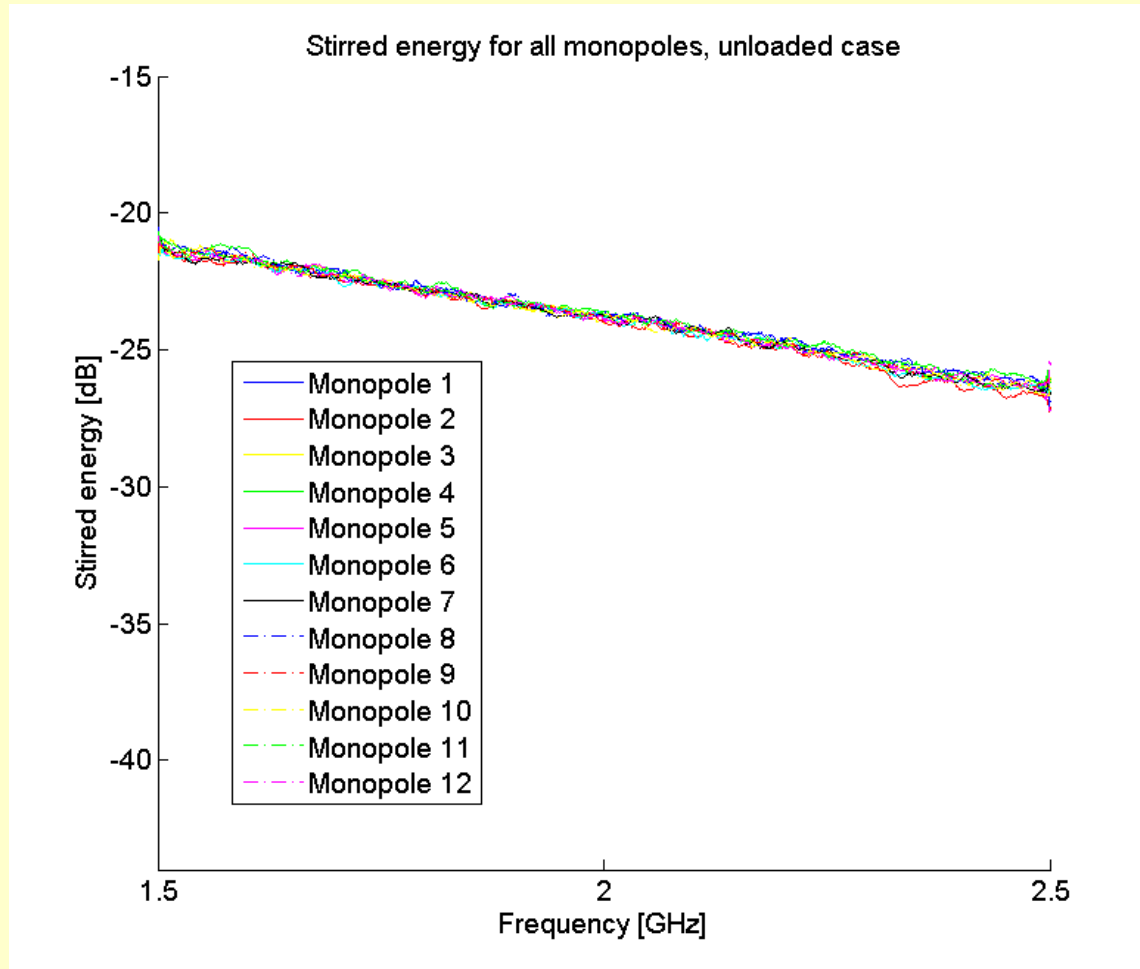
Standard bodies (e.g., IEC and CTIA) have various means of determining when a chamber meets a performance metric. Typically we would like the chamber to be “*statistically uniform*”.



**Metric:** The variance (or standard deviation) of the mean “stirred” power (averaged over all paddle positions) for the twelve test points are within some given value.

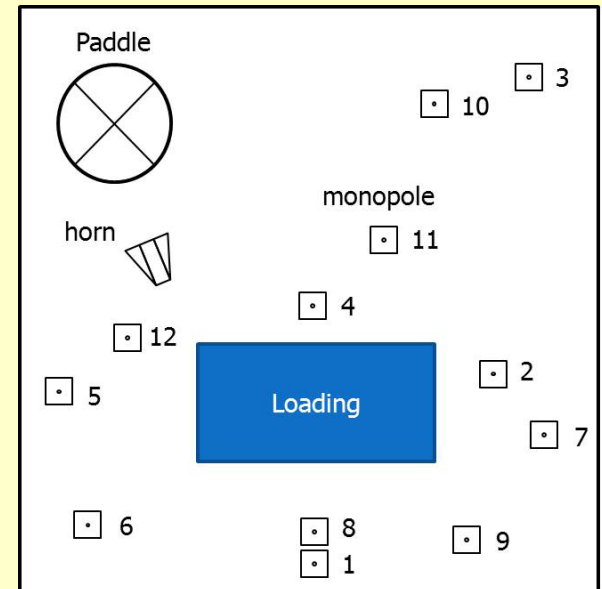
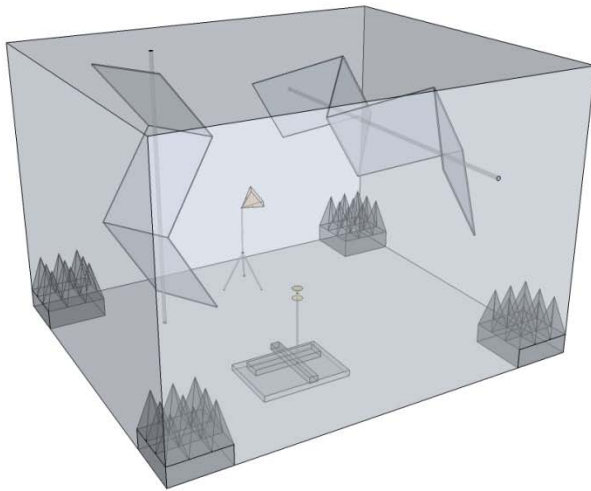
# Metric for a “Well” Performing Chamber

NIST Chamber: 2.9 M by 4.2 m by 3.6 m



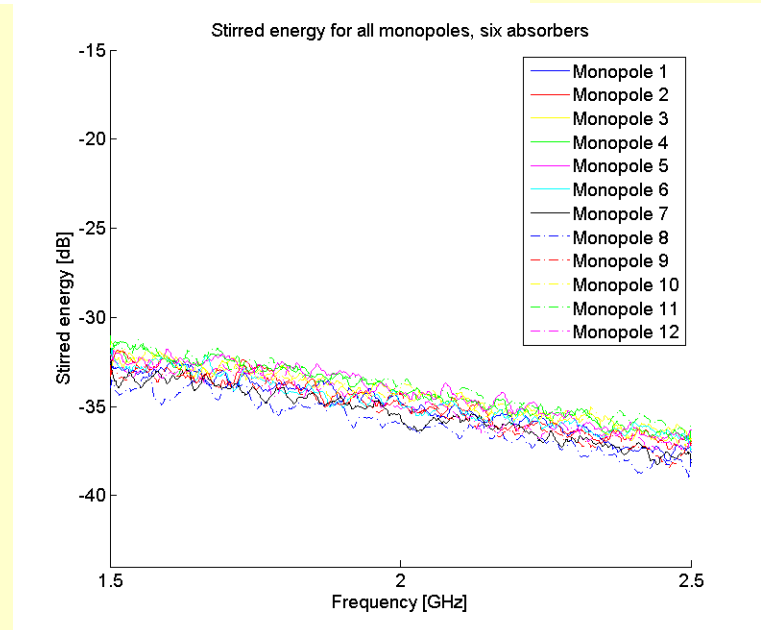
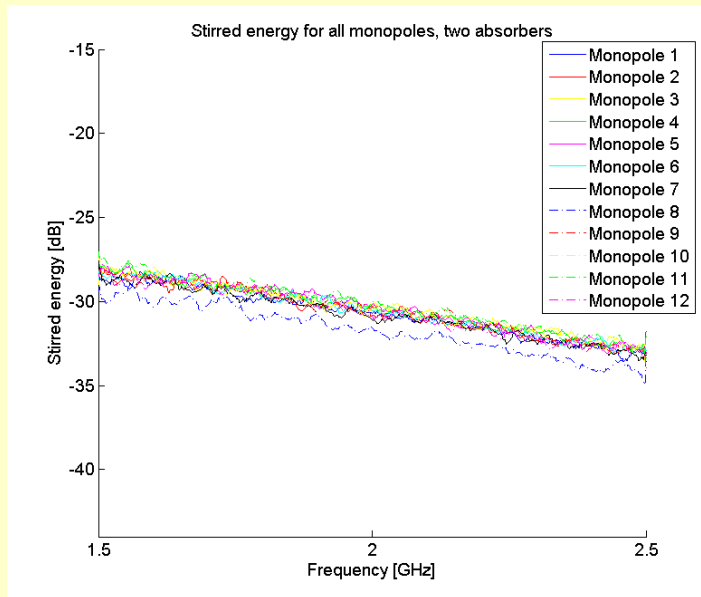
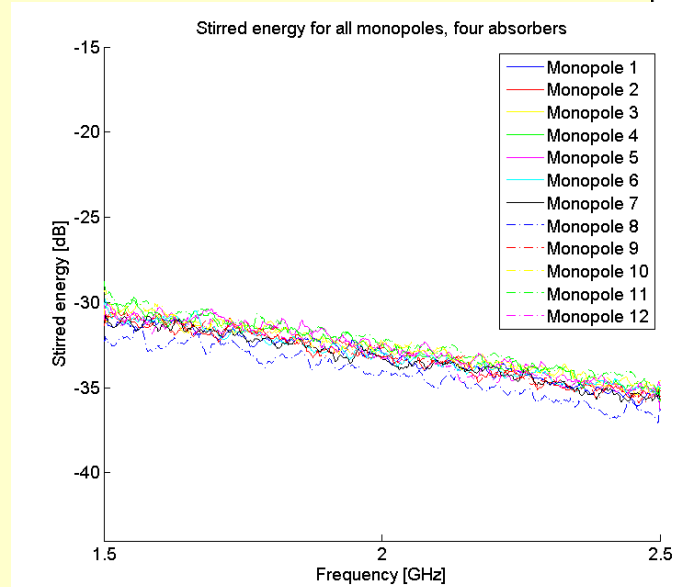
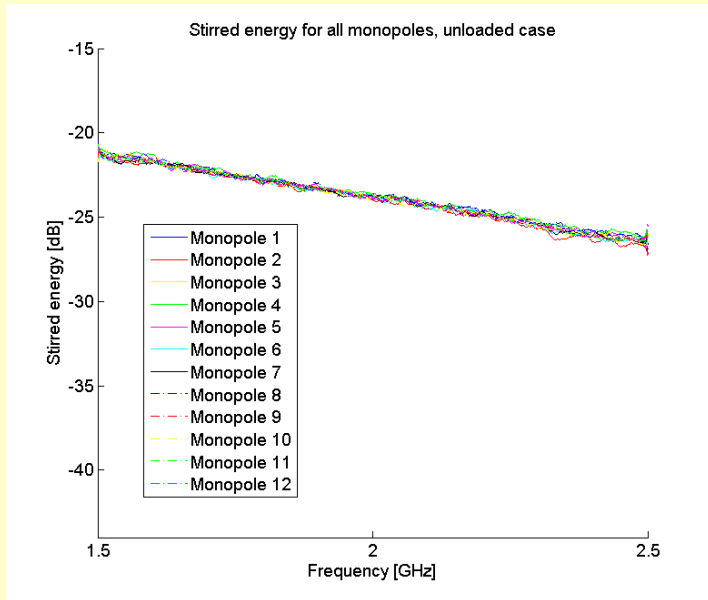
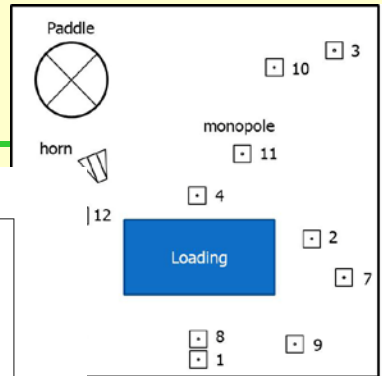
# Metric for a Loaded Chamber

Using reverberation chambers for testing wireless devices is getting a lot of attention in recent years. For the application, some type of rf absorber is used in the chamber in order to control the delay time in the chamber.



Loading a chamber has an adverse effect on its “*statistical uniformity*”.

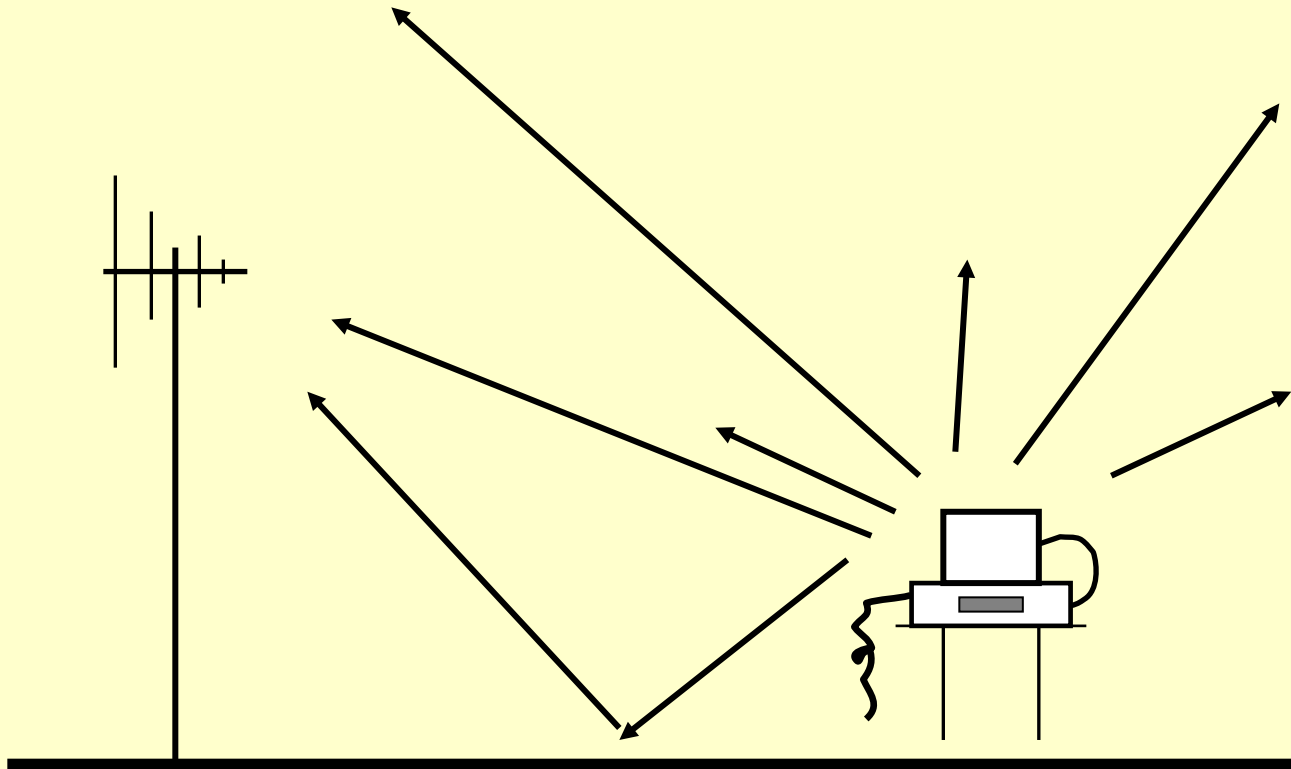
# Loaded Chamber



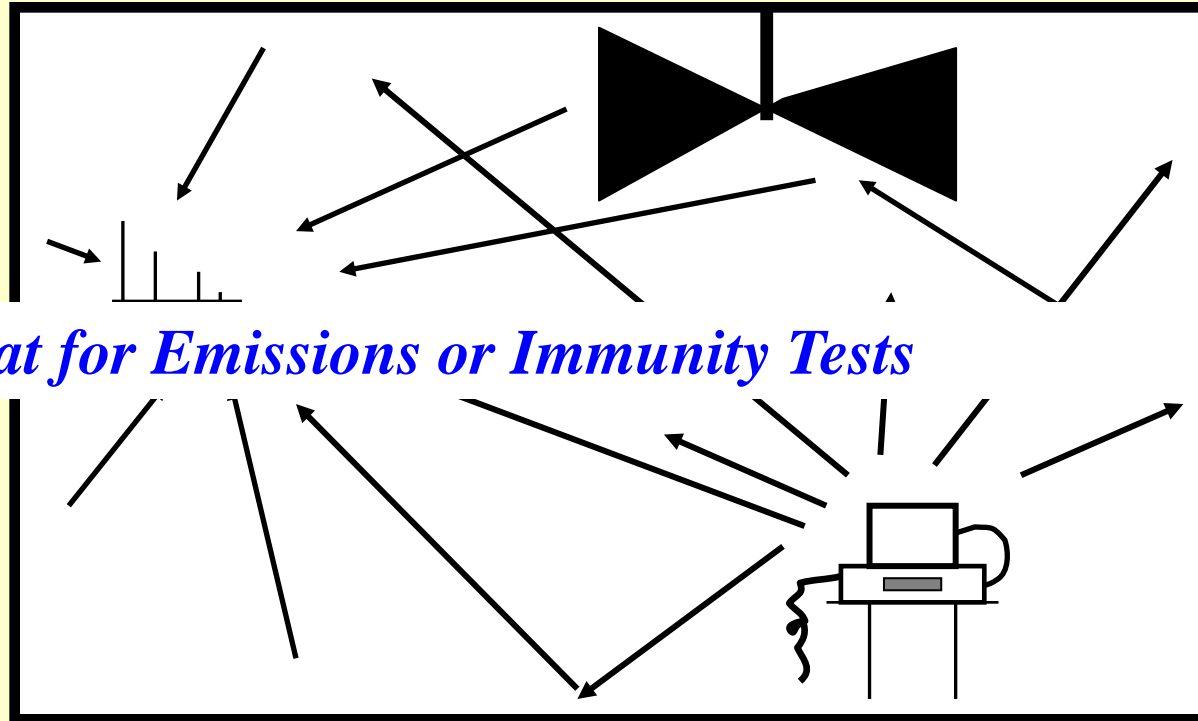
*EM / EMC / Wireless  
Applications*



# HIDING Emission Problems



# YOU CANNOT HIDE IN Reverberation Chamber

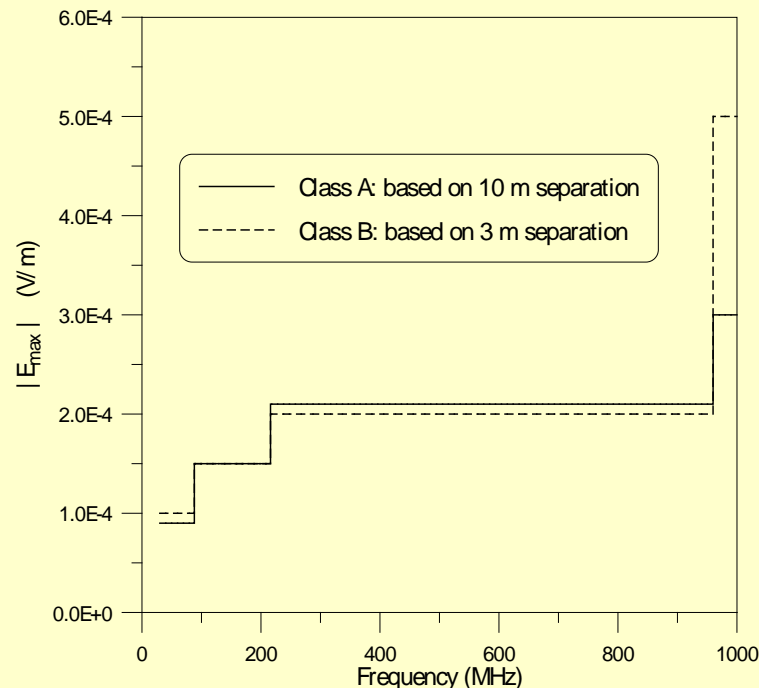


**In reverberation chambers you cannot hide emission problems.**

**Reverberation chambers will find problems.**

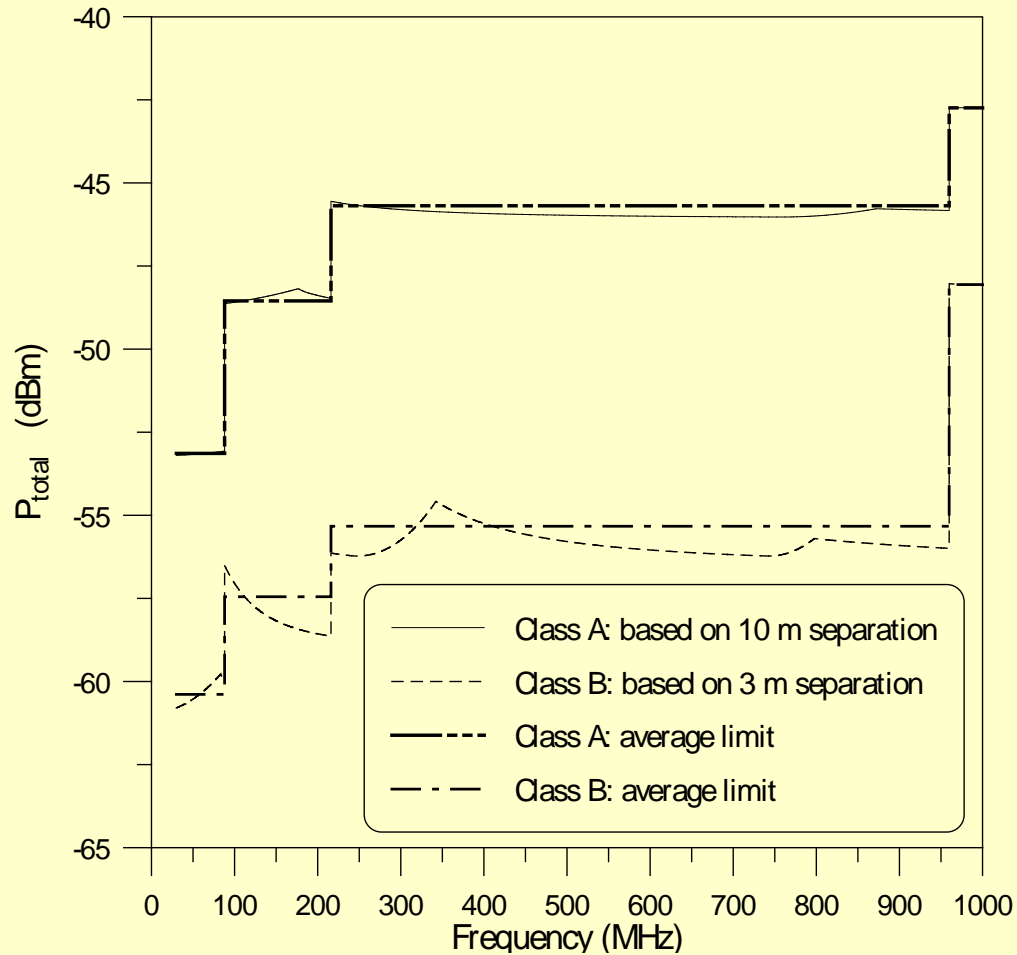
# EMISSION LIMITS

- Devices and/or products are tested for emissions to ensure that electromagnetic field strengths emitted by the device and/or product are below a maximum specified electric (E) field strength over the frequency range of 30 MHz to 1 GHz.
- These products are tested either on an open area test site (OATS) or in a semi-anechoic chamber.
- Products are tested for either Class A (commercial electronics) or Class B (consumer electronics) limits, Class A equipment have protection limits at 10 m, and Class B equipment have protection limits at 3 m.



# Total Radiated Power for Reverberation Chambers

Holloway et al., IEEE EMC Symposium

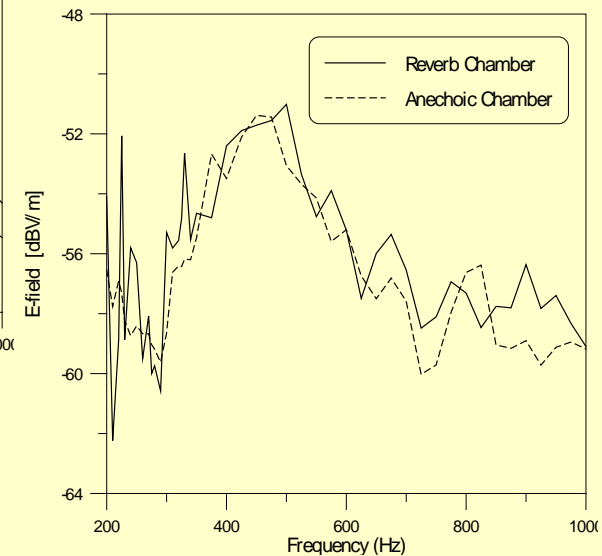
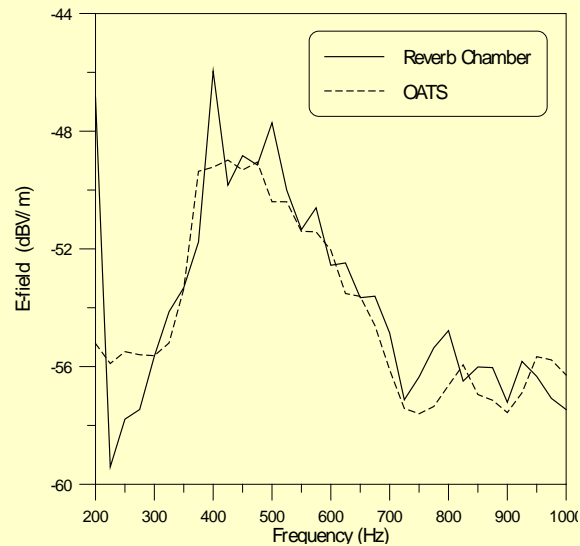


# Emission Measurements

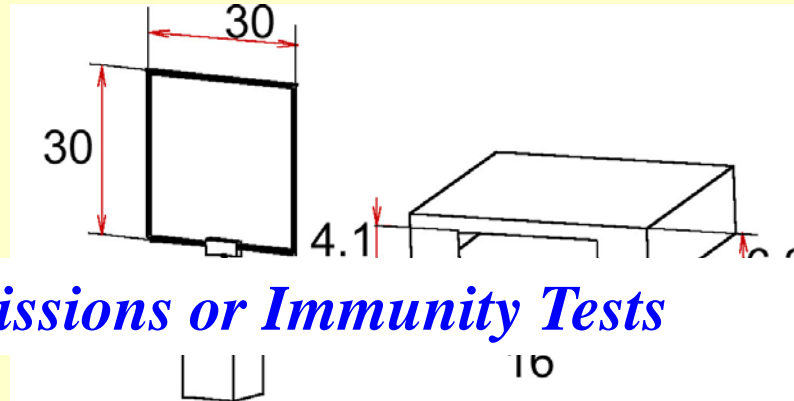


Relate total radiated power in reverberation chambers to measurements made on OATS with dipole correlation algorithms.

## Spherical Dipole

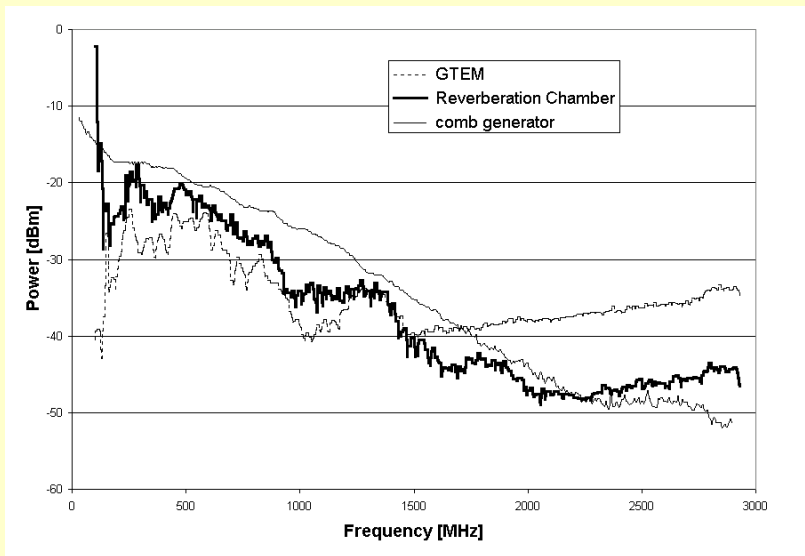


# Emissions Measurements of Devices

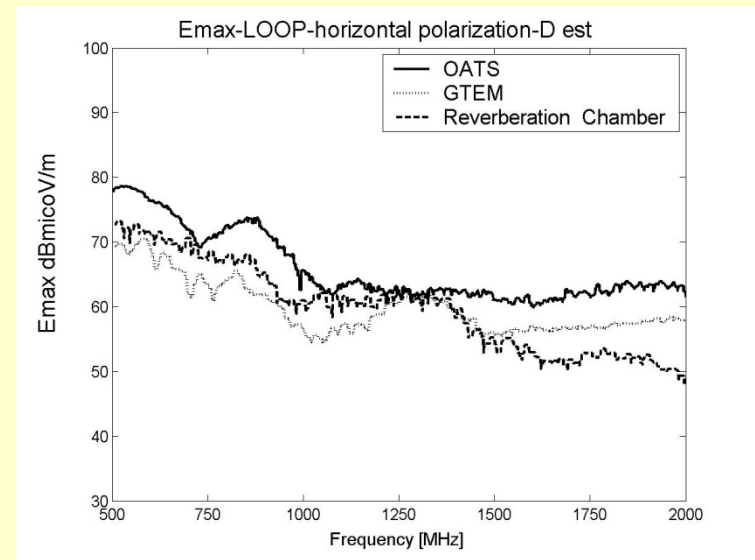


*Great for Emissions or Immunity Tests*

## Total Radiated Power Comparison



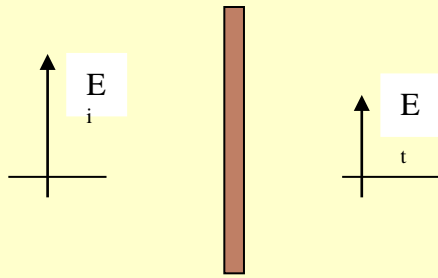
## Max Field Comparison





# Shielding Properties of Materials

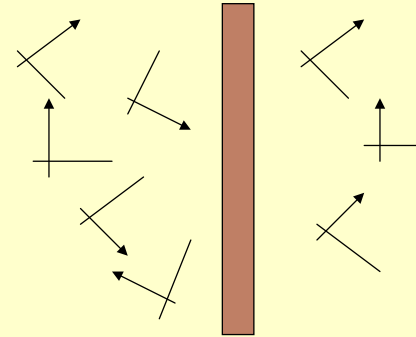
The conventional methods uses normal incident plane-waves, i.e., Coaxial TEM fixtures.



$$SE = -10 \text{Log}_{10} \left( \frac{P_t}{P_i} \right)$$

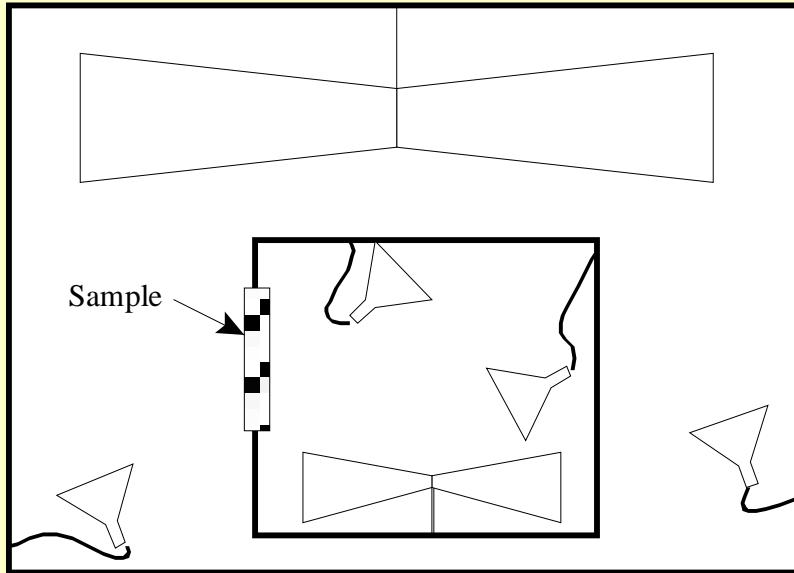
However, these approaches determine SE for only a very limited set of incident wave conditions.

In most applications, materials are exposed to complex EM environments where fields are incident on the material with various polarizations and angles of incidence.



Therefore, a test methodology that better represents this type of environment would be beneficial.

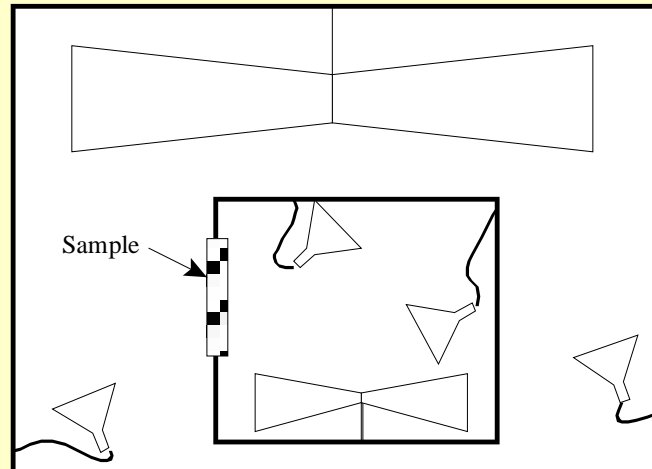
# *Nested Reverberation Chamber*



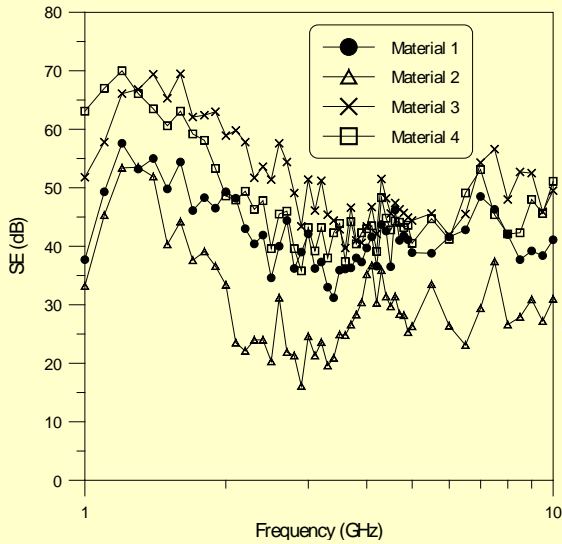
# *Nested Reverberation Chamber*

C.L. Holloway, D. Hill, J. Ladbury, G. Koepke, and R. Garzia, “Shielding effectiveness measurements of materials in nested reverberation chambers,” *IEEE Trans. on Electromagnetic Compatibility*, vol. 45, no. 2, pp. 350-356, May, 2003.

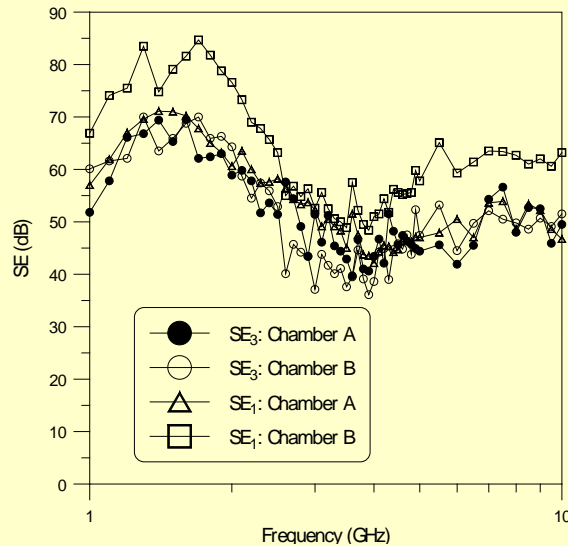
$$SE_3 = -10 \text{Log}_{10} \left( \frac{P_{r,in,s}}{P_{r,in,ns}} \frac{P_{r,o,ns}}{P_{r,o,s}} \frac{P_{rQ,in,ns}}{P_{rQ,in,s}} \frac{P_{tx,in,s}}{P_{tx,in,ns}} \right)$$



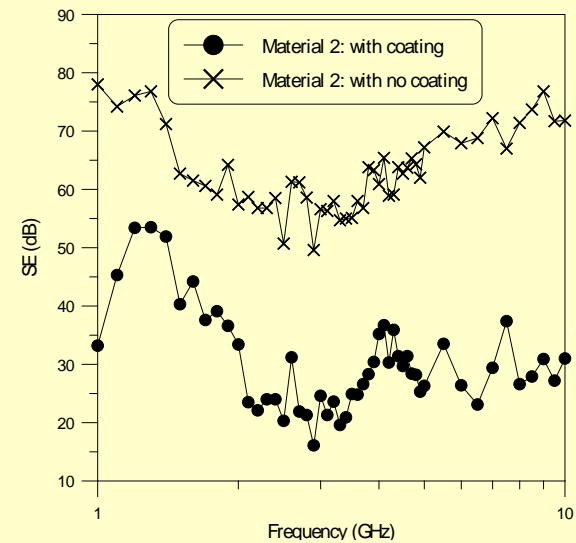
# Nested Reverberation Chamber



Different Materials



Different Chamber Sizes



Edge Effects

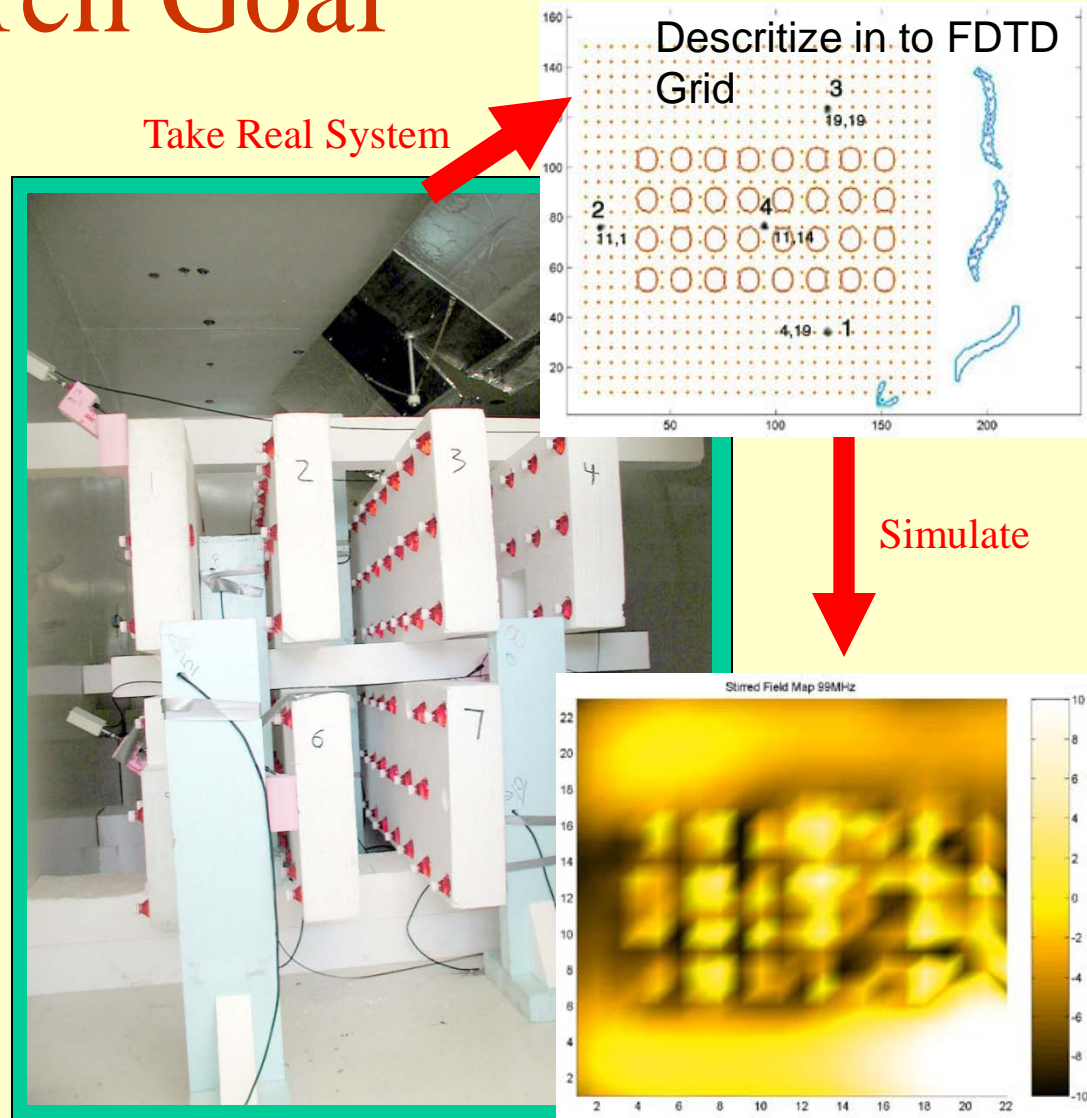
# *Loading Effects: Rat in a Cage*





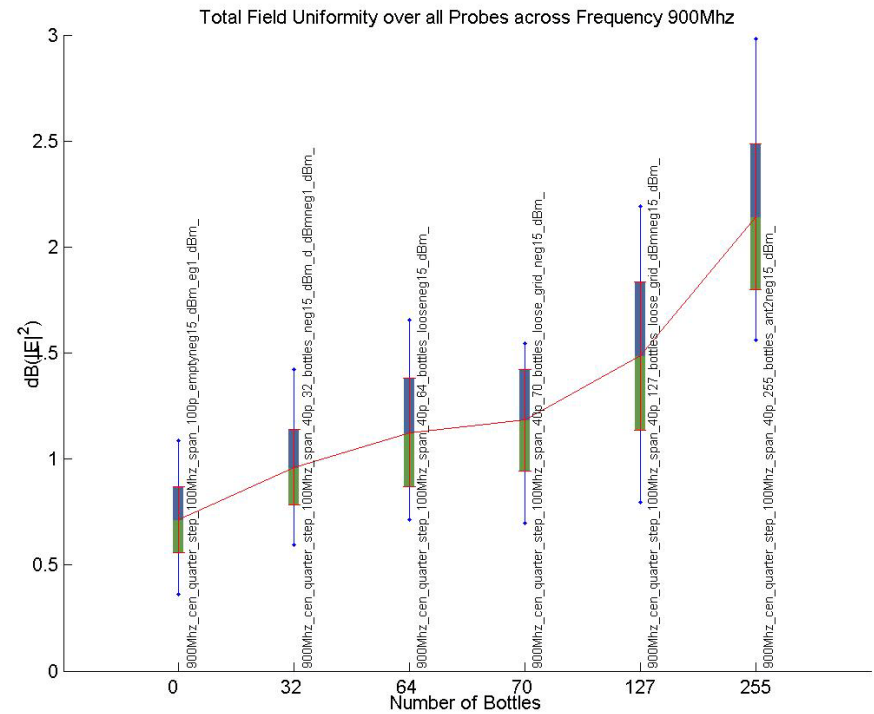
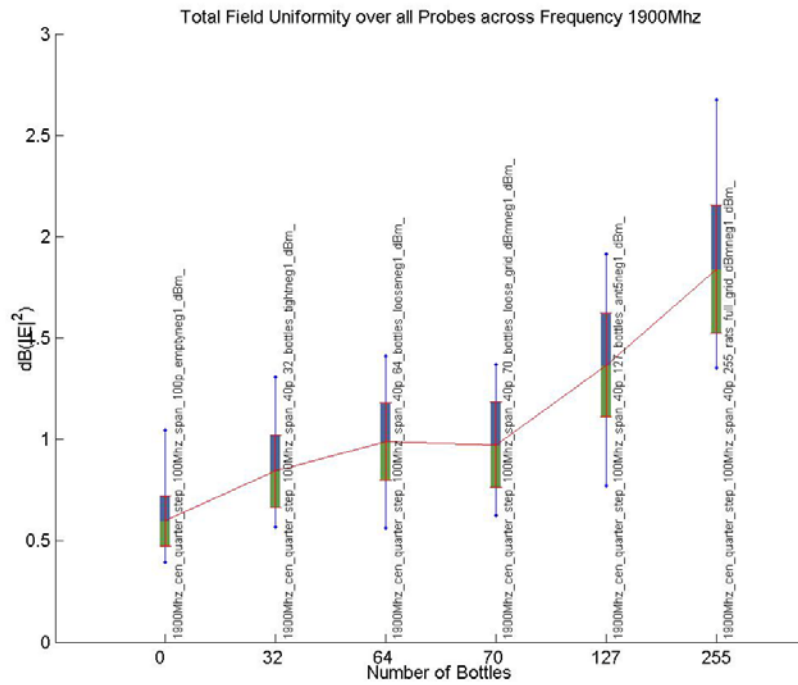
# Research Goal

- To provide a way to gain intuition into loaded chamber responses to better help measurements
- Ultimately correlate measured and modeled data, and use models to predict what we cant measure.
- Develop a fast and efficient numerical code to explore multiple chamber topologies. (FDTD)

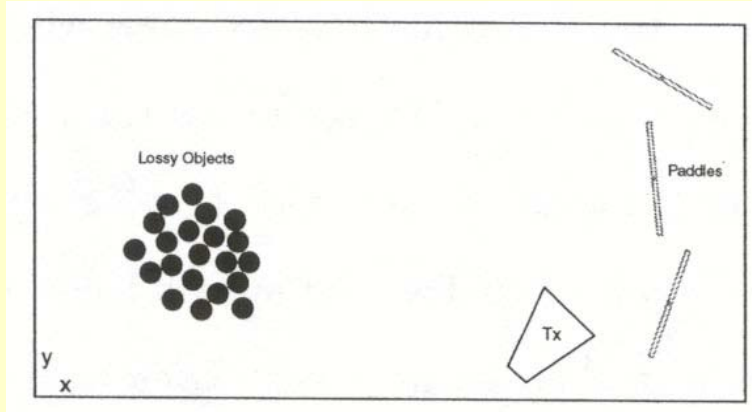


Predict Stirred Fields Computationally to give us **insight into chamber measurements** in a loaded environment

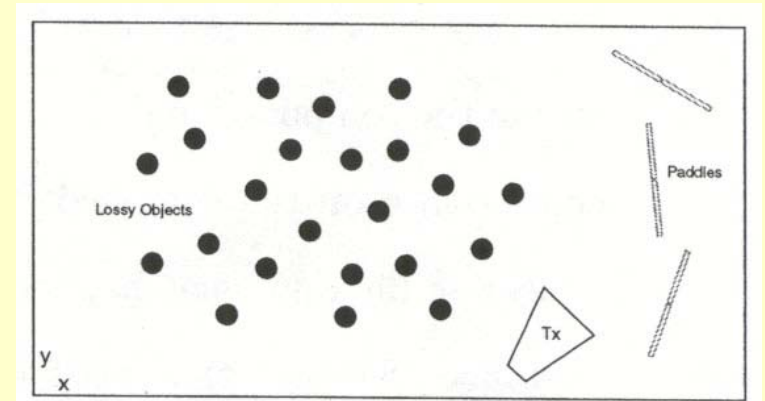
# Measurements of Fake Rats



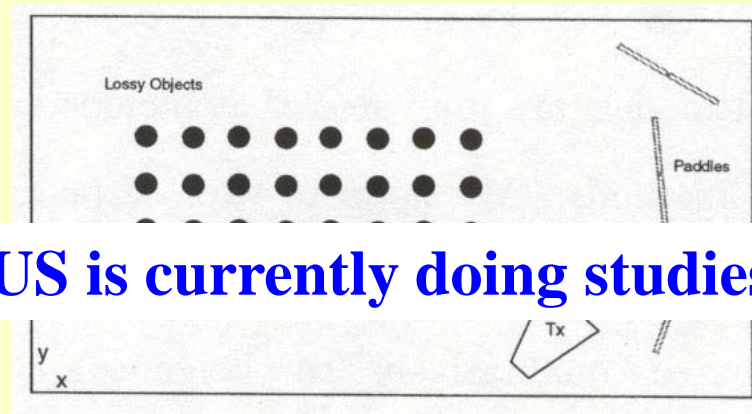
# Lossy Body Configuration



*Large Lossy Body*



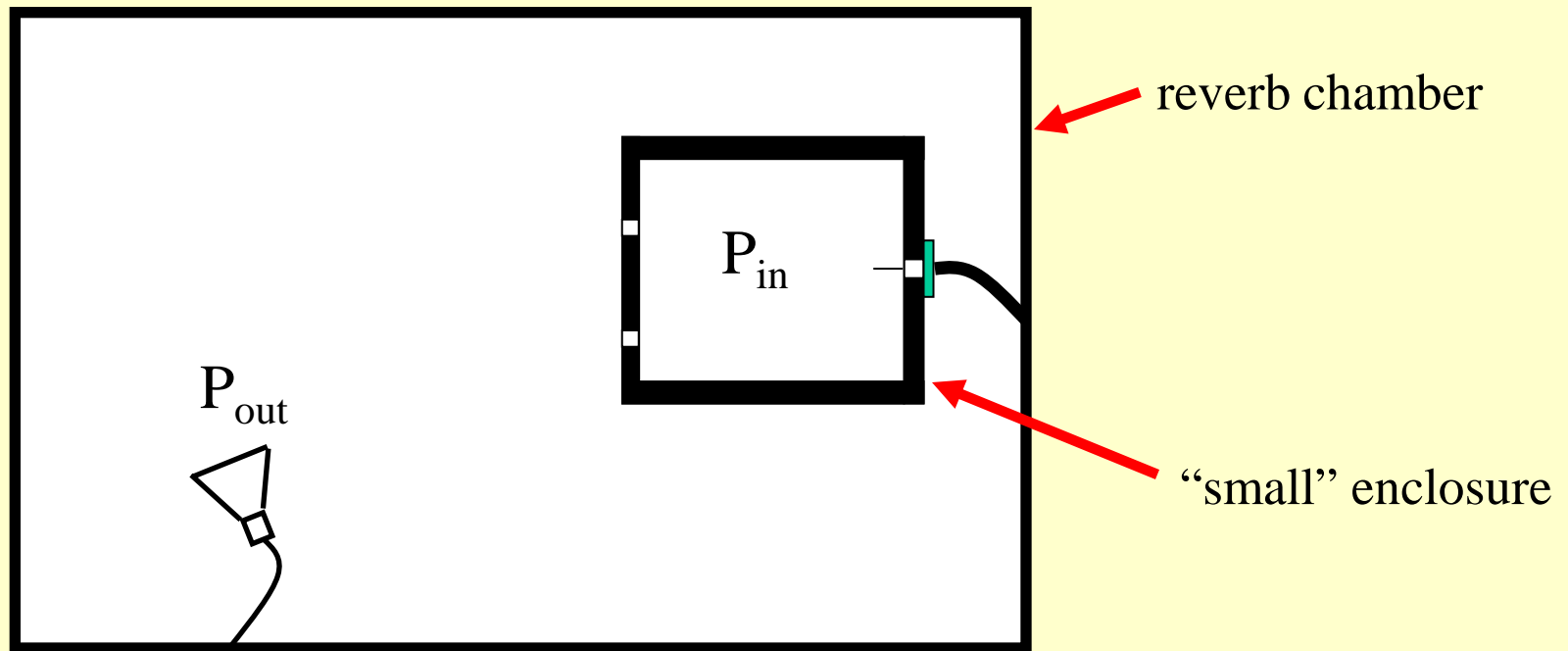
*Distributed Lossy Bodies*



**NIH in the US is currently doing studies in 22 chambers**

*Periodic Lossy Bodies*

# *Measuring Shielding for “small” Enclosures*

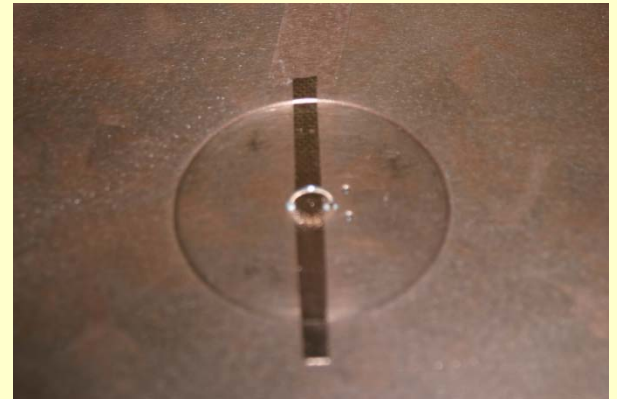
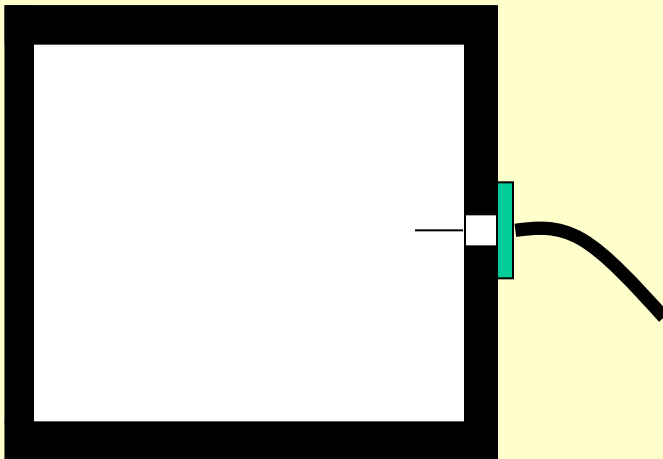


$$SE = -10 \text{ Log}(P_{in} / P_{out}): \text{ with frequency stirring}$$

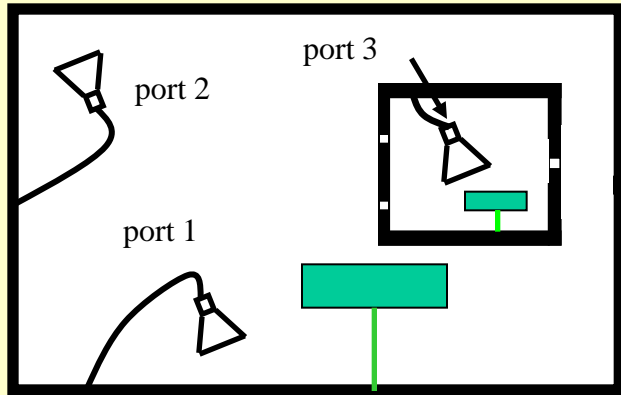
# *Problem with “small” Enclosures: Measuring the Fields Inside*

- However, Hill (IEEE Trans on EMC, 2005) has recently shown that the statistics for the normal component of the E-field at the wall are the same for the field in the center of the chamber.

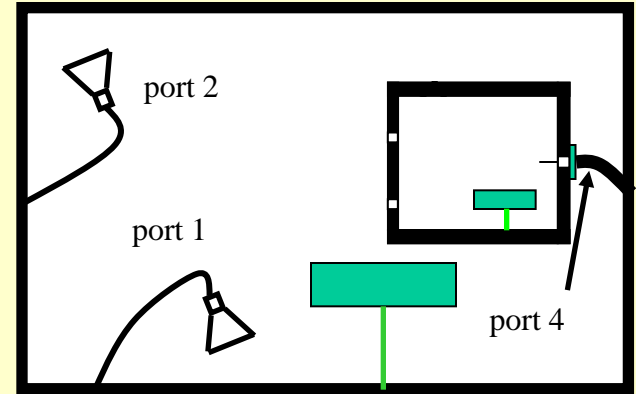
1. Thus, small monopole (or loop) probes attached to the wall can be used to determine the power in the center of a “small” enclosure.
2. Use frequency stirring for obtain samples.



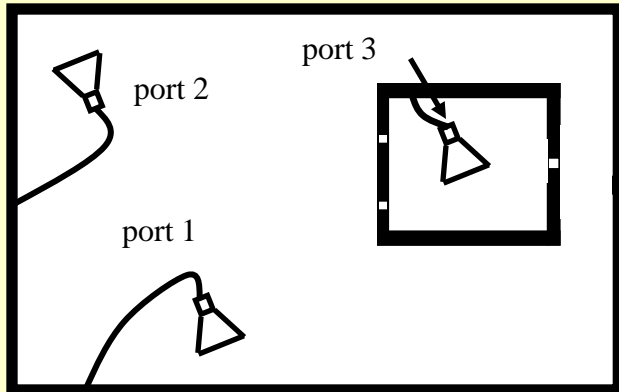
# Comparison with Different Reverberation Chamber Approaches



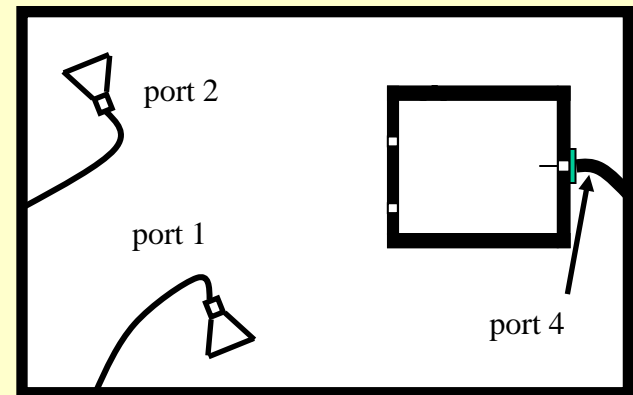
Mode-Stirred with a Horn Antenna:  $SE \Rightarrow S_{31}$



Mode-Stirred with a Monopole Antenna:  $SE \Rightarrow S_{41}$

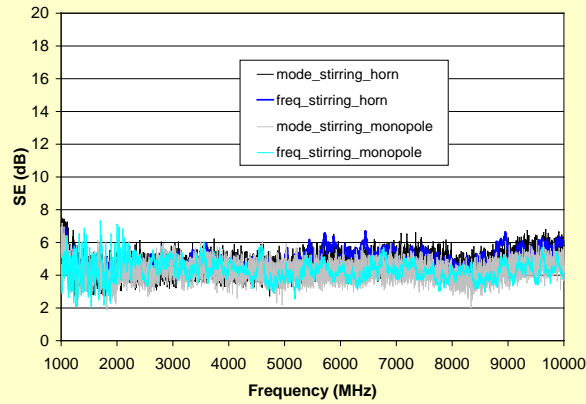


Frequency Stirring with a Horn Antenna:  $SE \Rightarrow S_{31}$

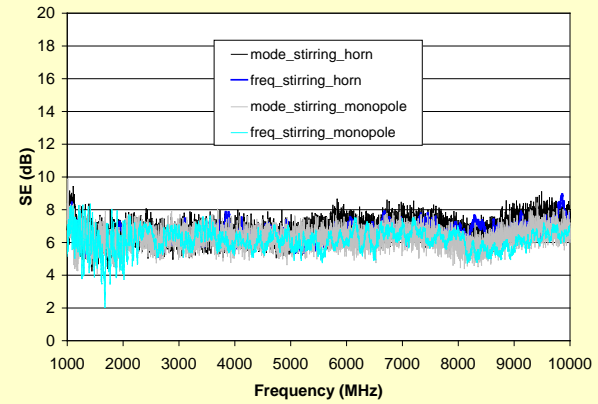


Frequency Stirring with a Monopole Antenna:  $SE \Rightarrow S_{41}$

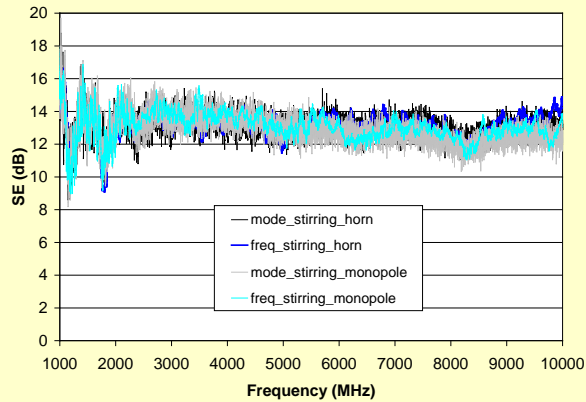
# Comparison with Different Approaches



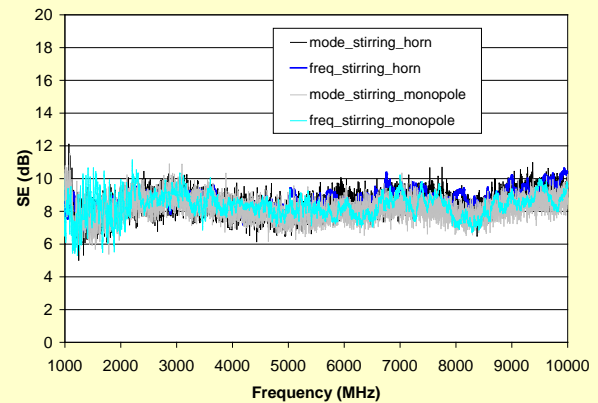
(a) open aperture



(b) half-filled aperture



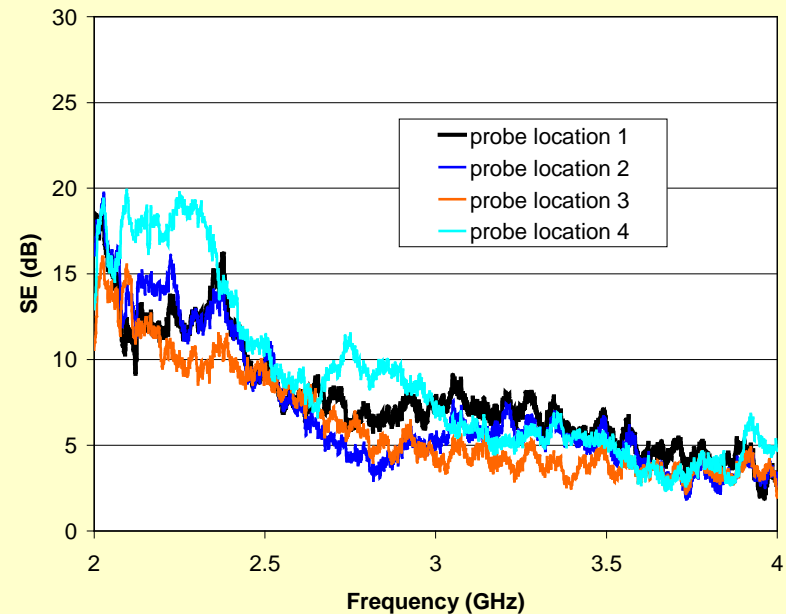
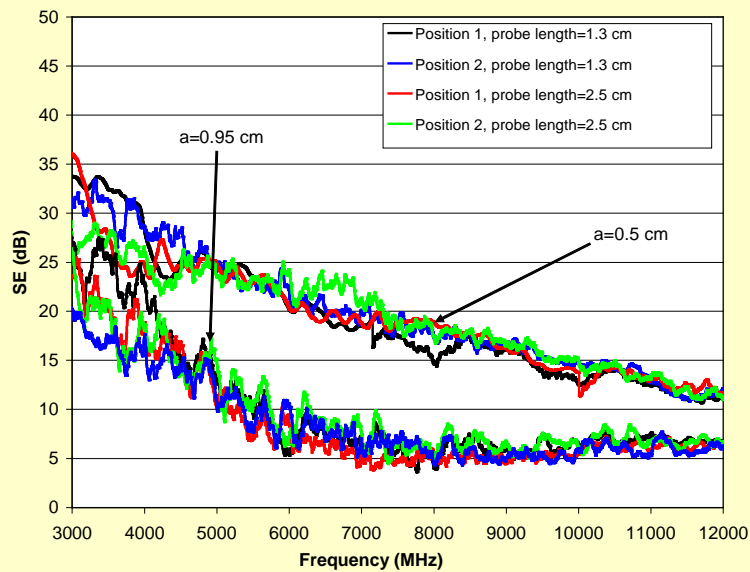
(c) narrow slot aperture



(d) generic aperture

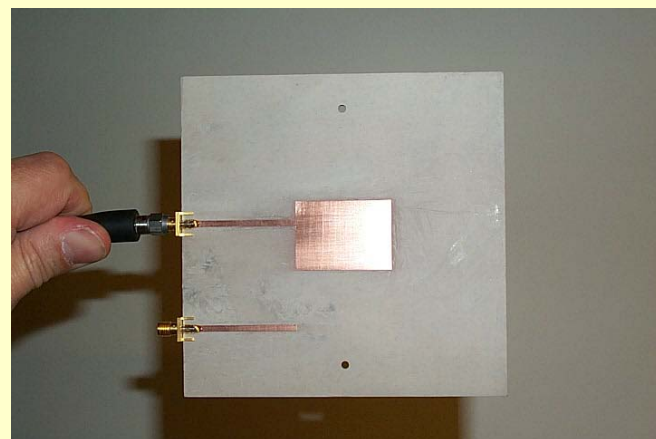


# Different Probe Lengths and Locations

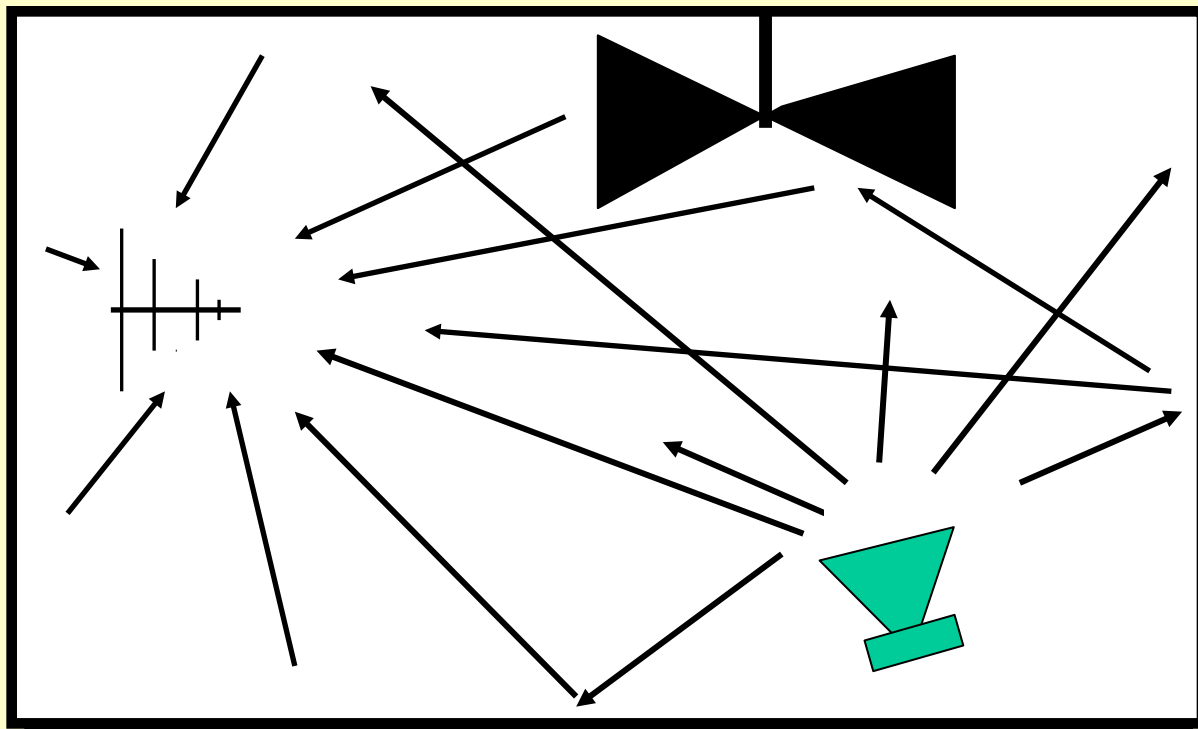


**This technique is currently being incorporated in the IEEE 299-1 standard**

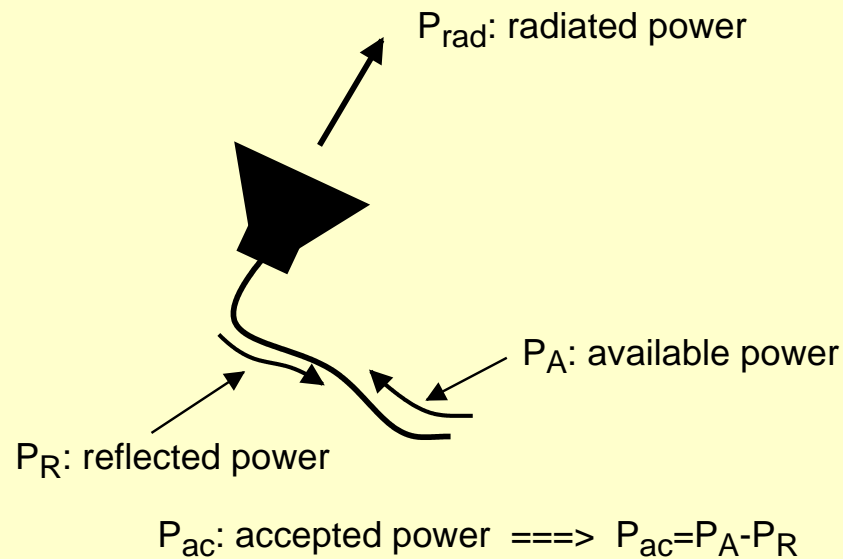
# Antenna Measurement:



# Reverberation Chambers are Natural Multipath Environments (Ideal for Antenna Measurements)



# Radiation and Total Efficiencies of Antennas

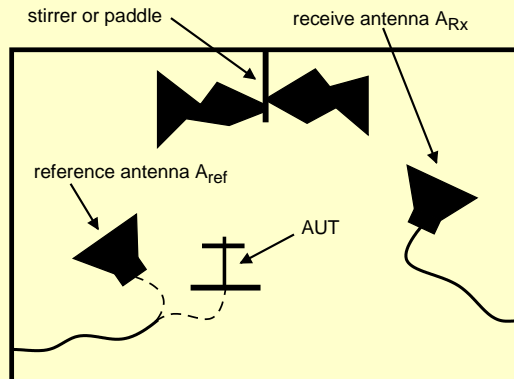


- total efficiency: defined as the ratio of the power radiated to the power available at the antenna port (including mismatch or reflection loss)
- radiation efficiency: defined as the ratio of the power radiated to the power accepted by the antenna port

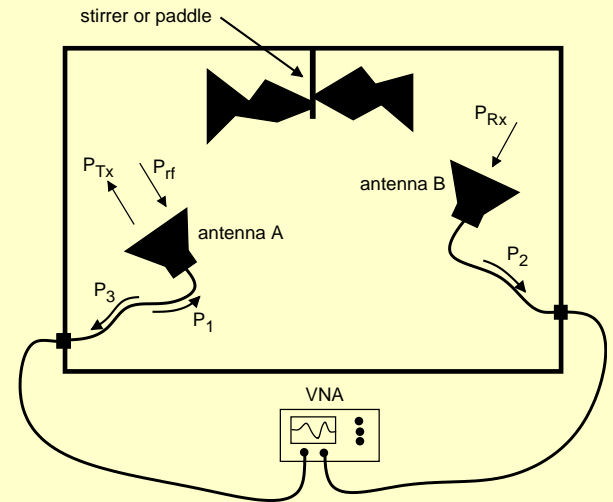
# Problems with Current Two Approaches

The two current reverberation chamber approaches have the following two problems:

- The first approach requires a reference antenna and it is assumed that the efficiency of the reference antenna is known.
- The problem with the second approach is that we only have one expression for the product of the two efficiencies. Thus, we “MUST” assume the two antennas are identical in order to determine the efficiencies.



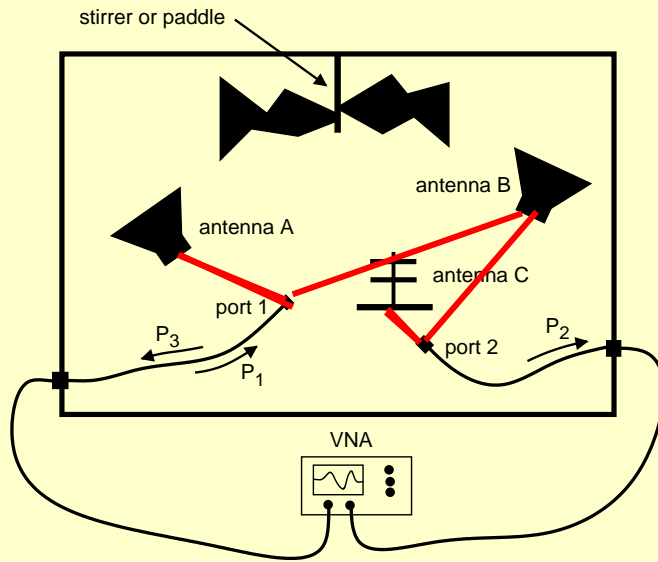
$$\eta_{\text{AUT}} = (P_{\text{AUT}}/P_{\text{ref}}) \eta_{\text{ref}}$$



$$\eta_B \eta_A = [C_{\text{RC}} / \omega] \cdot [ \langle |S_{21}|^2 \rangle / \tau_{\text{RC}} ]$$

# Three Antenna Approach

Holloway et al., "Reverberation Chamber Techniques for Determining the Radiation and Total Efficiency of Antennas"  
*IEEE Trans. on Antenna and Propagation*, vol. 60, no. 4, April 2012, pp. 1758-1770



## Antennas A & B

$$\eta_B \eta_A = [C_{RC} / \omega] M_{AB}$$

$$M_{AB} = [ \langle |S_{21}|^2 \rangle / \tau_{RC} ]_{AB}$$

## Antennas A & C

$$\eta_C \eta_A = [C_{RC} / \omega] M_{AC}$$

$$M_{AC} = [ \langle |S_{21}|^2 \rangle / \tau_{RC} ]_{AC}$$

## Antennas B & C

$$\eta_C \eta_B = [C_{RC} / \omega] M_{CB}$$

$$M_{CB} = [ \langle |S_{21}|^2 \rangle / \tau_{RC} ]_{CB}$$

unknown

obtained for a measurement

Three equation and three unknown:  $\eta_A$ ,  $\eta_B$  and  $\eta_C$

$$\eta_A^{total} = \sqrt{\frac{C_{RC}}{\omega}} \sqrt{\frac{M_{AB} M_{AC}}{M_{BC}}}$$

$$\eta_B^{total} = \sqrt{\frac{C_{RC}}{\omega}} \sqrt{\frac{M_{BC} M_{AB}}{M_{AC}}}$$

$$\eta_C^{total} = \sqrt{\frac{C_{RC}}{\omega}} \sqrt{\frac{M_{AC} M_{CB}}{M_{AB}}}$$

# Three Antenna Approach

Total efficiency (mismatch and ohmic loss)

$$\eta_A^{\text{total}} = \sqrt{\frac{C_{RC}}{\omega}} \sqrt{\frac{M_{AB} M_{AC}}{M_{BC}}}$$

$$\eta_B^{\text{total}} = \sqrt{\frac{C_{RC}}{\omega}} \sqrt{\frac{M_{BC} M_{AB}}{M_{AC}}}$$

$$\eta_C^{\text{total}} = \sqrt{\frac{C_{RC}}{\omega}} \sqrt{\frac{M_{AC} M_{BC}}{M_{AB}}}$$

Radiation efficiency (mismatch correction)

$$\eta_A^{\text{rad}} = \sqrt{\frac{C_{RC}}{\omega}} \sqrt{\frac{M_{AB,cor} M_{AC,cor}}{M_{BC,cor}}}$$

$$\eta_B^{\text{rad}} = \sqrt{\frac{C_{RC}}{\omega}} \sqrt{\frac{M_{BC,cor} M_{AB,cor}}{M_{AC,cor}}}$$

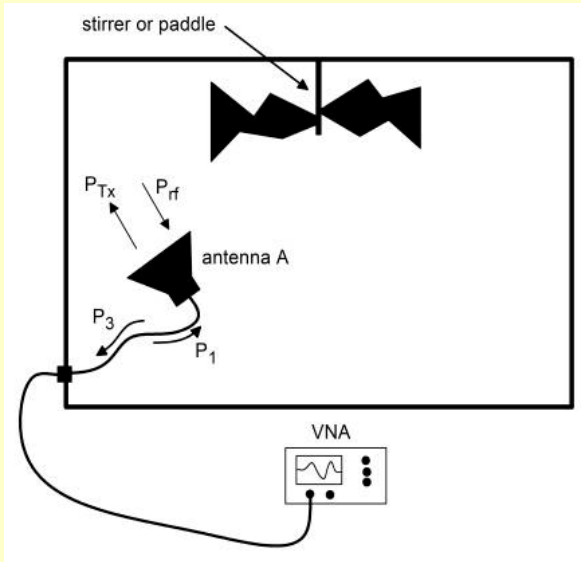
$$\eta_C^{\text{rad}} = \sqrt{\frac{C_{RC}}{\omega}} \sqrt{\frac{M_{AC,cor} M_{BC,cor}}{M_{AB,cor}}}$$

$$M_{AB,cor} = \frac{\langle |S_{21,s}|^2 \rangle_{ij,cor}}{\tau_{RCAB,ij}} = \frac{1}{\tau_{RCAB,ij}} \frac{\langle |S_{21,s}|^2 \rangle_{ij}}{(1 - |S_{11}|^2)(1 - |S_{22}|^2)}$$



# One Antenna Approach

Holloway et al., "Reverberation Chamber Techniques for Determining the Radiation and Total Efficiency of Antennas"  
*IEEE Trans. on Antenna and Propagation*, vol. 60, no. 4, April 2012, pp. 1758-1770



$$P_{TX} = \eta_A P_1 \quad ; \quad P_{rf} = P_2 / \eta_A$$

$$\langle P_{rf} \rangle / P_{TX} = \langle S_{11} \rangle / (\eta_A * \eta_A)$$

For an "ideal" chamber it can be shown that:  $\langle P_{rf} \rangle = 2 \langle P_{RX} \rangle$ .

This result is analogous to the enhanced backscatter that has been derived for scattering by a random medium.

$$(\eta_A)^2 = (\langle |S_{21}|^2 \rangle / 2) * (\langle P_{RX} \rangle / P_{TX}) \quad \text{and} \quad \langle P_{RX} \rangle / P_{TX} = Q / C_{RC}$$

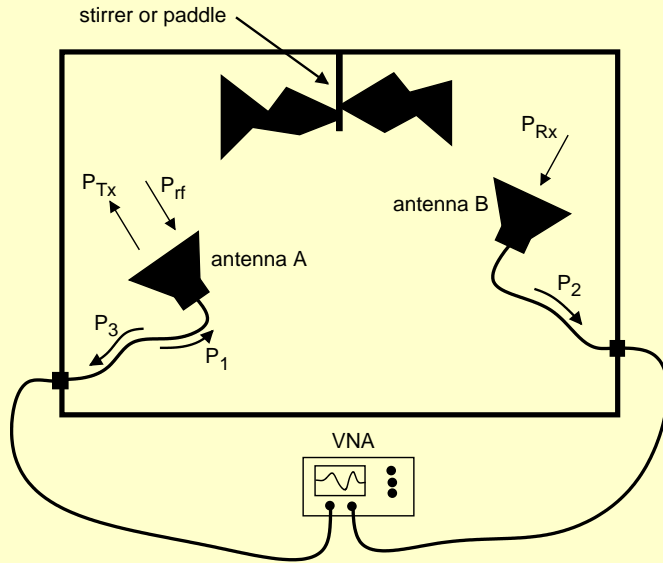
known

$$\eta_A = \sqrt{\frac{C_{RC}}{2\omega} \frac{\langle |S_{11}|^2 \rangle}{\tau_{RC}}}$$

unknown

obtained for a measurement

# Two Antenna Approach



Following a similar procedure as the one-antenna method, we can show:

$$\begin{aligned} \langle |S_{11}|^2 \rangle &= \eta_A^{total} \eta_A^{total} \frac{\langle P_{rf,1} \rangle}{P_{TX}} \\ \langle |S_{22}|^2 \rangle &= \eta_B^{total} \eta_B^{total} \frac{\langle P_{rf,2} \rangle}{P_{TX}} \\ \langle |S_{21}|^2 \rangle &= \eta_B^{total} \eta_A^{total} \frac{\langle P_{RX} \rangle}{P_{TX}} \end{aligned}$$

obtained for a measurement

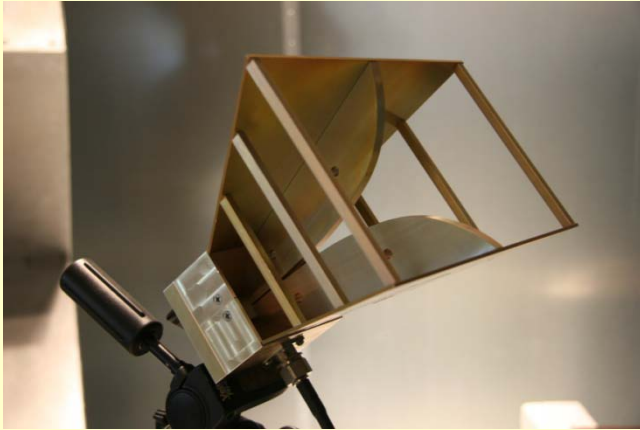
If we assume that  $\langle P_{rf,1} \rangle = e_b \langle P_{RX} \rangle$  and  $\langle P_{rf,2} \rangle = e_b \langle P_{TX} \rangle$  where  $e_b$  is the enhanced backscatter constant (and is 2 for an ideal chamber), then the two-antenna method reduces to the following

$$\eta_A^{total} = \sqrt{\frac{C_{RC} \langle |S_{11}|^2 \rangle}{\omega e_b \tau_{RC}}}$$

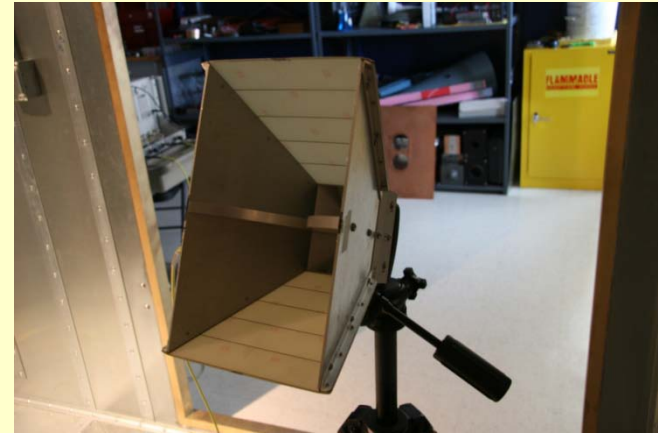
$$\eta_B^{total} = \sqrt{\frac{C_{RC} \langle |S_{22}|^2 \rangle}{\omega e_b \tau_{RC}}}$$

where  $e_b = \sqrt{\frac{\langle |S_{22}|^2 \rangle \langle |S_{21}|^2 \rangle}{\langle |S_{21}|^2 \rangle}}$

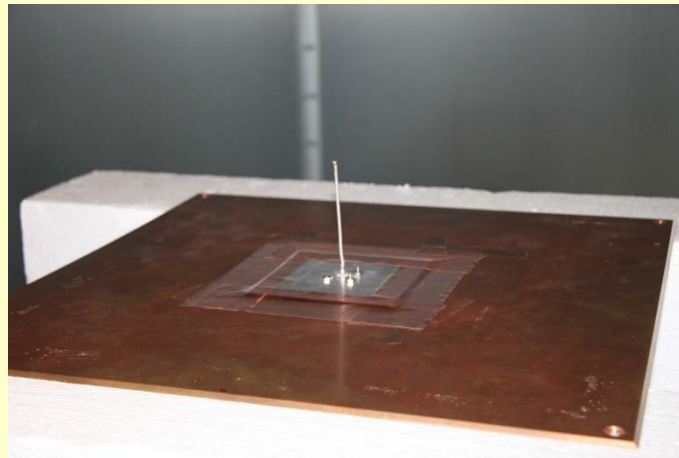
# Experimental Data for Three Antennas



Antenna A: 13.5 cm by 22.5 cm horn

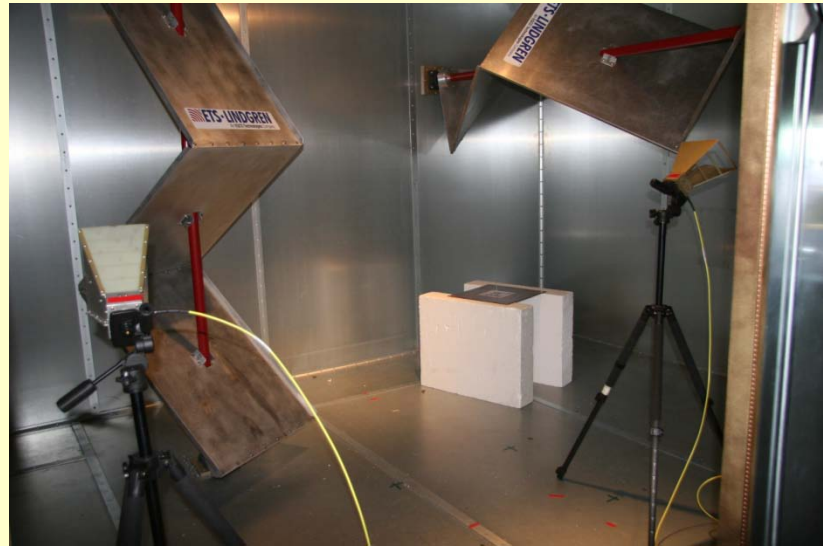


Antenna B: 13.5 cm by 24.5 cm horn



Antenna C: 9 cm monopole on 45.5 cm ground plane

# Experimental Data for Three Antennas



We performed three sets of measurements with a VNA:

- 1) Antennas A & B
- 2) Antennas A & C
- 3) Antennas B & C

We need a measurement of both  $\langle |S_{11}|^2 \rangle$  and  $\tau_{RC}$ .

# Determining $S_{11}$

$S_{11}$  is obtained for the experimental set-up shown in the figure, by first measuring  $S_{11}$  for each paddle position (100 positions were used in these measurements), then averaging  $|S_{11}|^2$  for these 100 positions to obtain the ensemble average  $\langle |S_{11}|^2 \rangle$ .

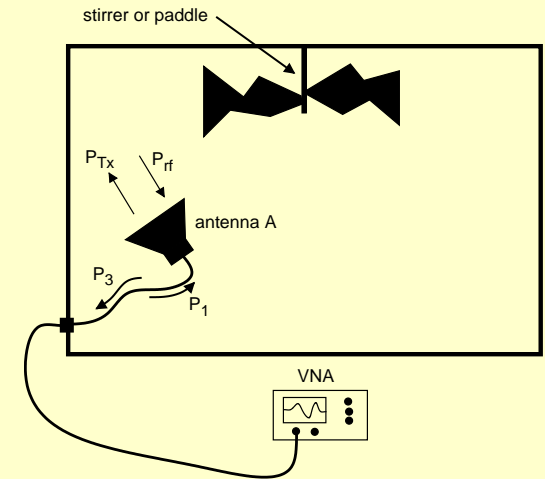
The formulation above requires  $\langle |S_{11}|^2 \rangle$  to have contributions from only the stirred energy in the RC.

$$\text{The formulation: } S_{11} = S_{11\text{unstirred}} + S_{11\text{stirred}}$$

In order to ensure that the unstirred contribution is removed,  $\langle |S_{11}|^2 \rangle$  is determined with the following:

$$\langle |S_{11}|^2 \rangle = \langle |S_{11} - \langle S_{11} \rangle|^2 \rangle$$

That is, we remove the average value,  $\langle S_{11} \rangle$ , from  $S_{11}$ .



# Determining $\tau_{RC}$

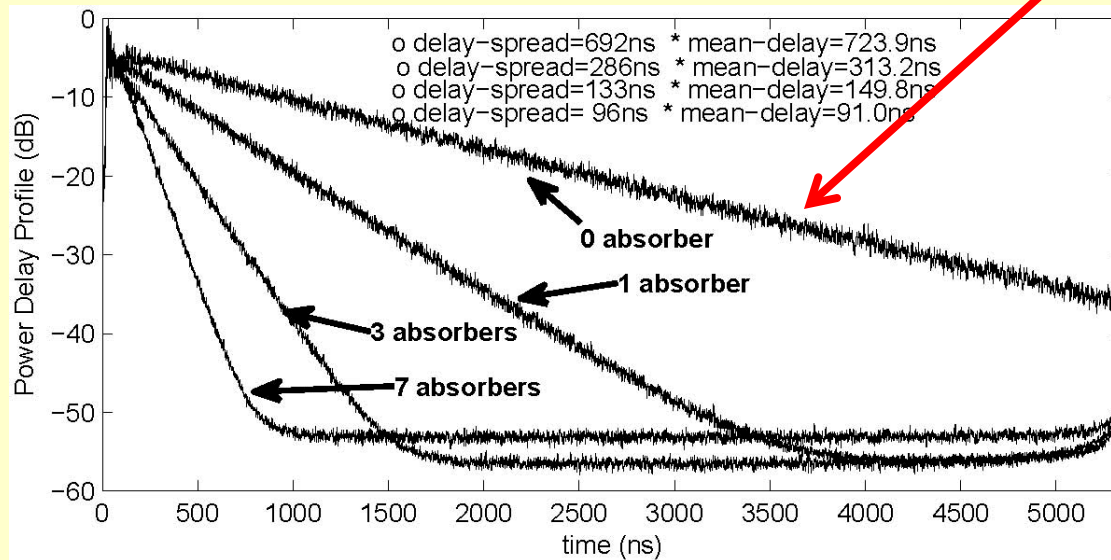
We determine  $\tau_{RC}$  from time-domain data

Power Delay Profile:

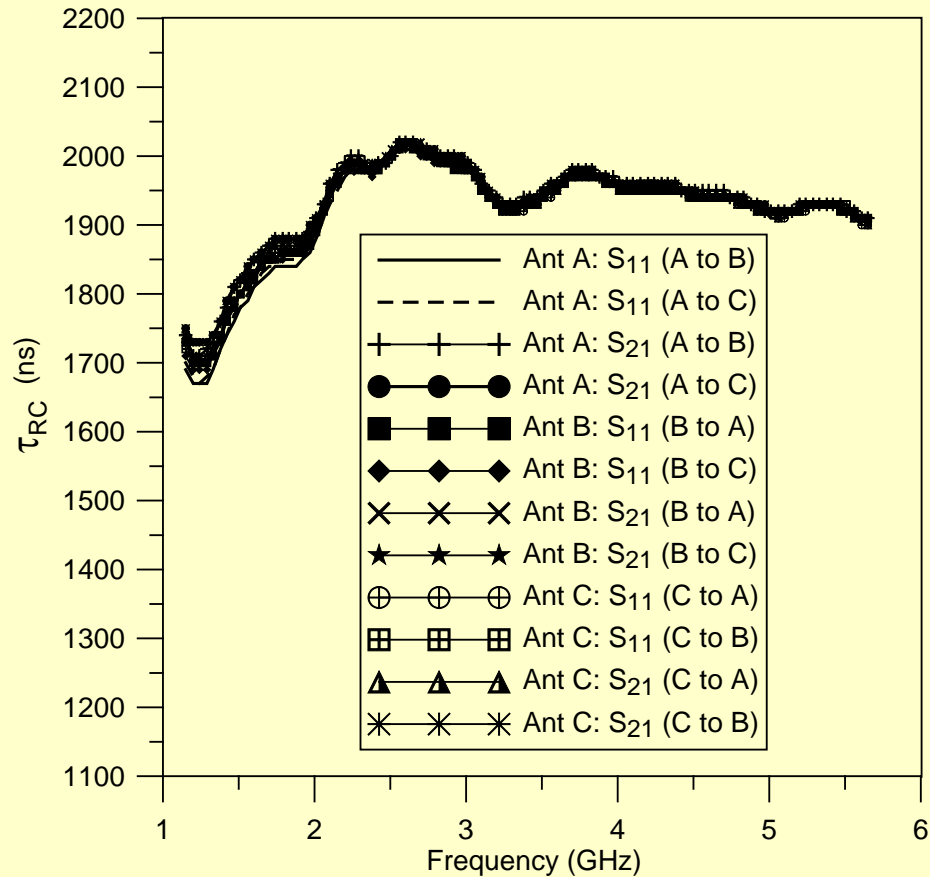
$$PDP(\tau) = \left\langle |h(t)|^2 \right\rangle$$

where  $h(t)$  is the Fourier transform of  $S_{21}(\omega)$

slope =  $1/\tau_{RC}$

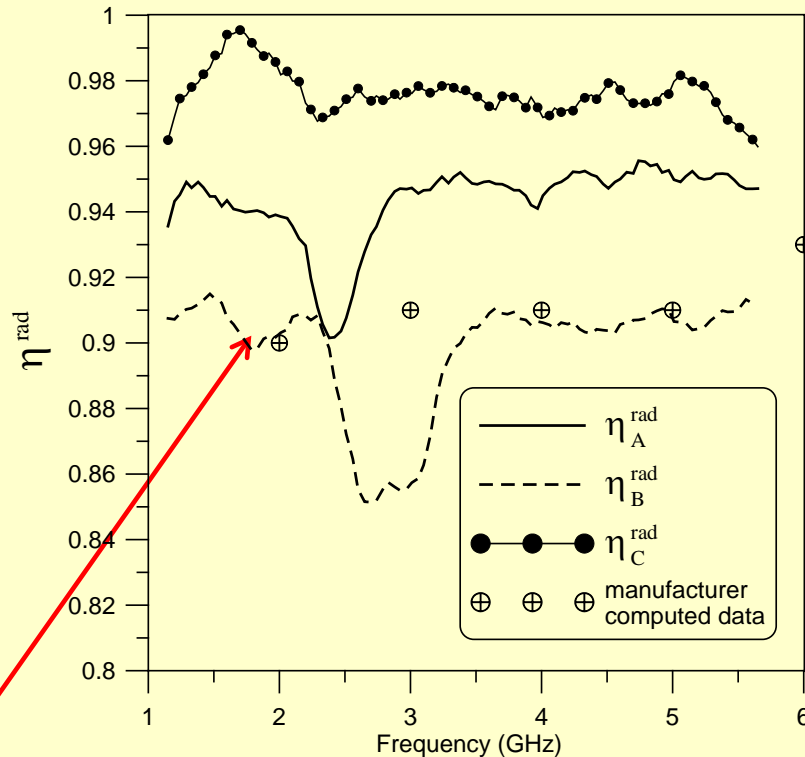


# Determining $\tau_{RC}$



This shows that  $\tau_{RC}$  is independent of location in the chamber and independent of the antenna use in the measurement.

# Radiation Efficiency



$$\eta_A^{\text{rad}} = \sqrt{\frac{C_{AC}}{W}} \sqrt{\frac{M_{AB,\text{cor}} M_{AC,\text{cor}}}{M_{BC,\text{cor}}}}$$

$$\eta_B^{\text{rad}} = \sqrt{\frac{C_{BC}}{W}} \sqrt{\frac{M_{BC,\text{cor}} M_{AB,\text{cor}}}{M_{AC,\text{cor}}}}$$

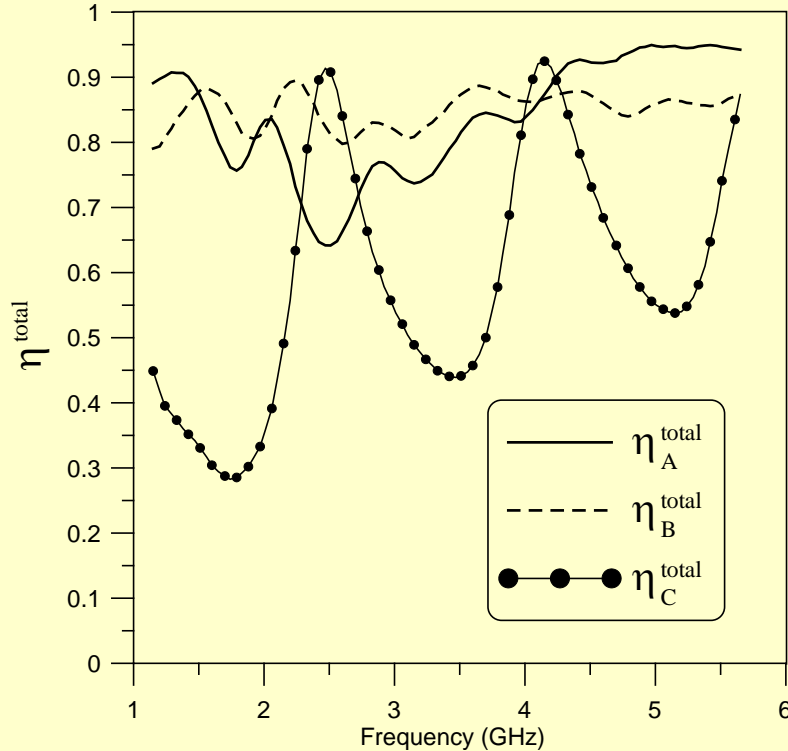
$$\eta_C^{\text{rad}} = \sqrt{\frac{C_{BC}}{W}} \sqrt{\frac{M_{AC,\text{cor}} M_{AC,\text{cor}}}{M_{AB,\text{cor}}}}$$

The manufacturer of antenna B state the radiation efficiency is 91 %.  
 (Danny Odum and Dr. Vince Rodriguez of ETS-Lindgren)

We see that the monopole antenna has the least ohmic loss of the three antennas.  
 Antenna B has the largest ohmic losses.



# Total Efficiency

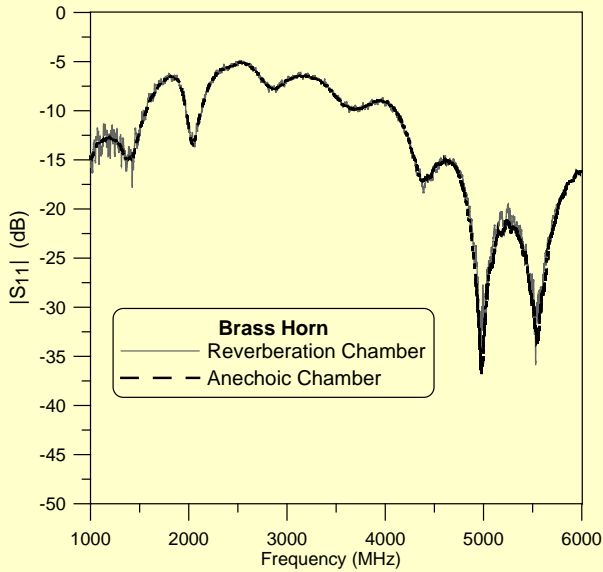


$$\eta_A^{\text{total}} = \sqrt{\frac{C_{RC}}{\omega}} \sqrt{\frac{M_{AB} M_{AC}}{M_{BC}}}$$
$$\eta_B^{\text{total}} = \sqrt{\frac{C_{RC}}{\omega}} \sqrt{\frac{M_{BC} M_{AB}}{M_{AC}}}$$
$$\eta_C^{\text{total}} = \sqrt{\frac{C_{RC}}{\omega}} \sqrt{\frac{M_{AC} M_{BC}}{M_{AB}}}$$

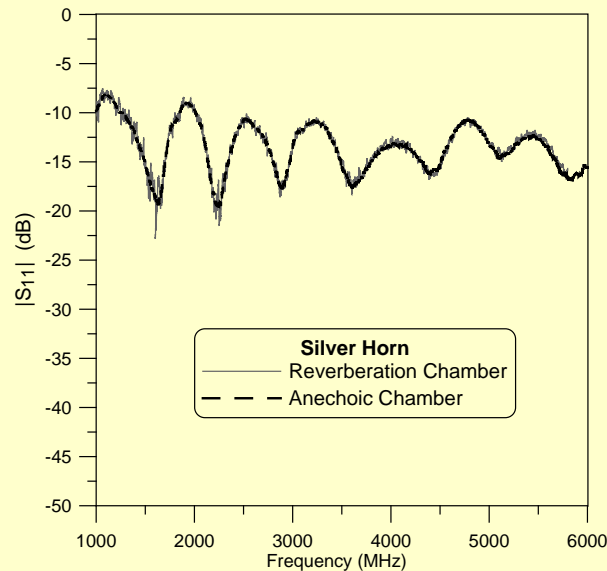
We see that the monopole antenna has the lowest total efficiency of the three antennas. This obviously implies that the monopole is the worst impedance matched antenna of the three.

# Measured $S_{11}$ for the Three Antennas

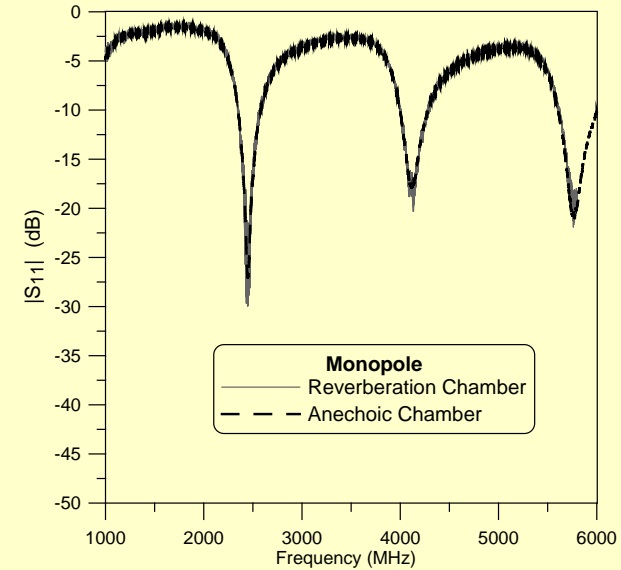
## Antenna A



## Antenna B



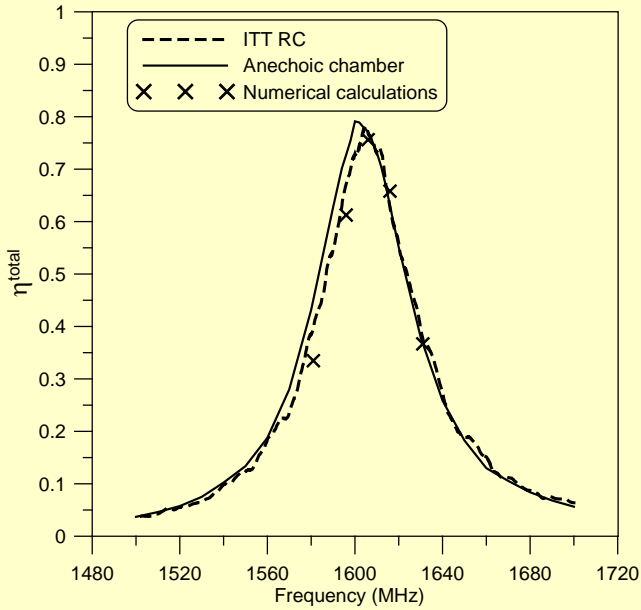
## Antenna C



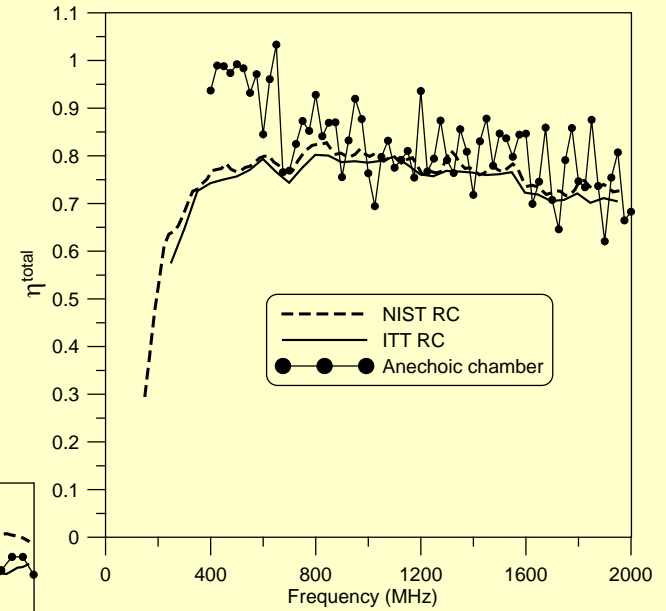
These comparisons illustrate that RC and anechoic chamber measurements give the same result for  $S_{11}$

# Comparisons to Other Chambers and Techniques

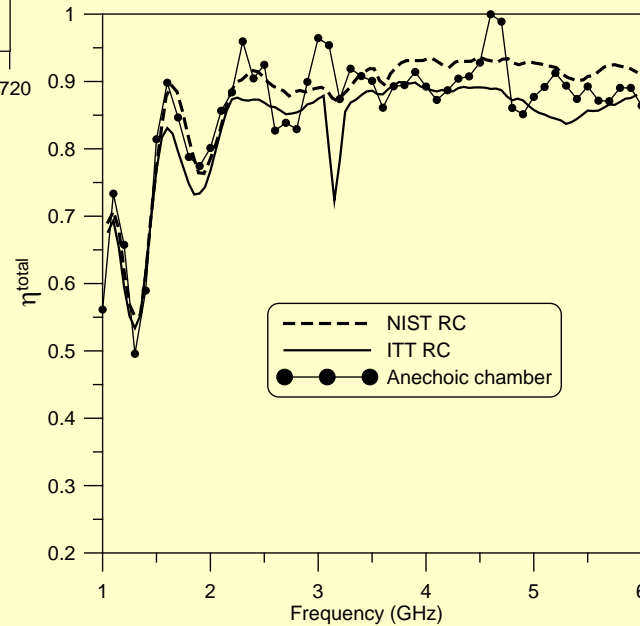
## Microstrip



## Log-periodic



## Horn



# Measurement Uncertainties

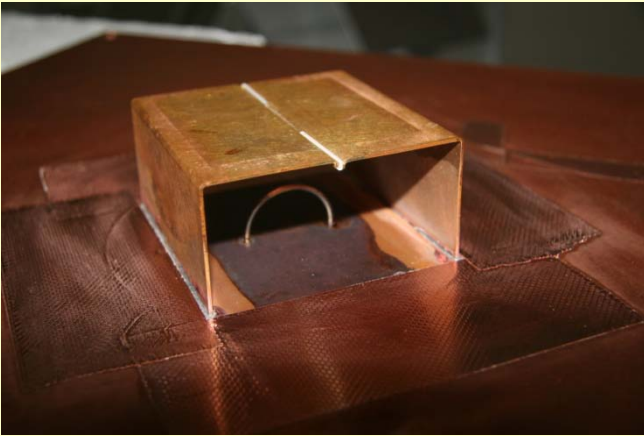
Uncertainty Source	uncertainty
Type A: $u_{S21}$	0.45 dB
$u_{\tau RC}$	0.048 dB
<b>Total: Type A</b>	<b>0.45 dB</b>
Type B: $u_{VNA}$	0.2 dB
<b>Total: Type B</b>	<b>0.2 dB</b>
<b>Total:</b>	<b>0.49 dB</b>

Total uncertainties for the three-antenna approach is  
0.49 dB or 12 %

However, by increasing the number of independent samples and employing a combination of paddle-averaging, frequency-averaging, and position-averaging (a common practice in RC measurements), the uncertainties can be reduced further to below 10 %.

# Magnetic Antenna

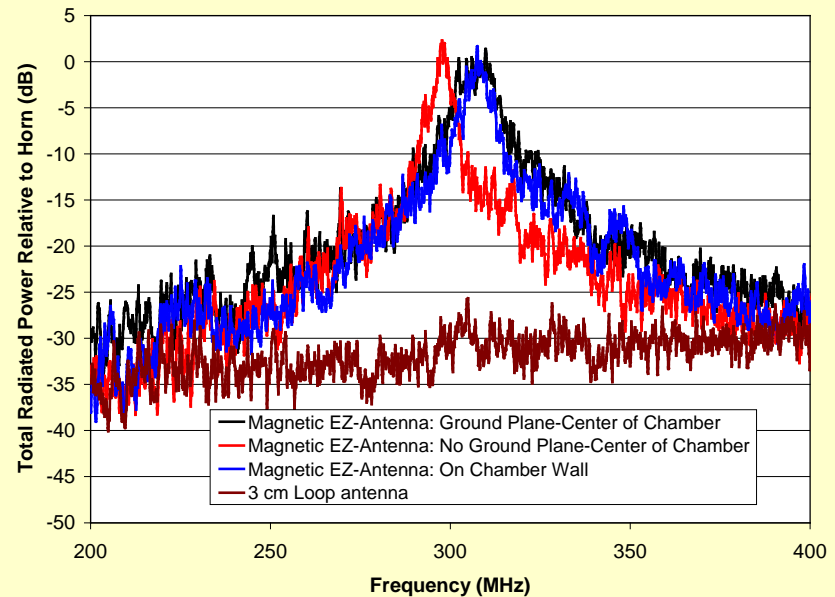
## New Magnetic Antenna



## Comparison to Horn



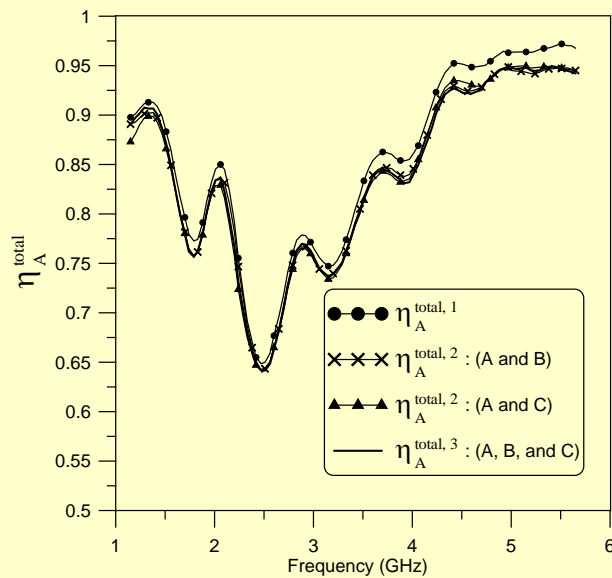
## Loop Antenna



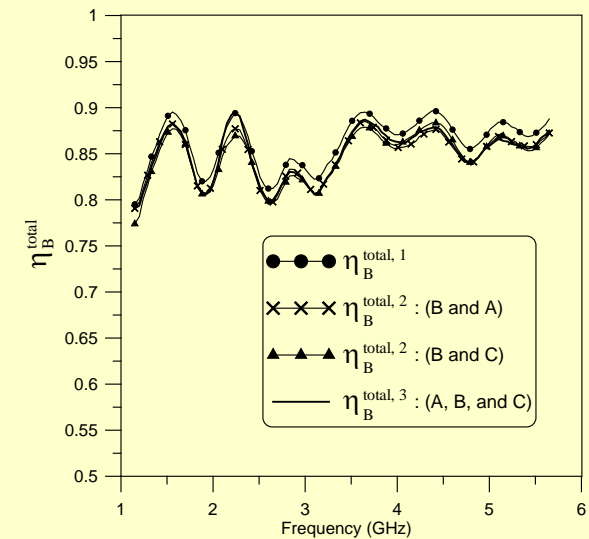
# Comparison of Total Efficiency with Other Methods

Holloway et al., "Reverberation Chamber Techniques for Determining the Radiation and Total Efficiency of Antennas"  
*IEEE Trans. on Antenna and Propagation*, vol. 60, no. 4, April 2012, pp. 1758-1770

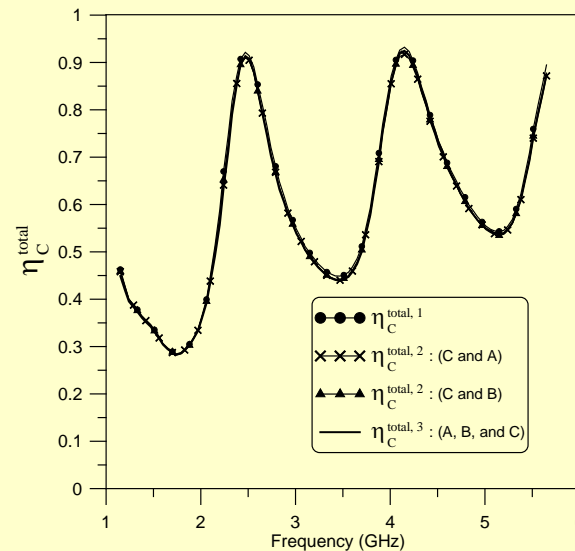
## Antenna A



## Antenna B



## Antenna C



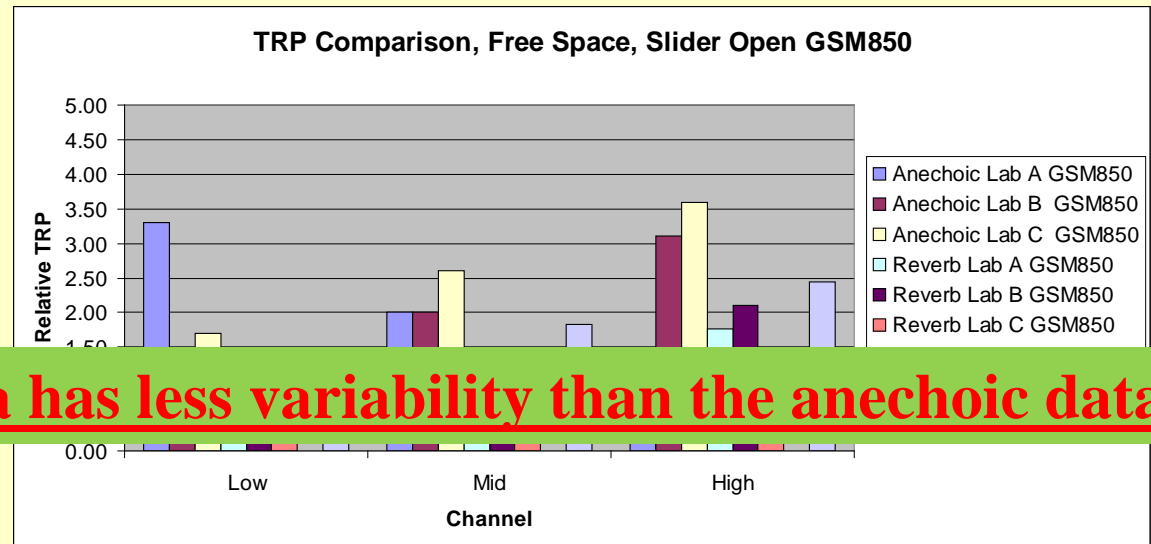
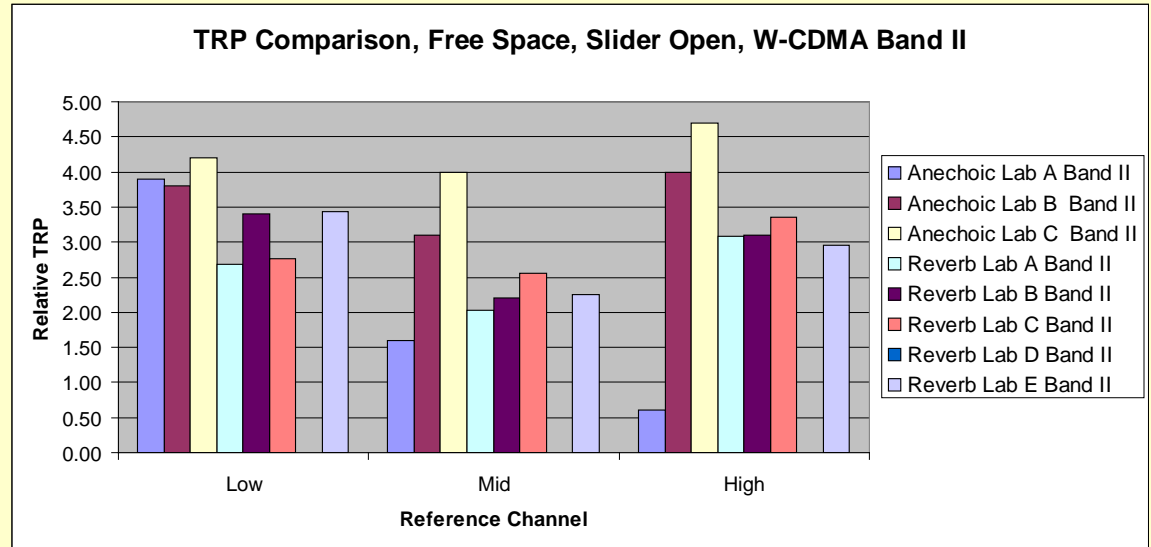
# Standardization of Wireless Measurements

Can we use a reverberation chambers as a reliable and repeatable test facilities that has the capability of simulating any multipath environment for the testing of wireless communications devices?

If so, such a test facility will be useful in wireless measurement standards.

# Total Radiated Power from Cell-Phones

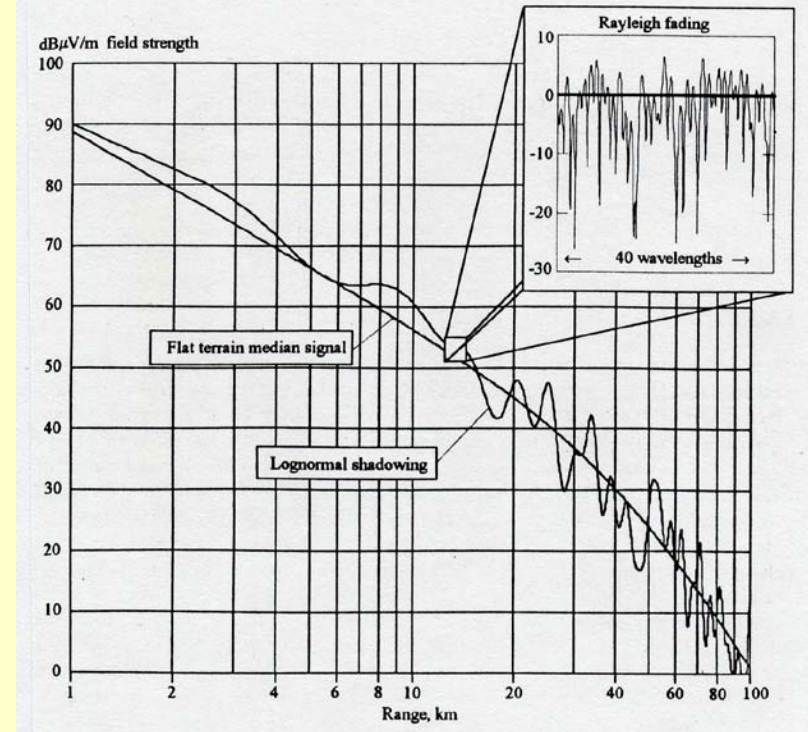
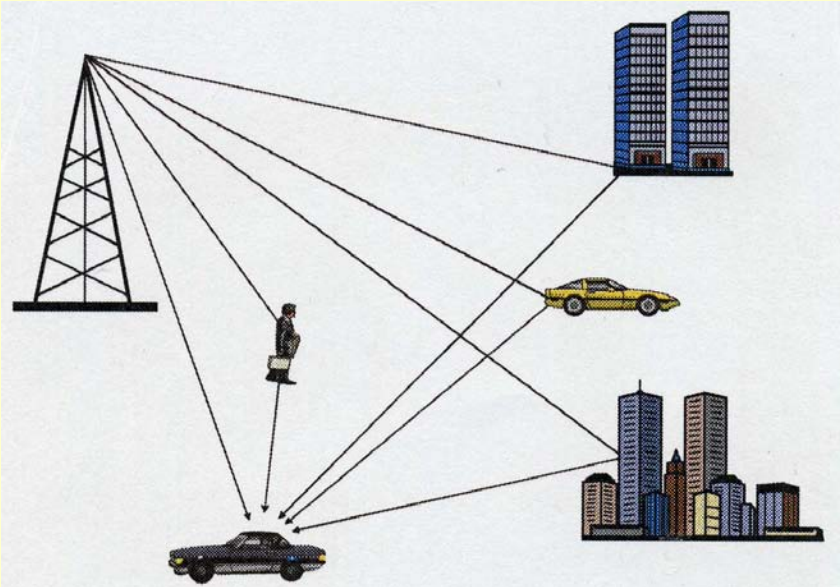
Data from CTIA working group on total radiate power (TRP) testing:



**Reverb chamber data has less variability than the anechoic data!**



# Multipath Environments



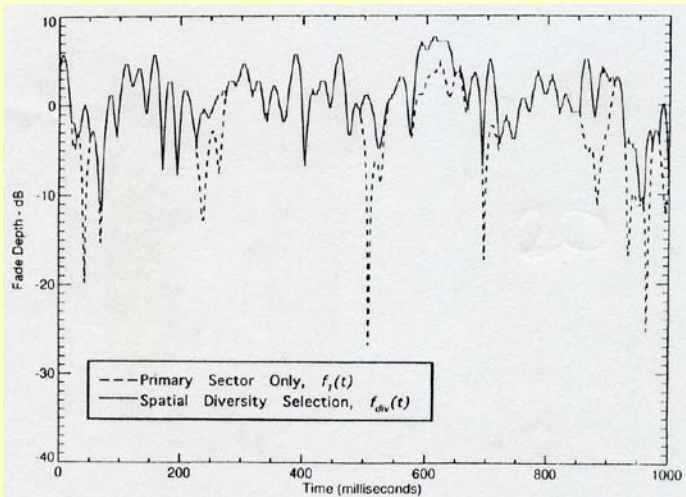
# Multipath Environments

Extensive measurements have shown that when light of sight (LOS) path is present the radio multipath environment is well approximated by a **Ricean** channel, and when no LOS is present the channel is well approximated by a **Rayleigh** channel:

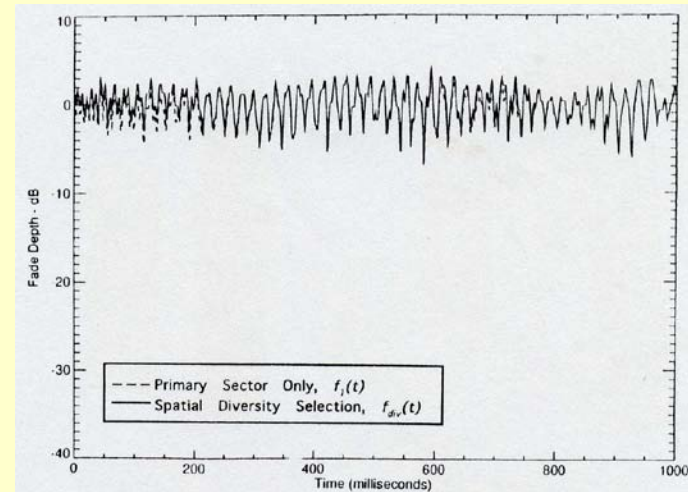
$$E = A_{LOS} \cos(2\pi f_c t) + \sum_{n=1}^N A_n \cos[2\pi(f_c + f_n)t + \phi_n]$$

The Amplitude of  $E$  is either Rayleigh or Ricean depending if a LOS path is present.

## Urban Environment



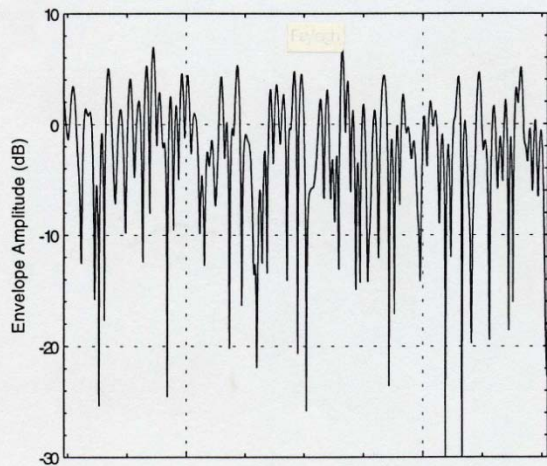
## Rural Environment



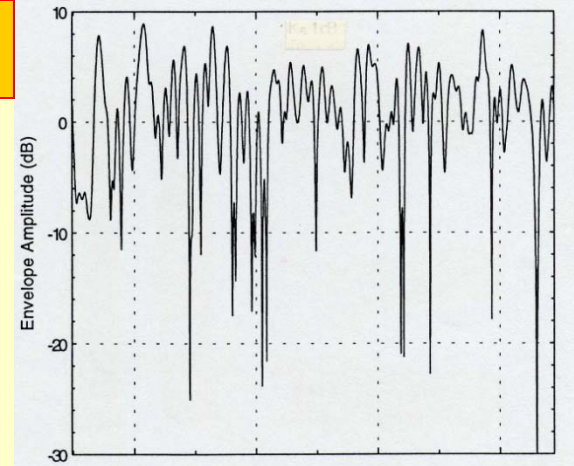
# Ricean K-factor

**K-factor:**  $k = \frac{\text{direct component}}{\text{scattered components}}$  or  $K = 10 \text{ Log}(k)$

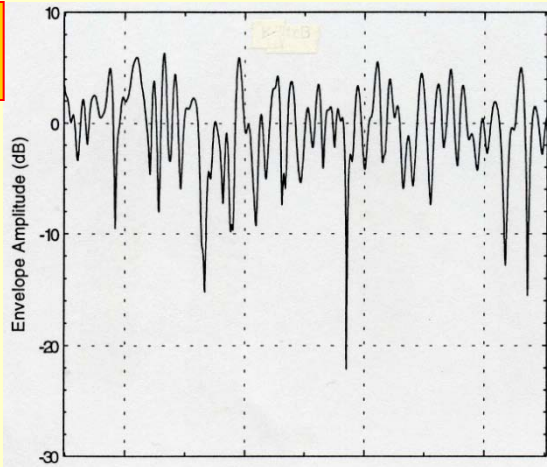
**K = -∞ dB  
(Rayleigh)**



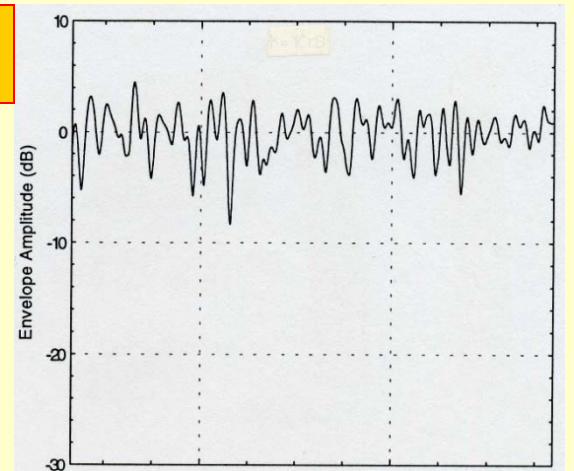
**K = 1 dB**



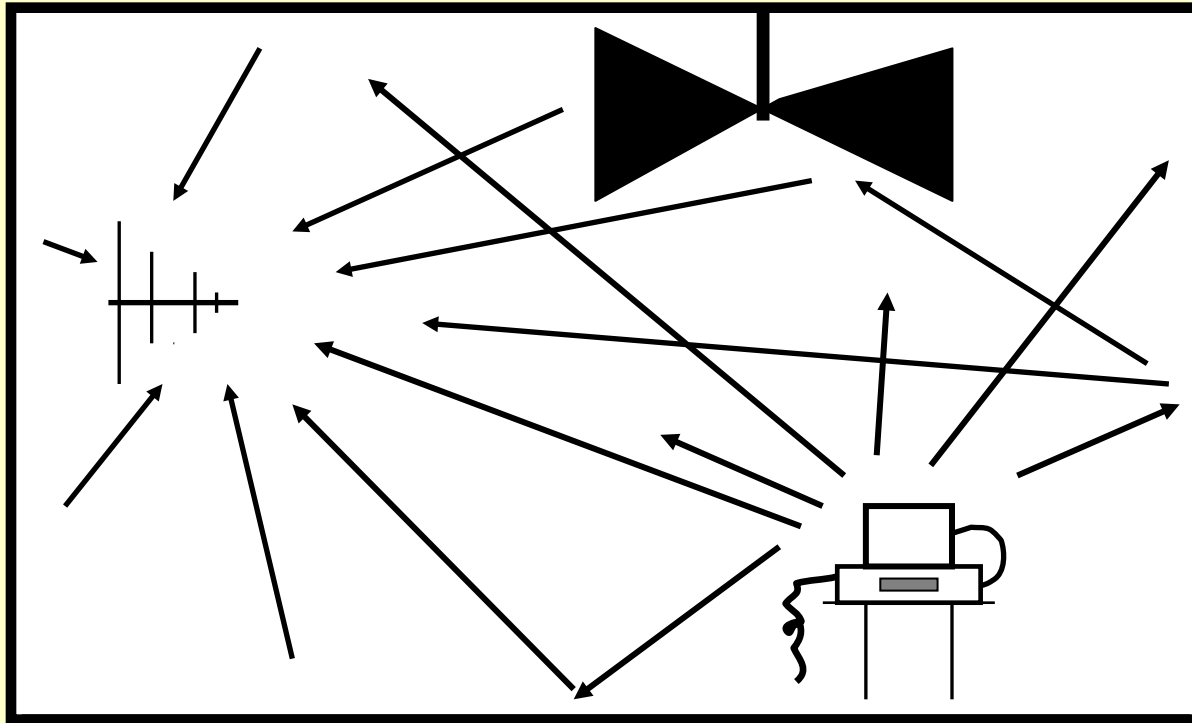
**K = 4 dB**



**K = 10 dB**

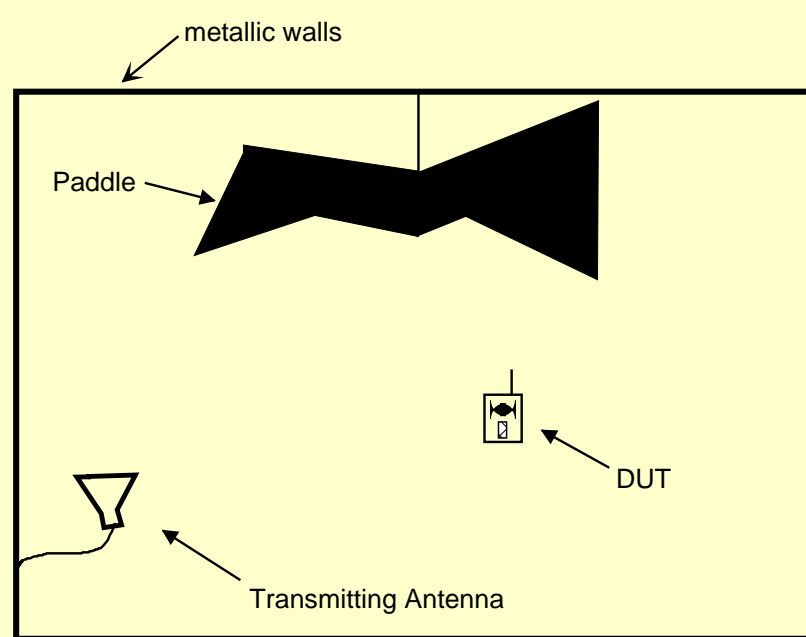


# Reverberation Chambers are Natural Multipath Environments



# Typical Reverberation Chamber Set-up

Antenna pointing away from probe (DUT)

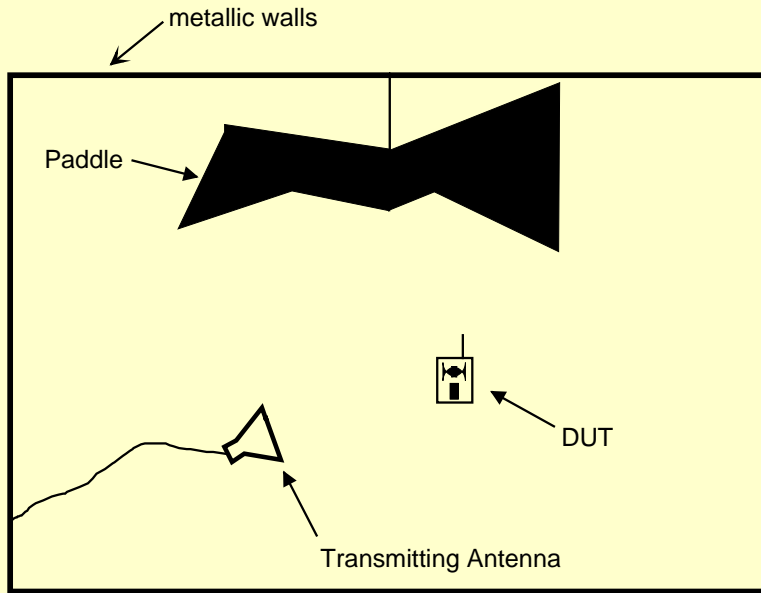


**A Rayleigh test environment**

**Can we generate a Ricean environment?**

# Chamber Set-up for Rician Environment

## Antenna pointing toward (DUT)



*We will show that by varying the characteristics of the reverberation chamber and/or the antenna configurations in the chamber, any desired Rician K-factor can be obtained.*

# Reverberation Chamber Ricean Environment

It can be shown: see Holloway et al, *IEEE Trans on Antenna and Propag.*, vol. 54, no. 11, pp. 3167-3177, November 2006.

$$K = \frac{3}{2} \frac{V}{\lambda} \frac{D}{Q r^2}$$

## Note:

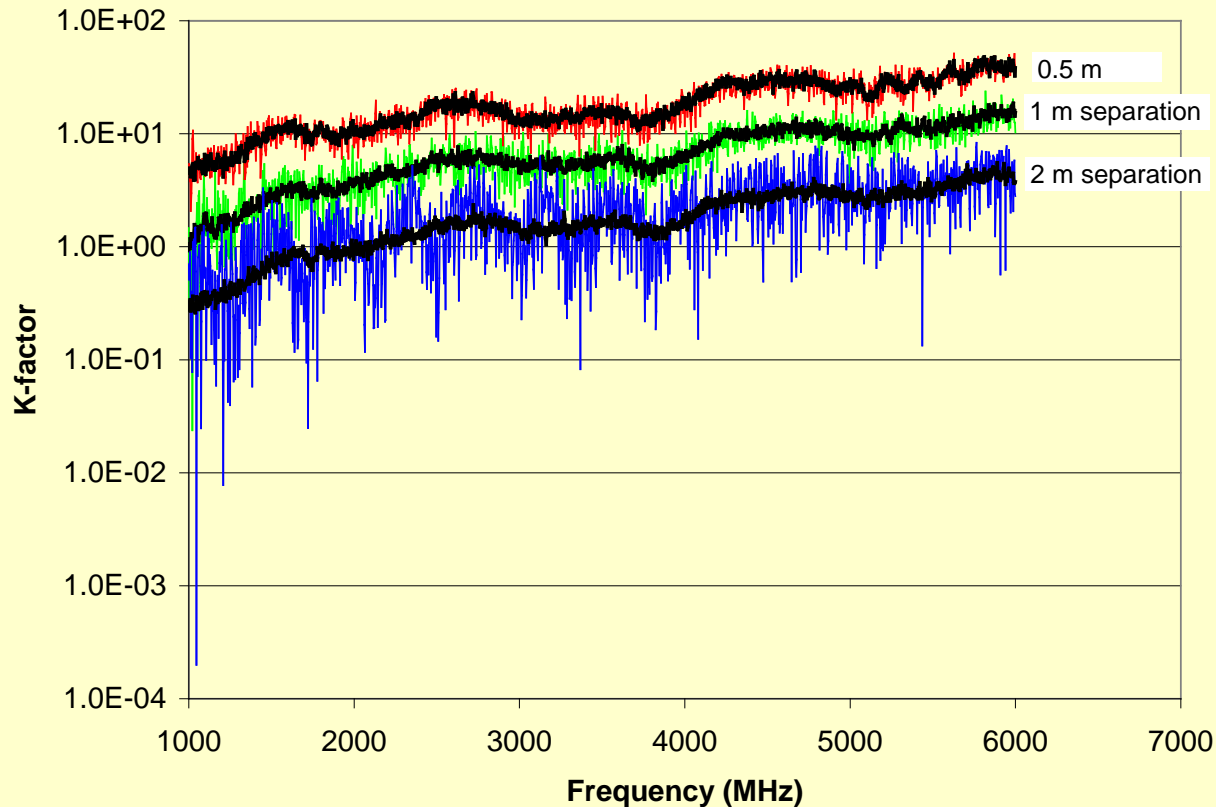
- We see that  $K$  is proportional to  $D$ . This suggests that if an antenna with a well defined antenna pattern is used, it can be rotated with respect to the DUT, thereby changing the  $K$ -factor.
- Secondly, we see that if  $r$  is large,  $K$  is small (approaching a Rayleigh environment); if  $r$  is small,  $K$  is large. This suggests that if the separation distance between the antenna and the DUT is varied, then the  $K$ -factor can also be changed to some desired value.
- Next we see that by varying  $Q$  (the chamber quality factor), the  $K$ -factor can be changed to some desired value. The  $Q$  of the chamber can easily be varied by simply loading the chamber with lossy materials.

Also, if  $K$  becomes small, the distribution approaches Rayleigh.

Thus, varying all these different quantities in a judicious manner can result in controllable  $K$ -factor over a reasonably large range.



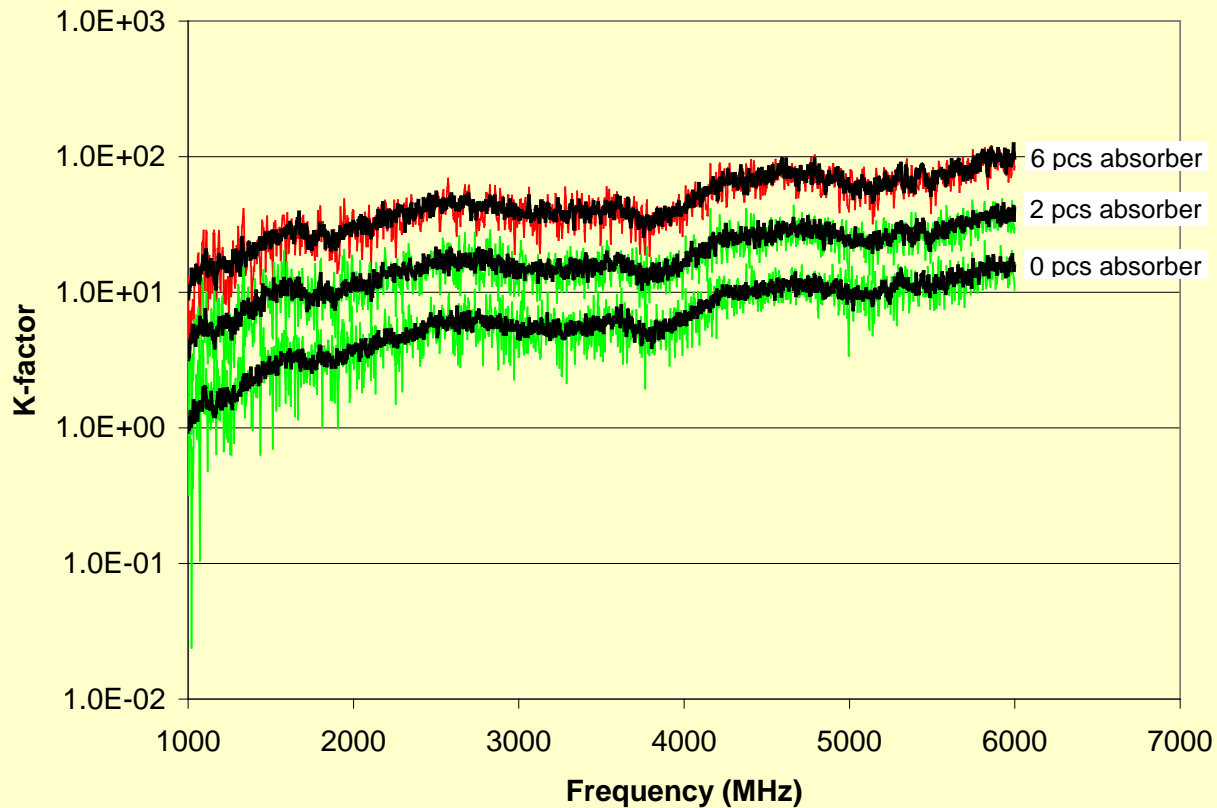
# Measured K-factor for Different Antenna Separation



Each set of curves represents a different distance of separation. The thick black curve running over each data set represents the  $K$ -factor obtained by using  $d$  determined in the anechoic chamber.

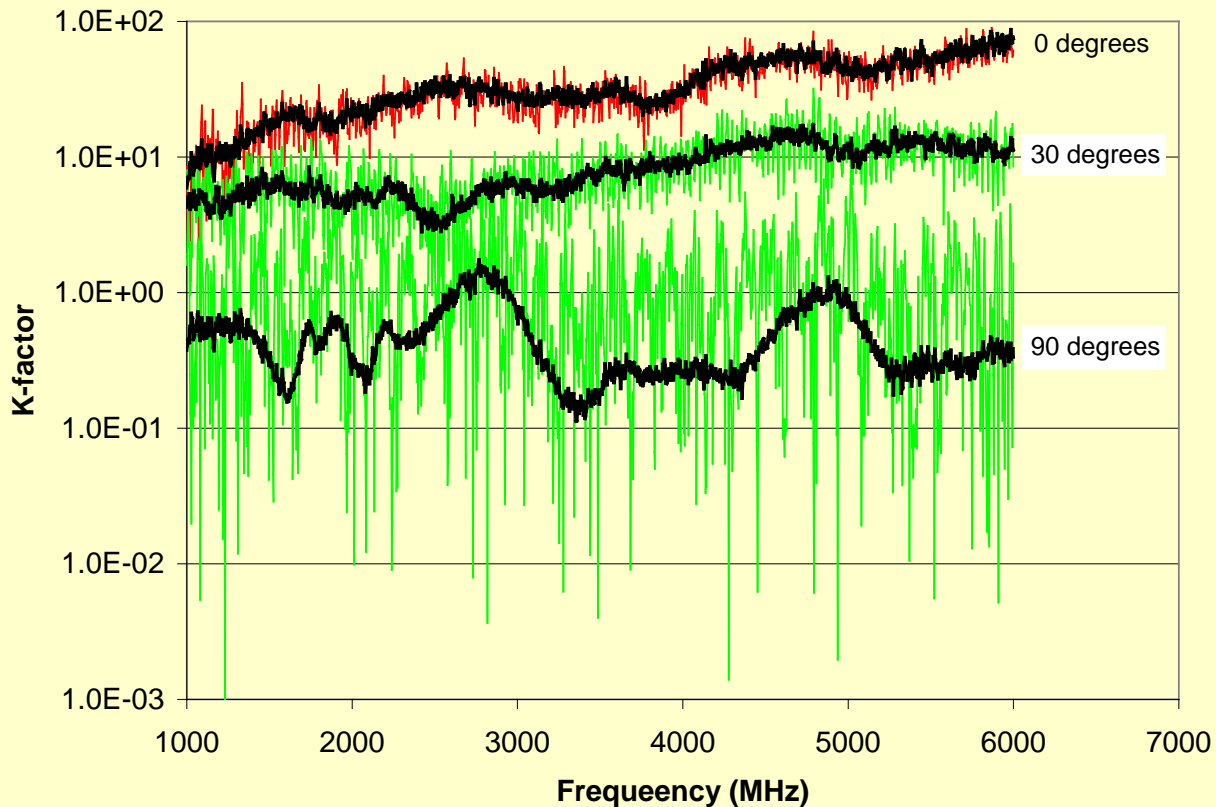


# Measured K-factor for Chamber Loading



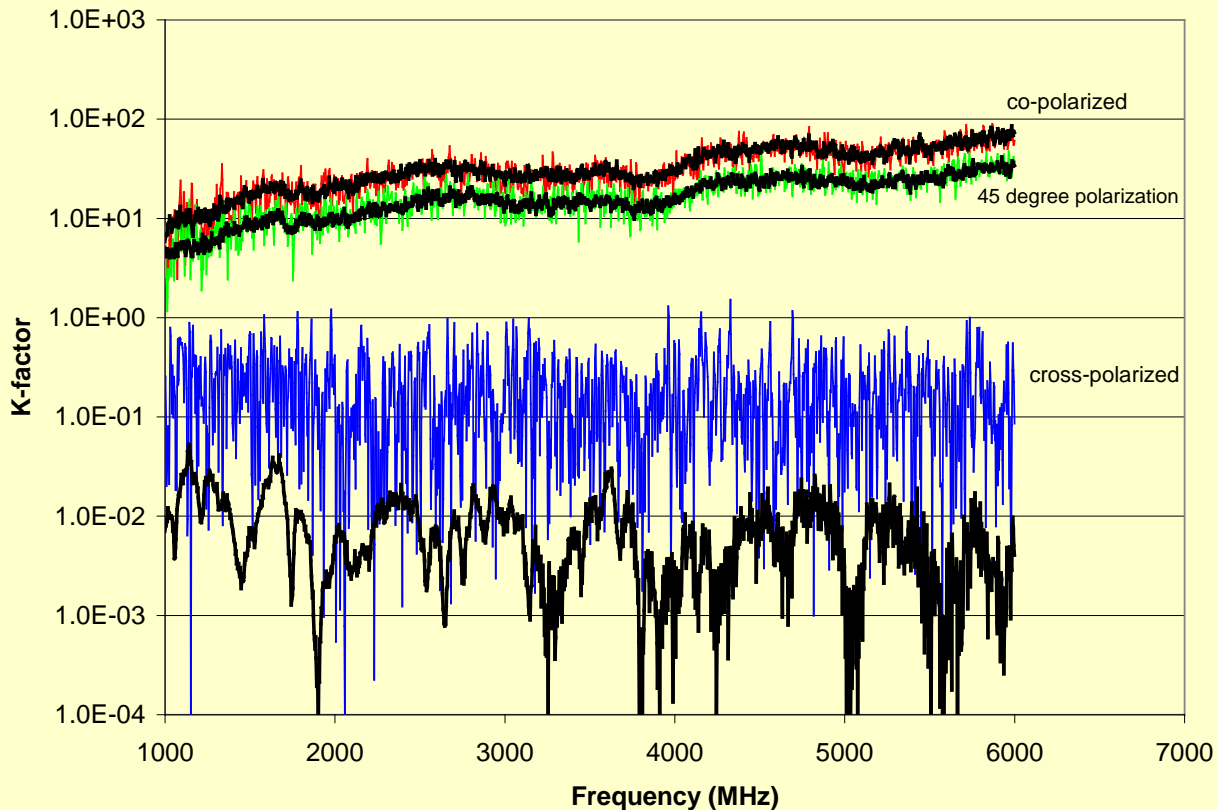
The thick black curve running over each data set represents the  $K$ -factor obtained by using  $d$  determined in the anechoic chamber.

# Measured K-factor for Different Antenna Rotations



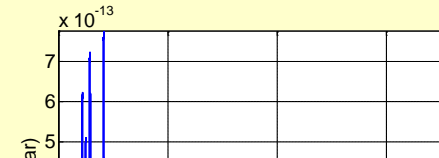
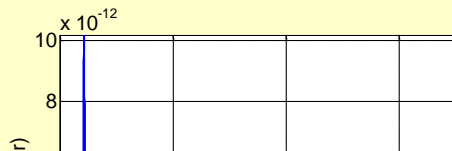
The thick black curve running over each data set represents the  $K$ -factor obtained by using  $d$  determined in the anechoic chamber. Each data set was taken at 1 m separation and with 4 pieces of absorber in the chamber.

# Measured K-factor for Different Antenna Polarizations

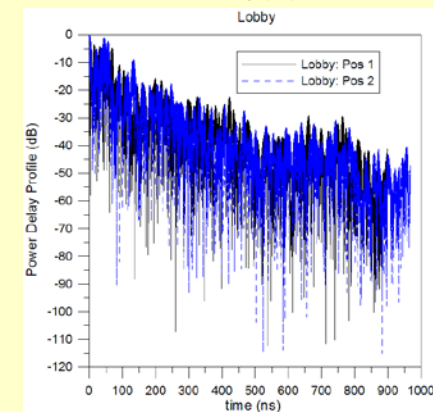
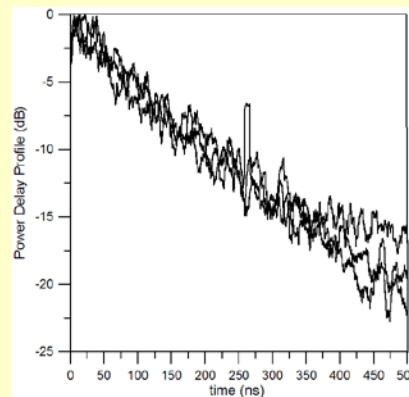
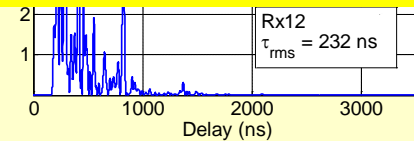
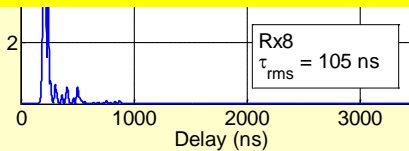
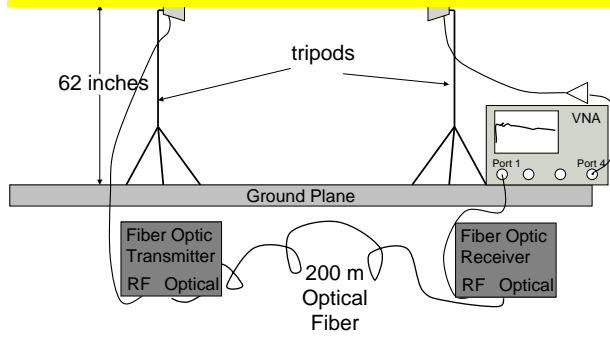


The thick black curve running over each data set represents the  $K$ -factor obtained by using  $d$  determined in the anechoic chamber. Each data set was taken at 1 m separation and with 4 pieces of absorber in the chamber.

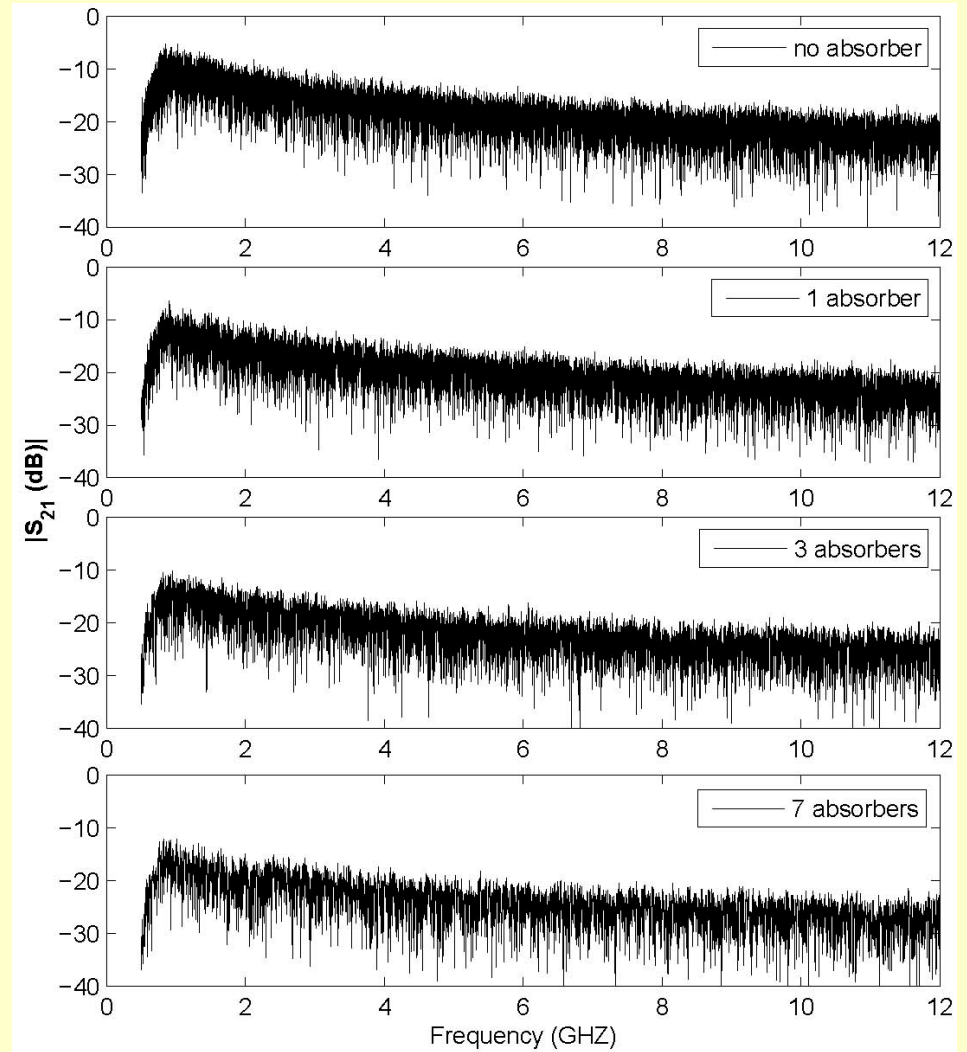
# Simulating Propagation Environments with Different Impulse Responses and rms Delay Spreads



Can we simulate these different PDP(t) in a reverberation chamber?



# $S_{21}$ Measurements: Loading the Chamber



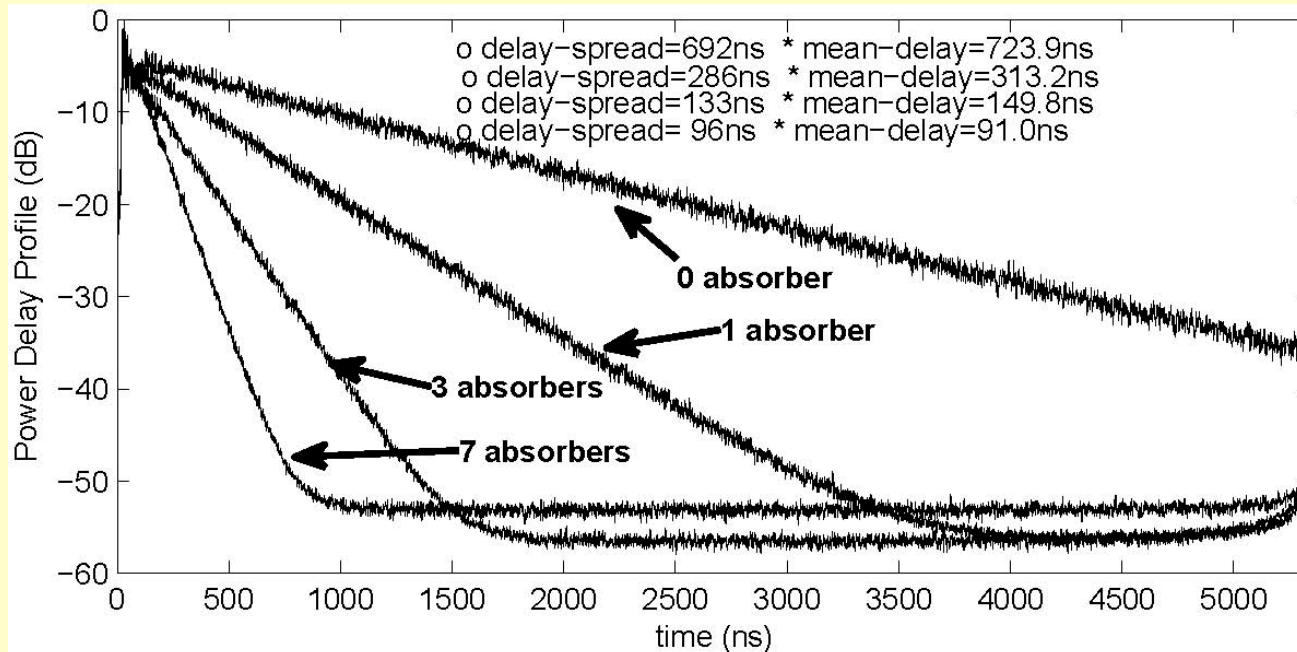
# Impulse Responses and Power Delay Profiles

Power Delay Profile:

$$PDP(\tau) = \langle |h(t)|^2 \rangle$$

where  $h(t)$  is the Fourier transform of  $S_{21}(\omega)$

## Loading the Chamber





# rms Delay Spreads

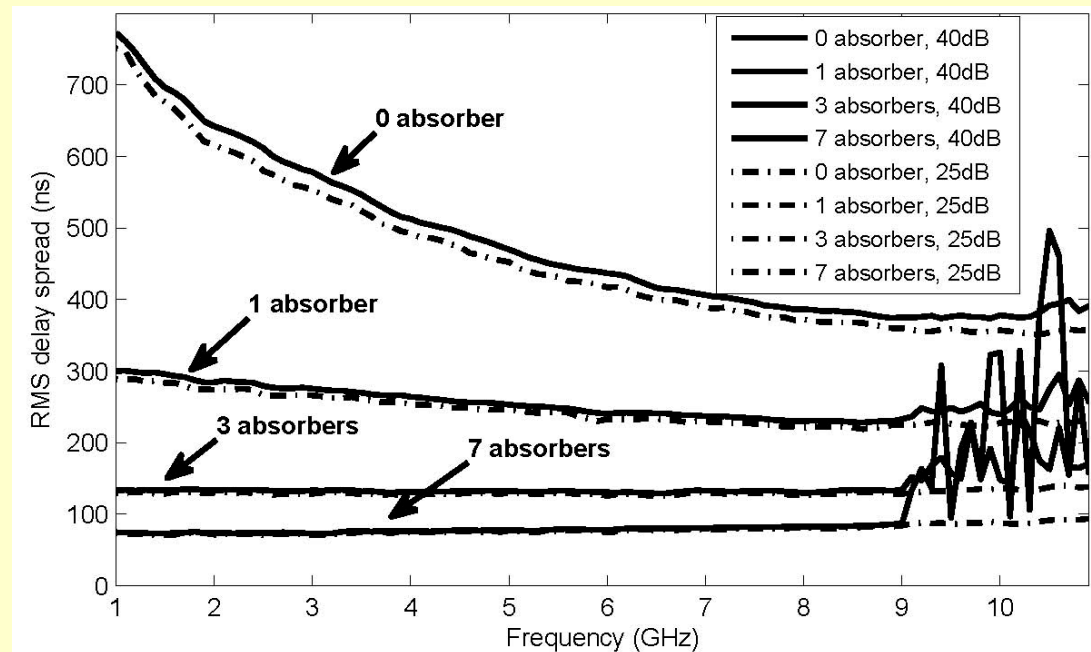
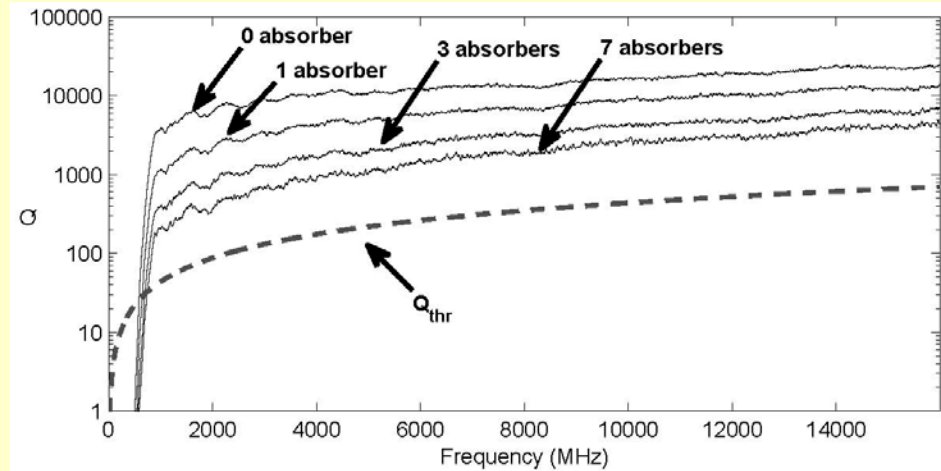
One characteristic of the PDP that has been shown to be particularly important in wireless systems that use digital modulation is the *rms* delay spread of the PDP:

$$\tau_{rms} = \frac{\int_0^{\infty} (t - \tau_o)^2 P(t) dt}{\int_0^{\infty} P(t) dt}$$

where  $\tau_o$  is the mean delay of the propagation channel, given by

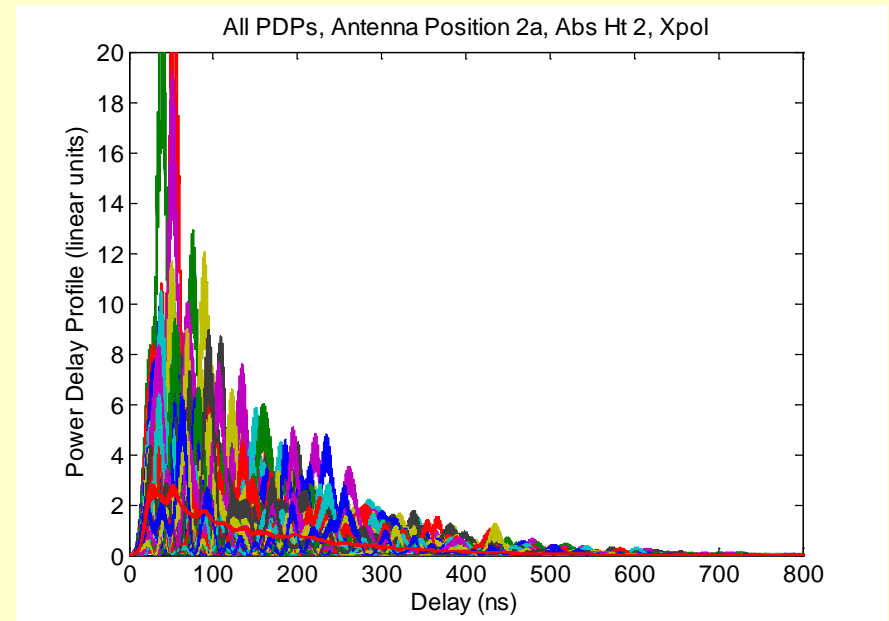
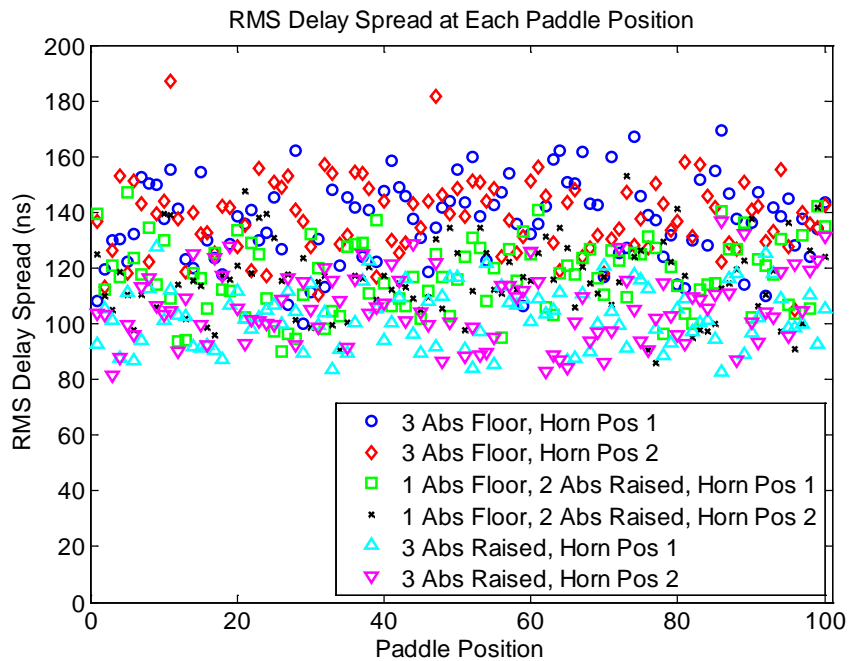
$$\tau_o = \frac{\int_0^{\infty} tP(t) dt}{\int_0^{\infty} P(t) dt}$$

# Impulse Responses and rms Delay Spreads (200 MHz bandpass filter on $S_{21}$ data)





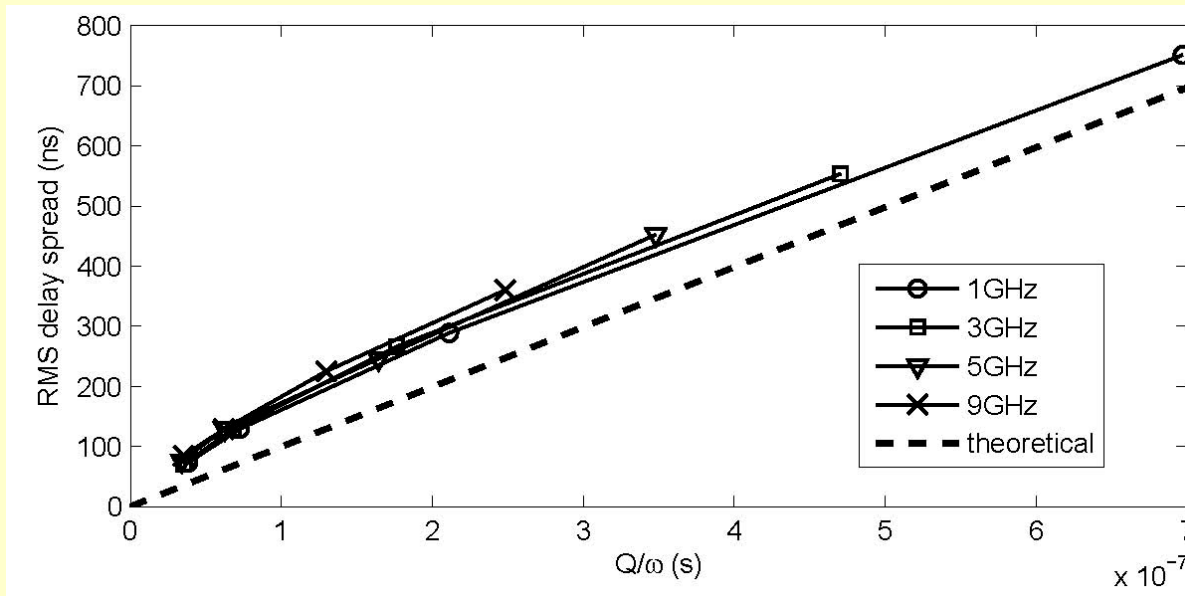
# Instantaneous Results Can Vary



## rms Delay Spreads from Q measurements

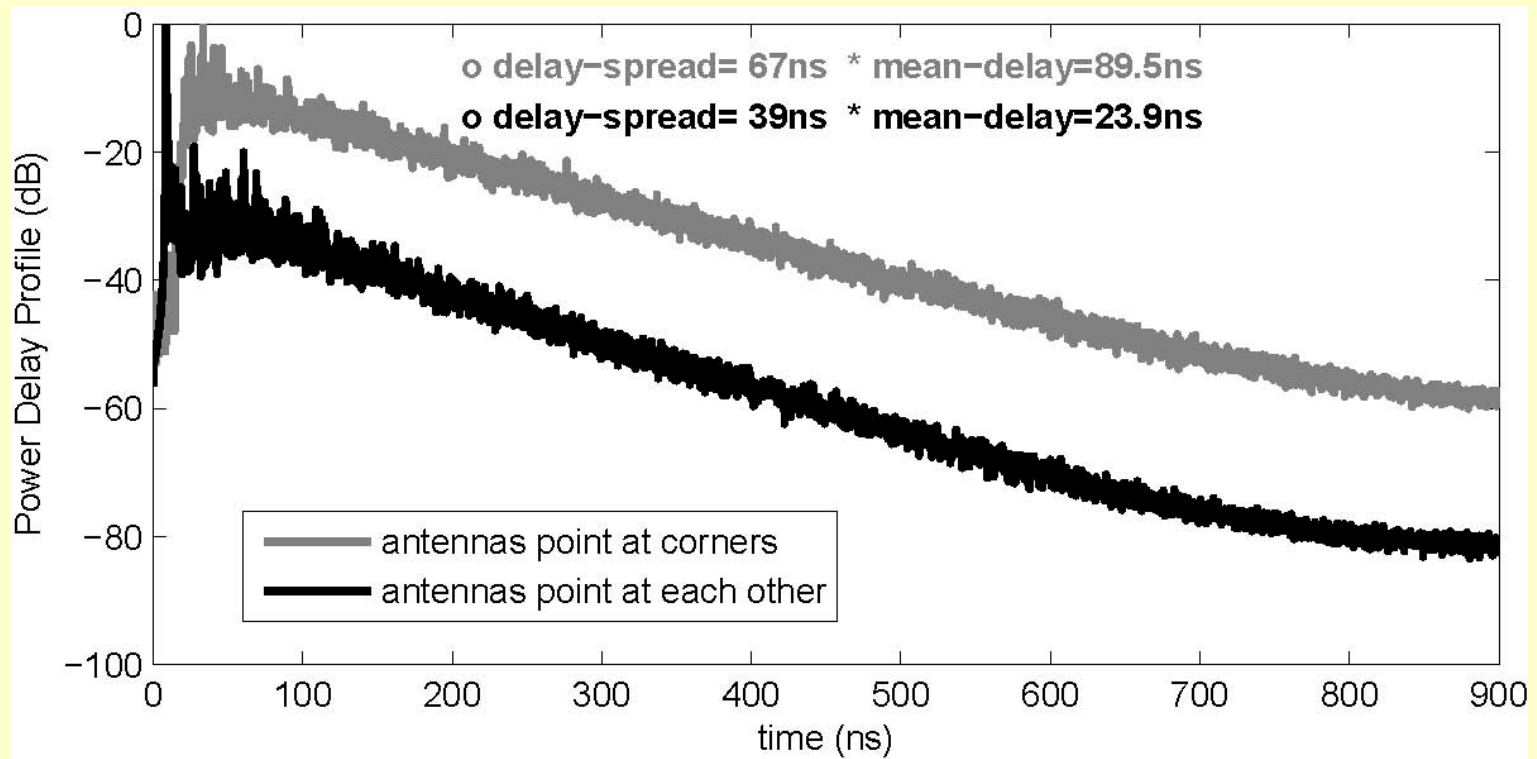
$$\tau_{rms} = \frac{Q}{\omega} \sqrt{\frac{2\alpha \ln(\alpha) - \ln^2(\alpha)\varepsilon - 2\alpha + 2}{(1-\alpha) + K} - \frac{(\alpha \ln(\alpha) + 1 - \alpha)^2}{((1-\alpha) + K)^2}}$$

where K is the K-factor and  $\alpha$  threshold.



Thus, once we have  $Q$ , we can estimate  $\tau_{rms}$

# Impulse Responses and rms Delay Spreads for Different Ricean K-factors



# Testing Wireless Devices in Realistic Environments

# Difficult Radio Environments



Apartment Building



Oil Refinery



Office Corridor



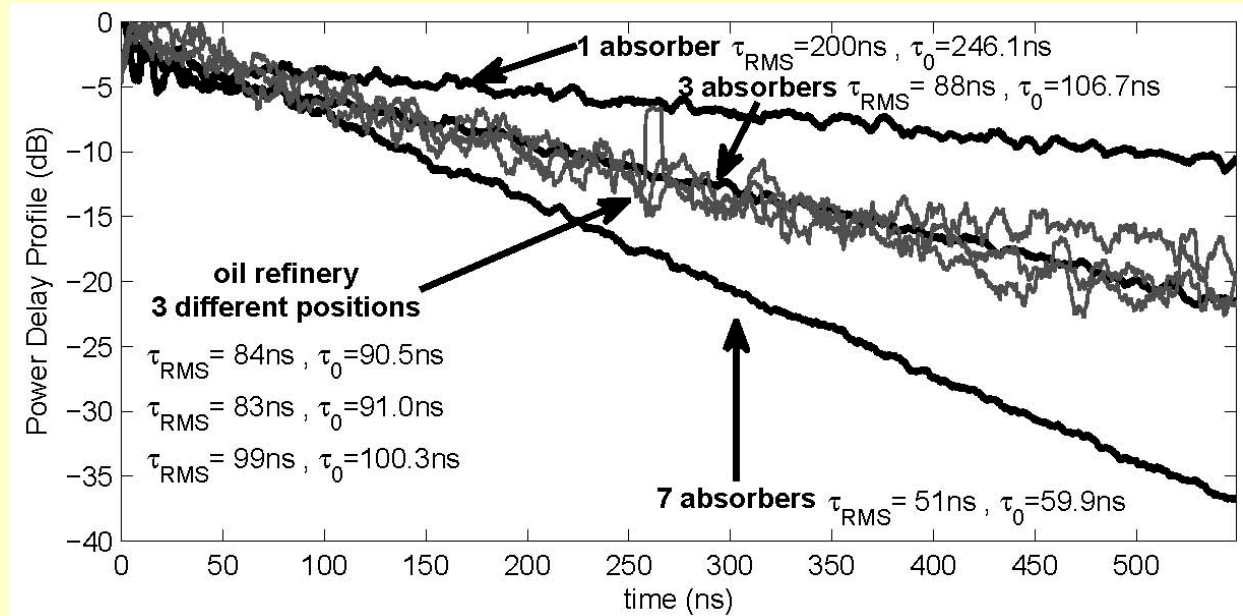
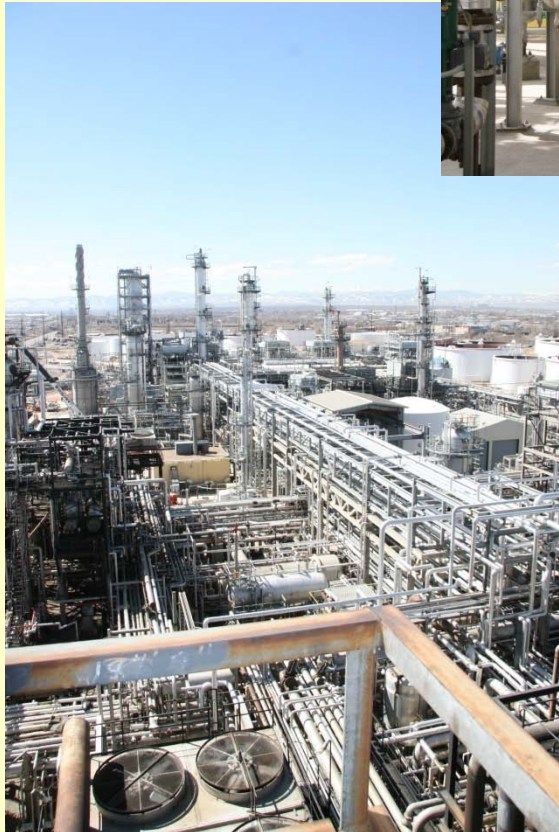
Subterranean Tunnels

NIST is measuring signal penetration and multipath in representative emergency response environments to provide data for improved wireless device design, standards development, and better channel models.

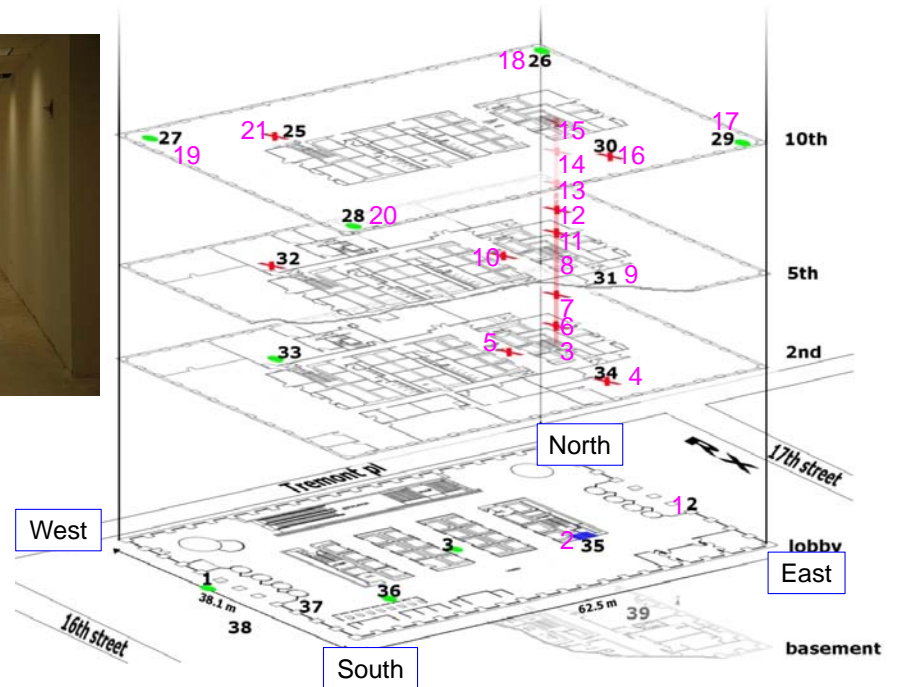


# How Well Can we Simulate a Real Environment?

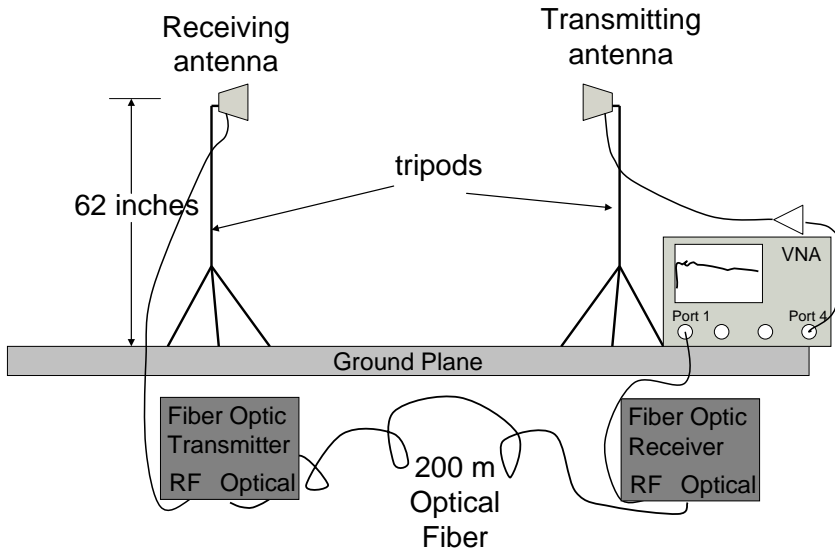
Power Delay Profile in an oil refinery.



# Example: Denver Highrise Tests



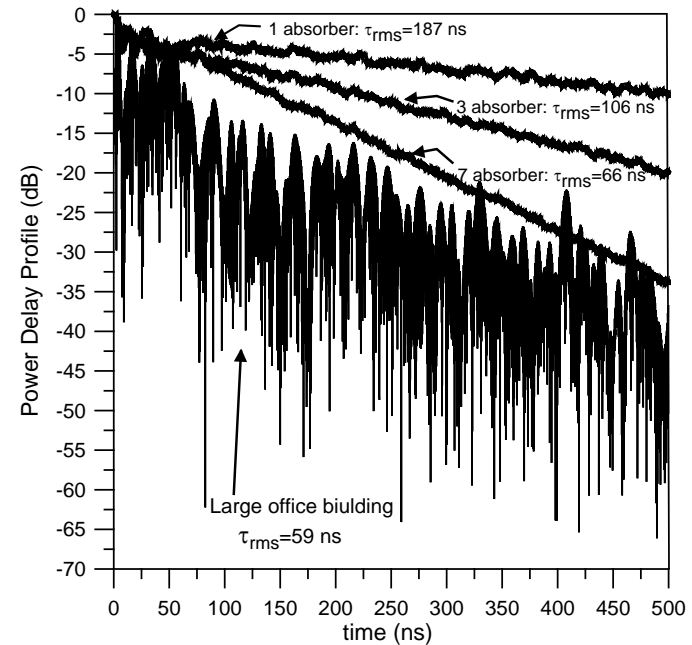
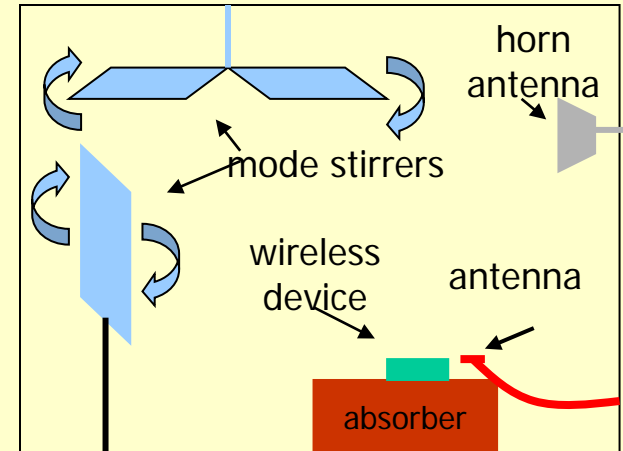
VNA measurement test locations are in pink



# Replicate Environment in Reverb Chamber

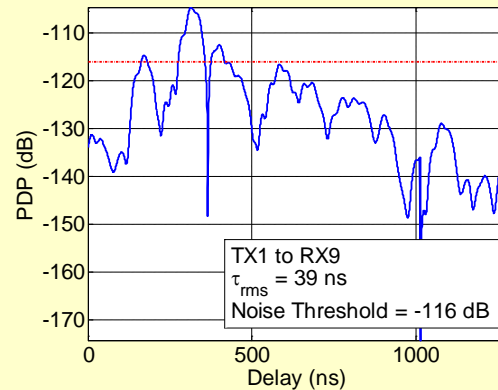
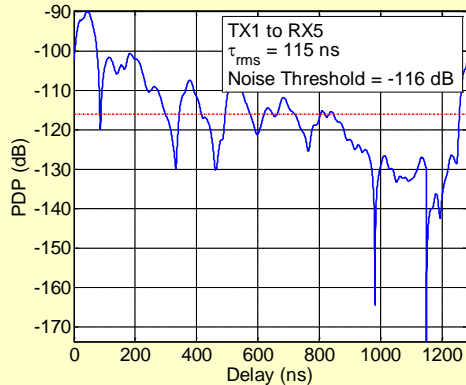


Reverberation chamber with absorbing material and phantom head

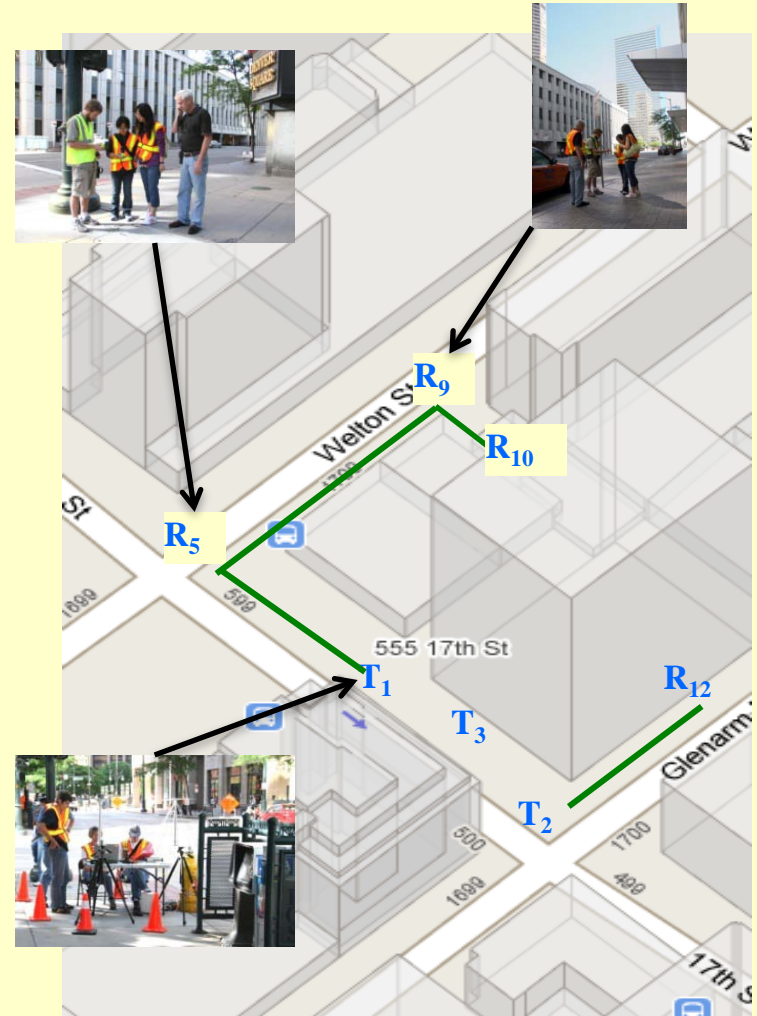




# Adding More Realism to the PDP: Urban Canyon

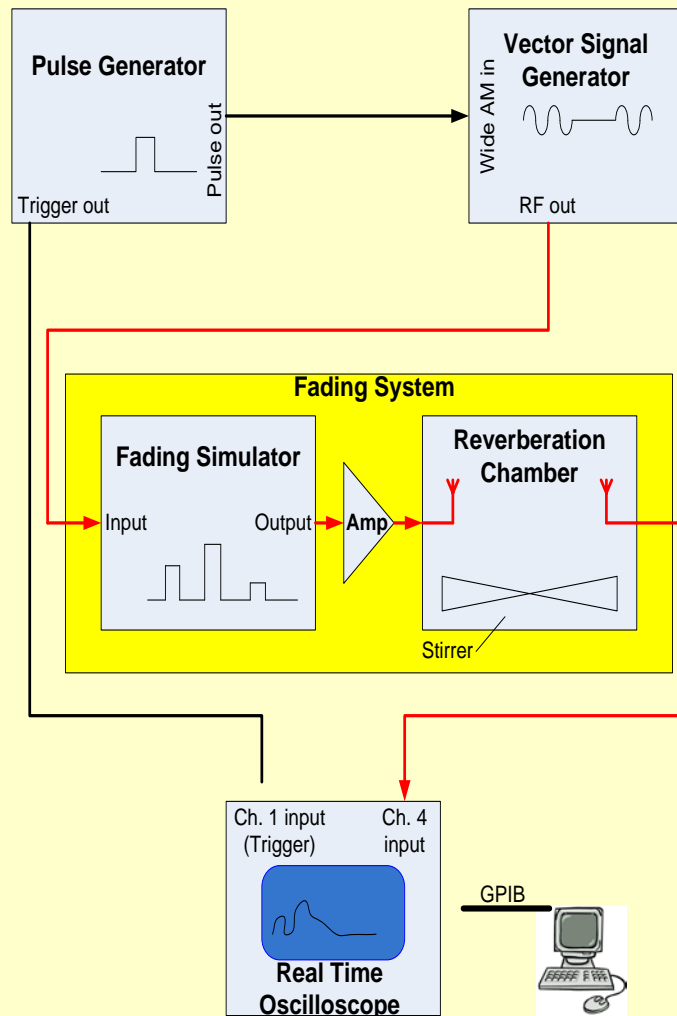


- Mean of 27 NLOS measurements made in Denver urban canyon.
- Channel characterization and wireless device measurements.

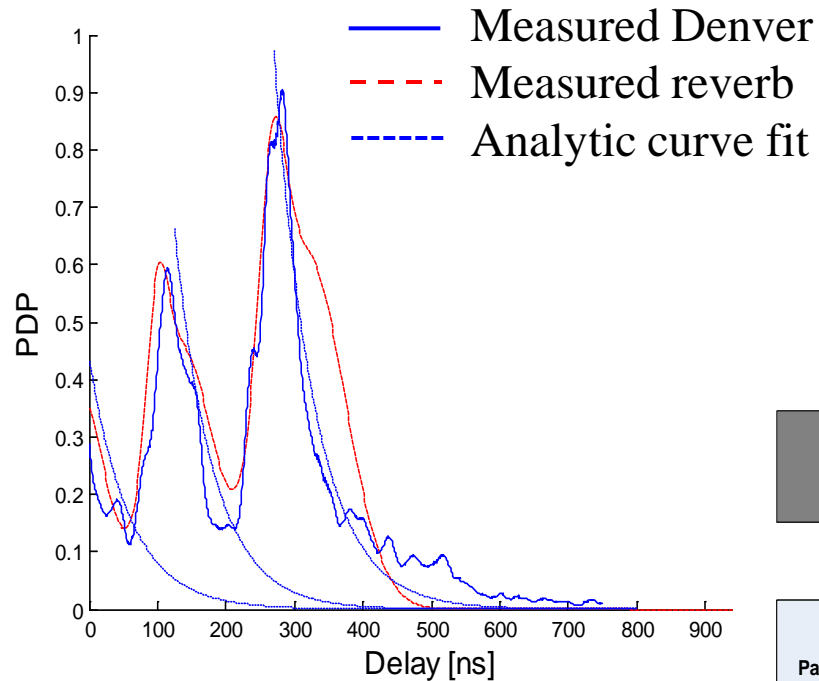


# Combine Fading Simulator with Reverb Chamber

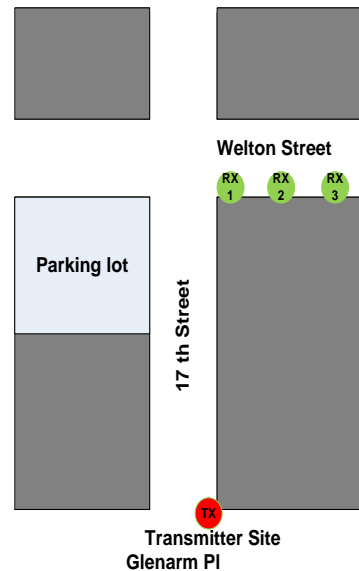
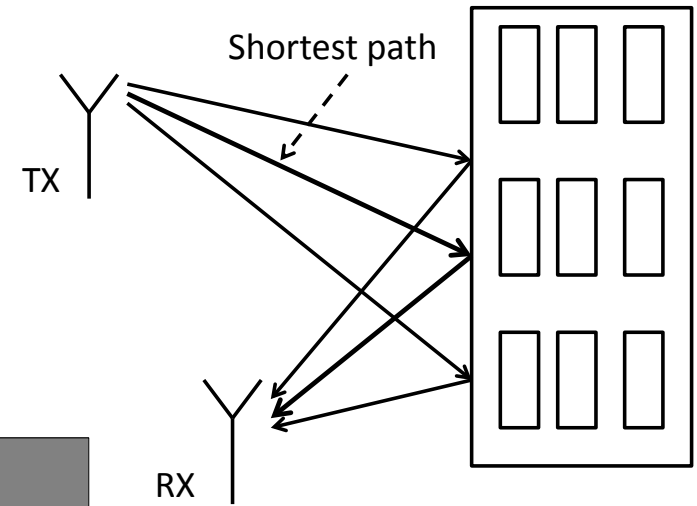
- Pulse generator used to amplitude modulate RF, creates short-duration pulse
- Fading simulator replicates delayed, scaled versions
- Reverb chamber introduces exponential profile



# Clustering of Multipath is Common in Urban Environments



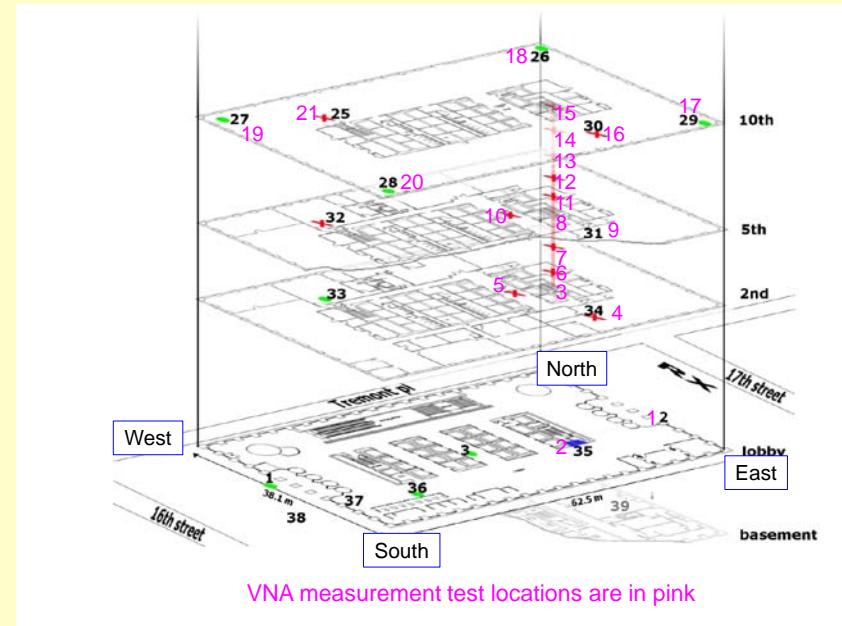
Excite reverberation chamber with channel emulator to create multipath clusters



Clusters of exponential distributions off of buildings

# NIST's Goal: Lab-Based Test Methods

Location and Notes	Test Point	VNA Loss Data (dB)	Path Loss @700 MHz (dB)	RMS Delay Spread @700 MHz (ns)
<b>Republic</b>	1	7.23	68.6149	44.99
Notes:	2	27.06	88.4449	39.52
- System 1	3	38.15	99.5349	52.30
repeater at test point 2.	4	37.60	98.9849	133.41
	5	37.18	98.5649	81.25
	6	42.26	103.6449	102.78
	7	46.04	107.4249	138.29
	8	44.88	106.2649	104.69
	9	48.30	109.6849	376.10
	10	45.34	106.7249	338.17
	11	50.25	111.6349	167.91
	12	50.48	111.8649	231.57
	13	50.98	112.3649	209.07
	14	51.82	113.2049	192.25
	15	49.60	110.9849	240.20
	16	44.64	106.0249	377.45
	17	29.28	90.6649	296.87
	18	30.45	91.8349	161.75
	19	42.24	103.6249	429.90
	20	39.30	100.6849	333.25
	21	47.07	108.4549	453.47



Replicate field-tested wireless device performance in the reverberation chamber

Used for standardized testing of wireless devices:

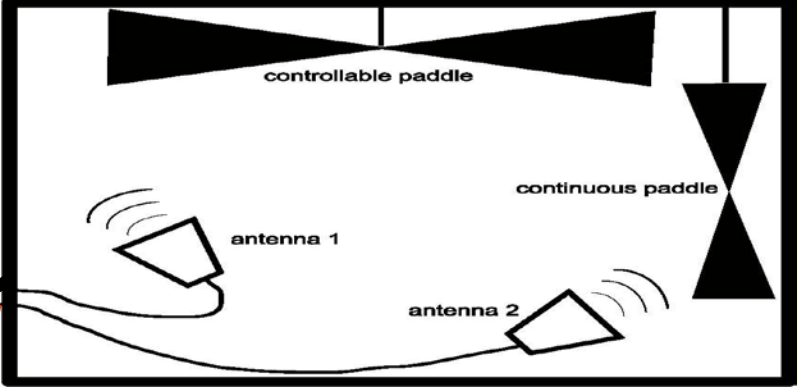
- public-safety community (NFPA)
- wireless sector (CTIA)

# BER Measurements - setup

Agilent 4438C Vector Signal Generator

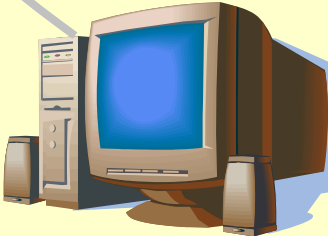


Reverberation chamber



External trigger

GPIB connection  
to control VSG



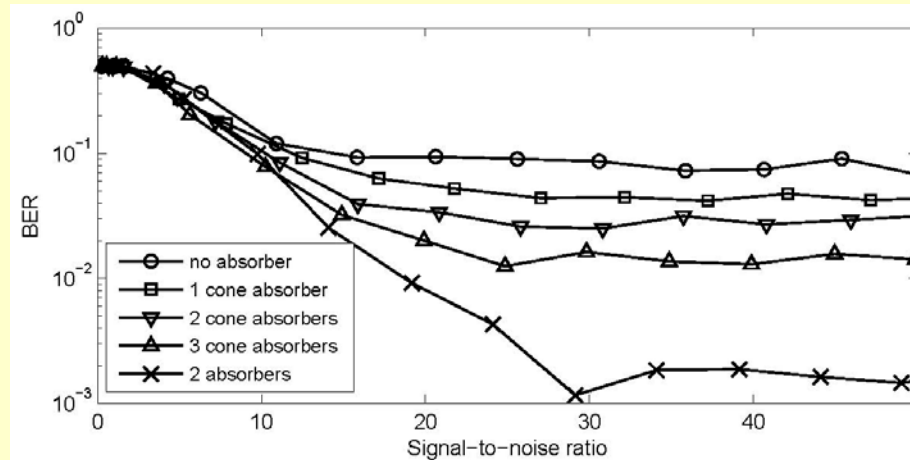
Firewire connection  
to control VSA

Agilent 89600 Vector Signal Analyzer

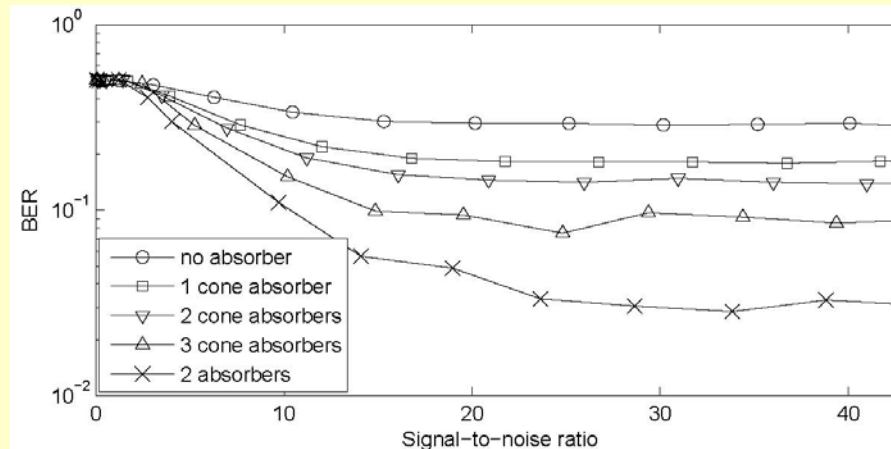


# BER Measurements

BER for a 243 kbps BPSK signal

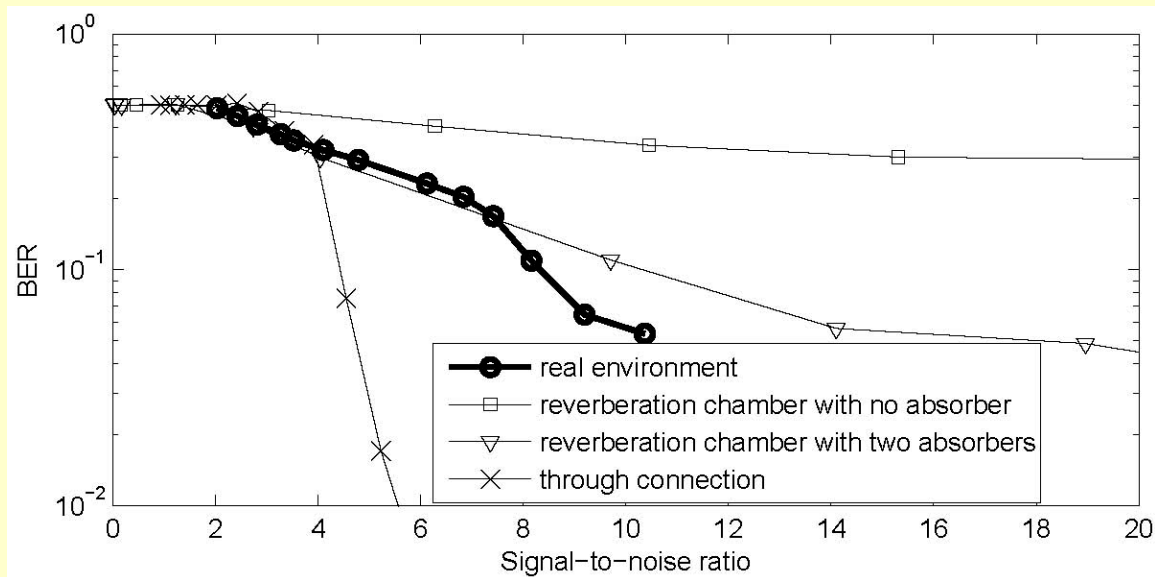


BER for a 786 kbps BPSK signal



# How Well Can we Simulate a Real Environment?

BER measurement in a laboratory.



# Reverberation Chamber Test Environment for MIMO Systems

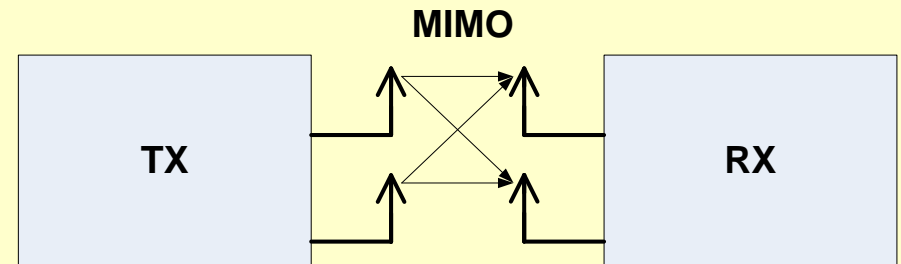
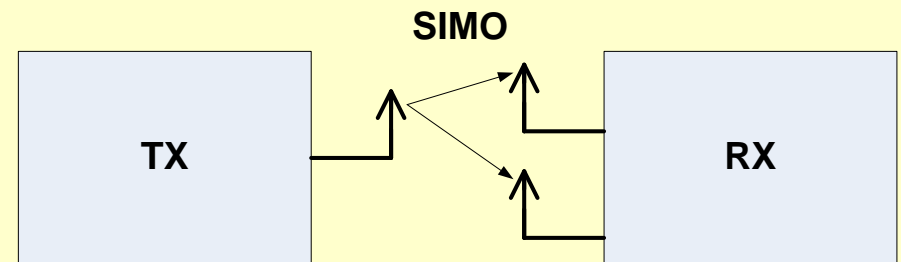
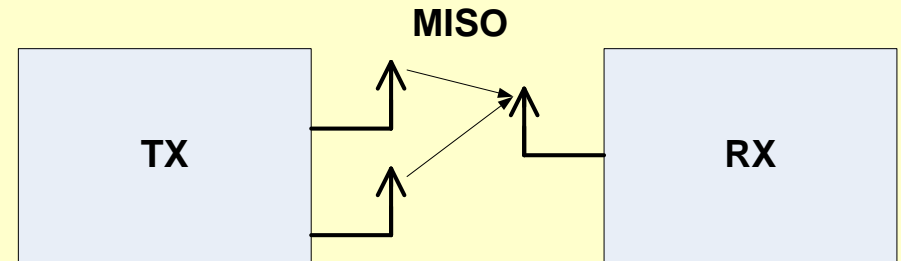
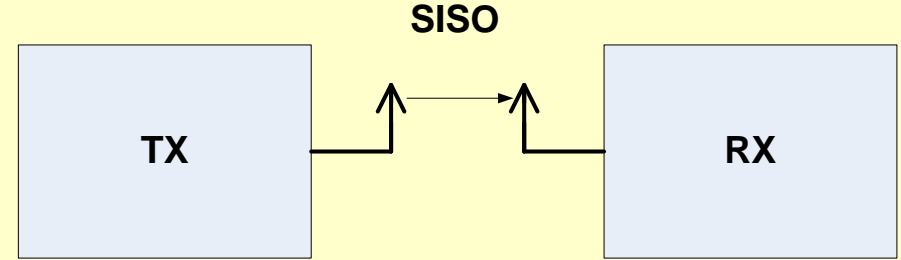


# Motivation

Alternative transmit/receive configurations can improve wireless reception in weak-signal and multipath environments

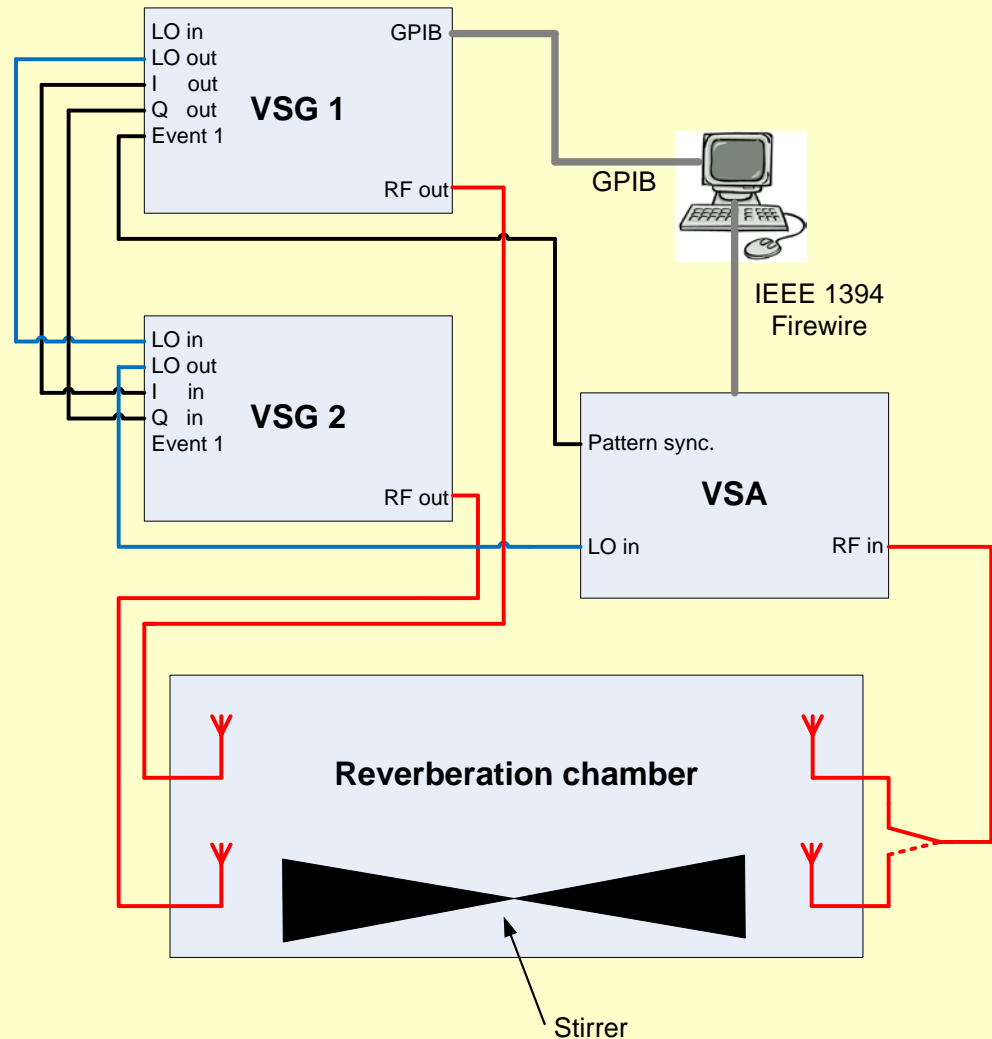
To verify performance of multiple antenna algorithms, testing in a multipath environment is desirable

We discuss methods for implementing such test environments using reverberation chambers



# Measurement Set-up

- Multiple TX simulated using 2 VSGs
- Vector signal analyzer provides channel power and demodulated data
- BPSK modulated signal; random, equal distribution; 2048 bits
- Error correction only to recover constellation after deep fade
- Paddle stepped



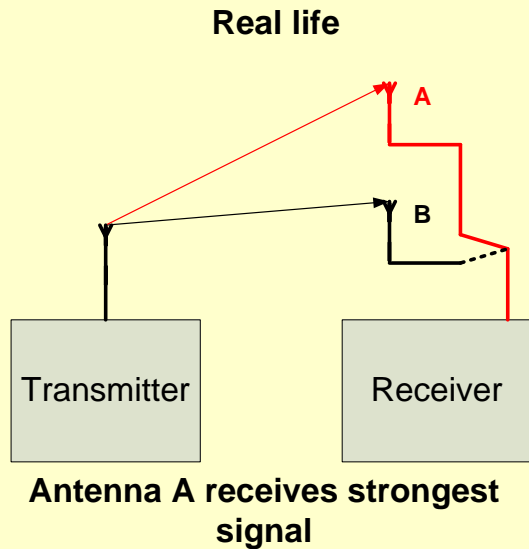
# NIST Chamber Characteristics

- Chamber dimensions:  
4.28m x 3.66m x 2.90m

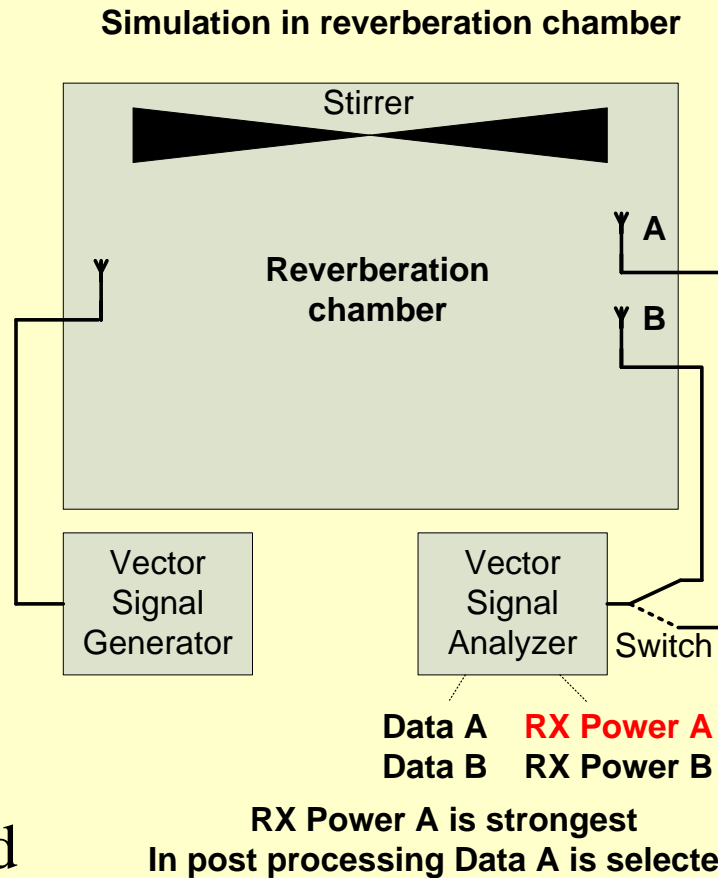
- Two paddles: vertical  
and horizontal

- Table shows Q, RMS  
delay spread, and  
coherence bandwidth  
for various numbers of  
absorbing blocks

Absorber	Q	$\tau_{\text{RMS}}$ [ns]	$\Delta f$ [MHz]
0	47130	3121.99	0.32
1	8505	563.38	1.77
2	3319	220.08	4.54
3	2051	136.01	7.35
4	1479	98.06	10.20
5	1407	93.32	10.71
6	1067	70.66	14.14
7	918	60.82	16.42
8	765	50.71	19.72
9	731	48.48	20.62
10	550	36.49	27.40
11	551	36.55	27.36
12	435	28.83	34.68
13	399	26.47	37.77
14	369	24.48	40.84
15	340	22.57	44.30
16	332	22.03	45.38



## SIMO

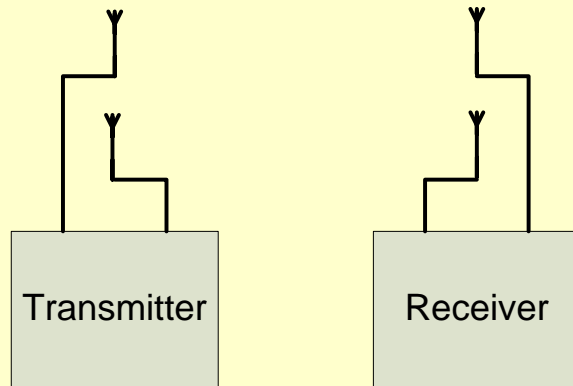


- Also called Diversity
- Power meter monitors received signal strength
- Strongest signal demodulated by receiver

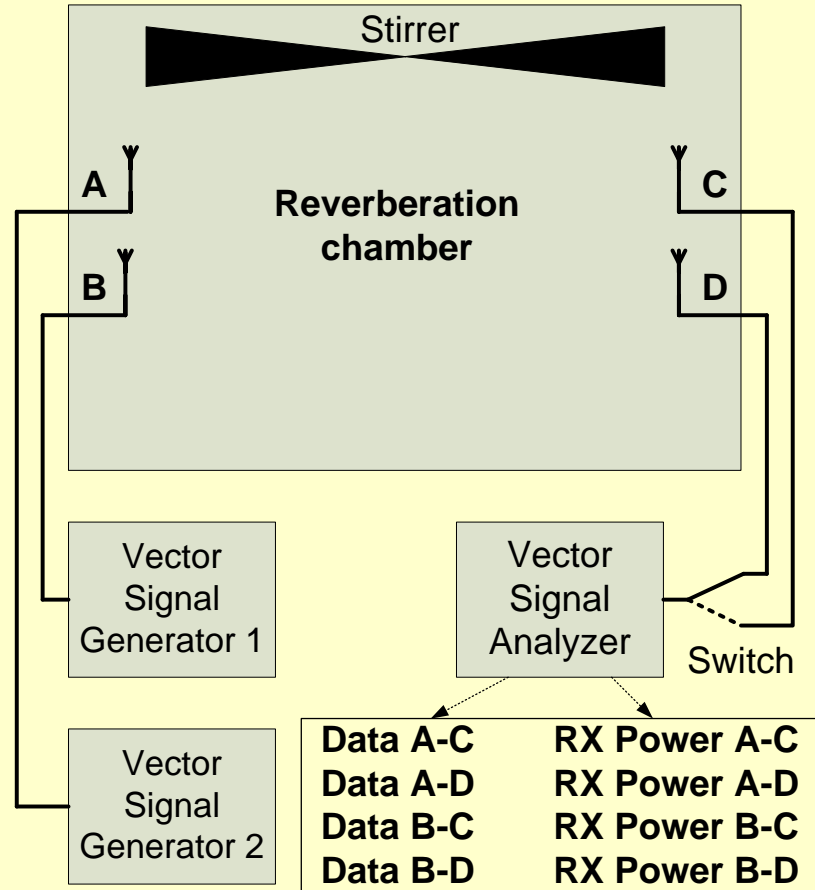
- VSA provides channel power
- Data from strongest signal chosen in post processing

# MIMO

Real life



Simulation in reverberation chamber



## Various schemes:

- **Precoding** (like beamforming)
- **Spatial multiplexing** (data broken into multiple streams, TX on uncorrelated channels)
- **Diversity coding** (identical data streams TX using orthogonal codes. RX decides which one to use)

- **MISO => MIMO** using post processing

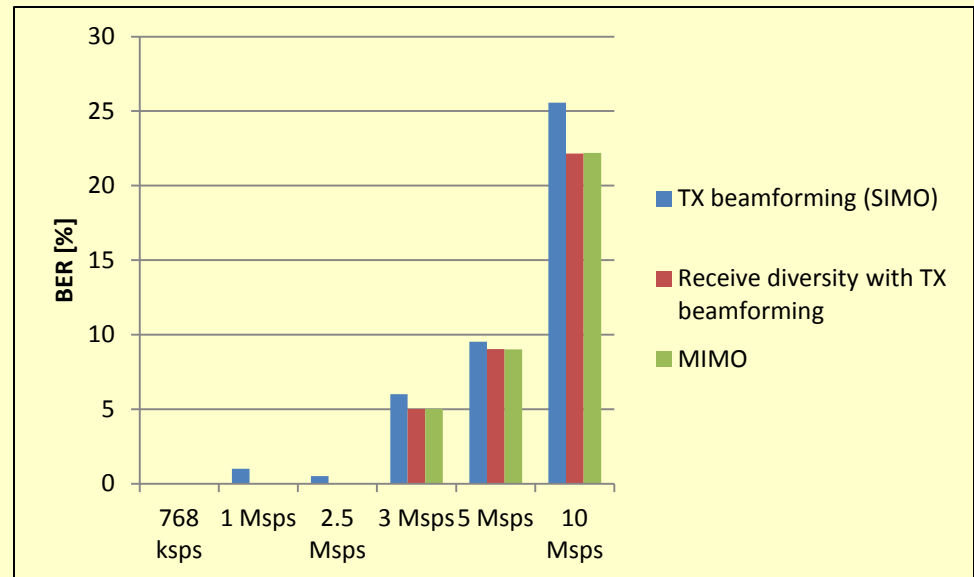
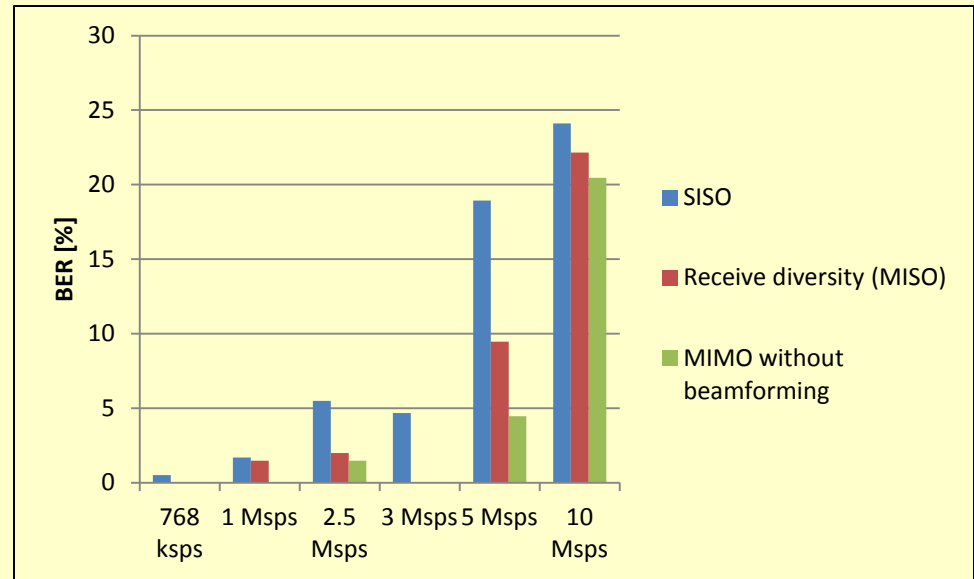
# Measured Results: Various Data Rates

- Best performance:  
RX diversity with TX beamforming  
and MIMO
- Huge increase in BER for high data  
rates may be affected by coherence  
BW of chamber

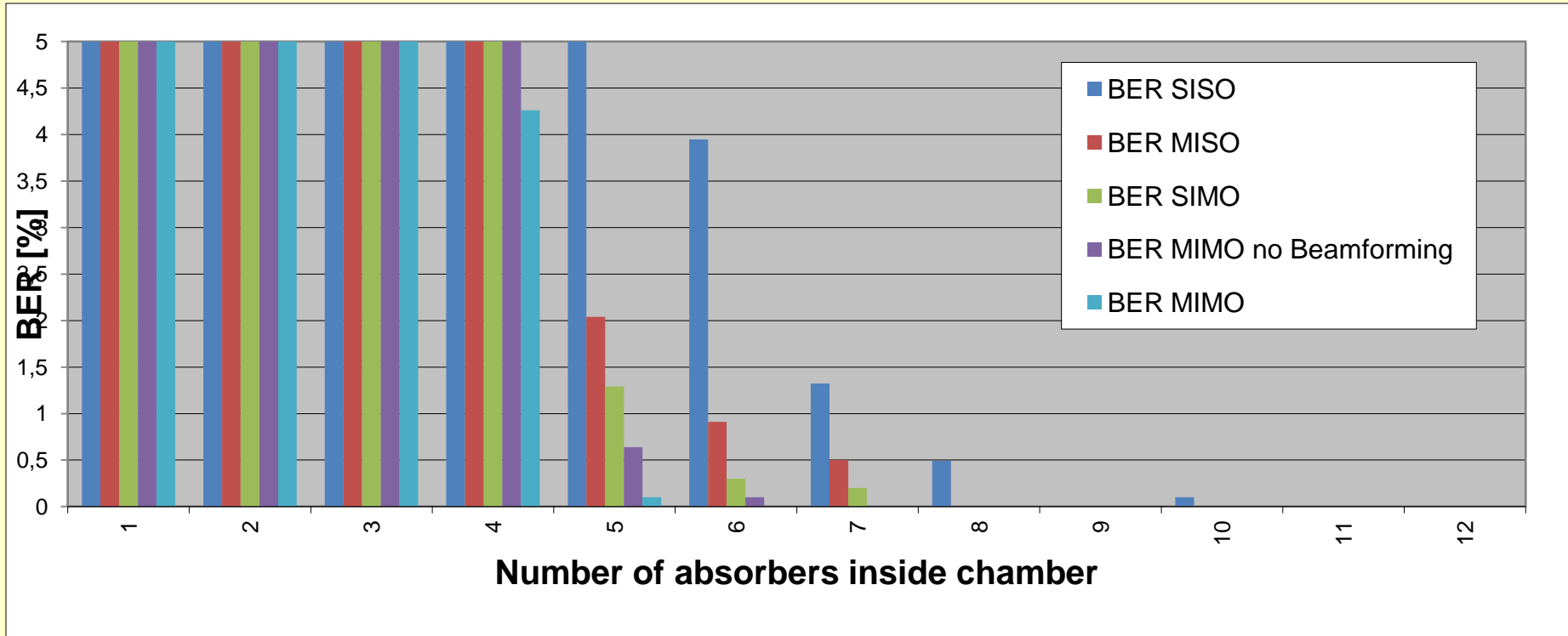
Frequency = 2.4 GHz

$P_{\text{out}} = -50$  dBm

BPSK modulated signal



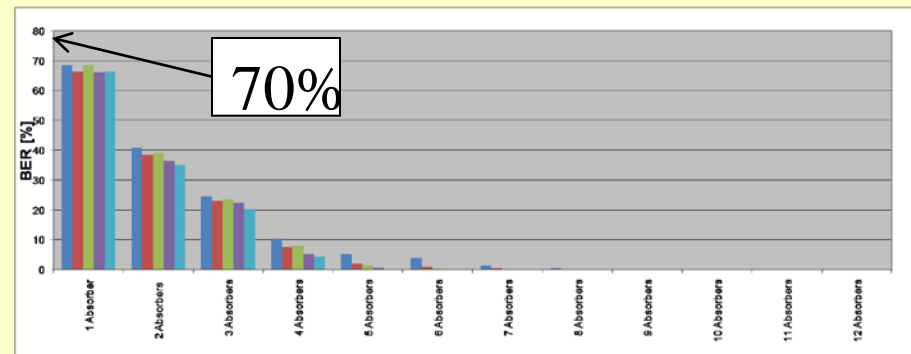
# Number of Absorbers



Frequency = 2.4 GHz

$P_{out} = -50$  dBm

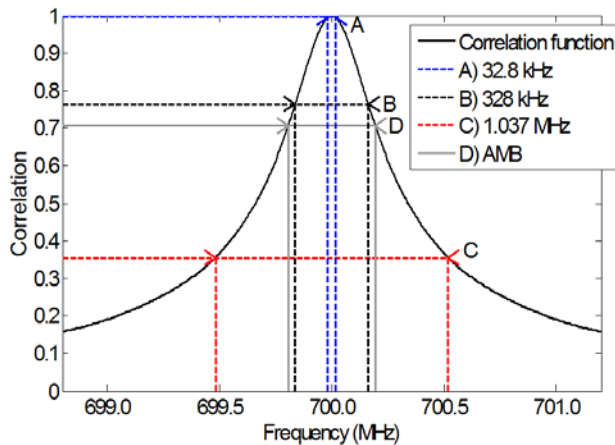
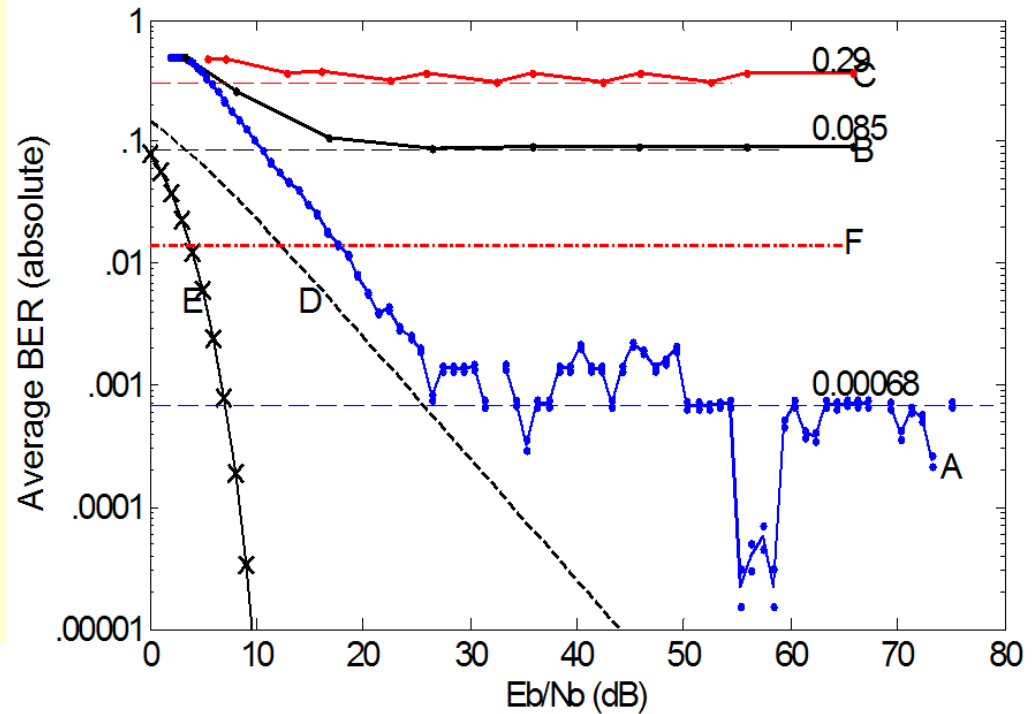
BPSK modulated signal, 768 ksps



# Modulated-Signal, BER Measurements

BER as a function of received power: BER increases for

- lower power levels
- wide modulation bandwidths

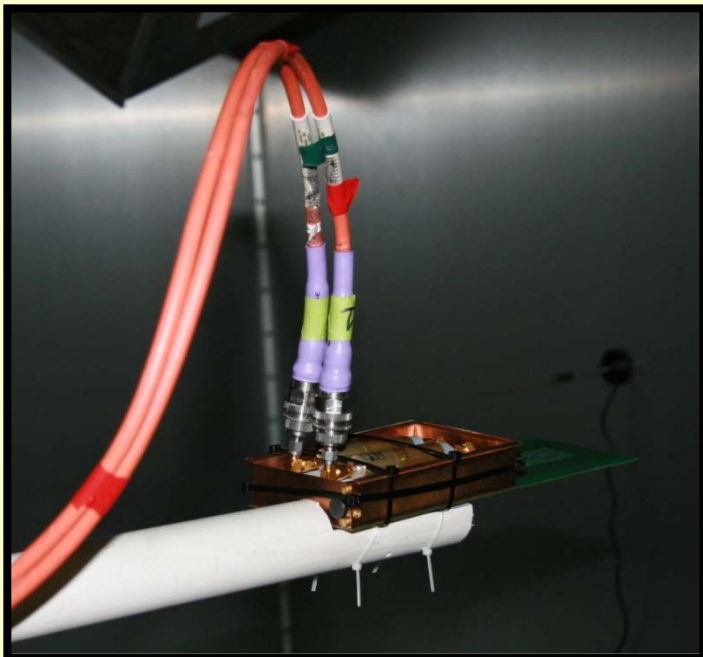


Coherence bandwidth of chamber interacts with signal bandwidth

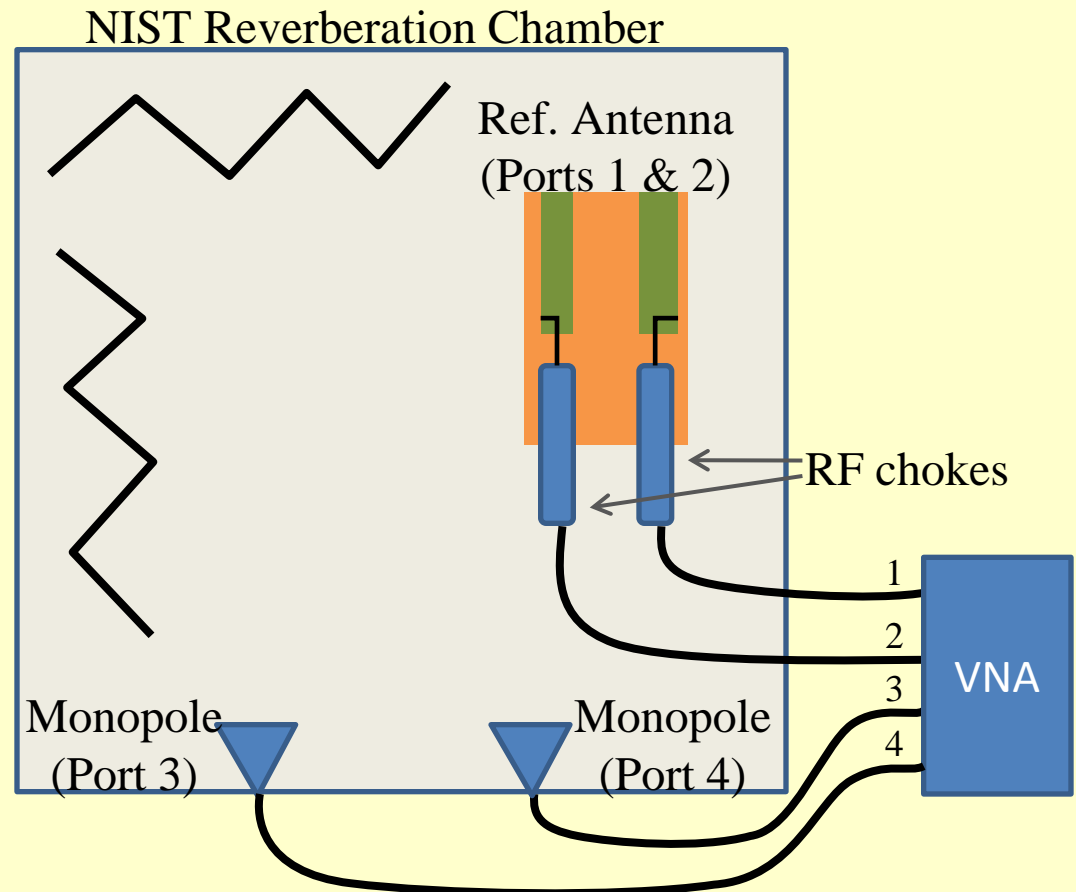


# MIMO Antenna Testing

CTIA “reference antennas” developed to ensure test chamber’s ability to distinguish “good”, “nominal”, and “bad antenna performance

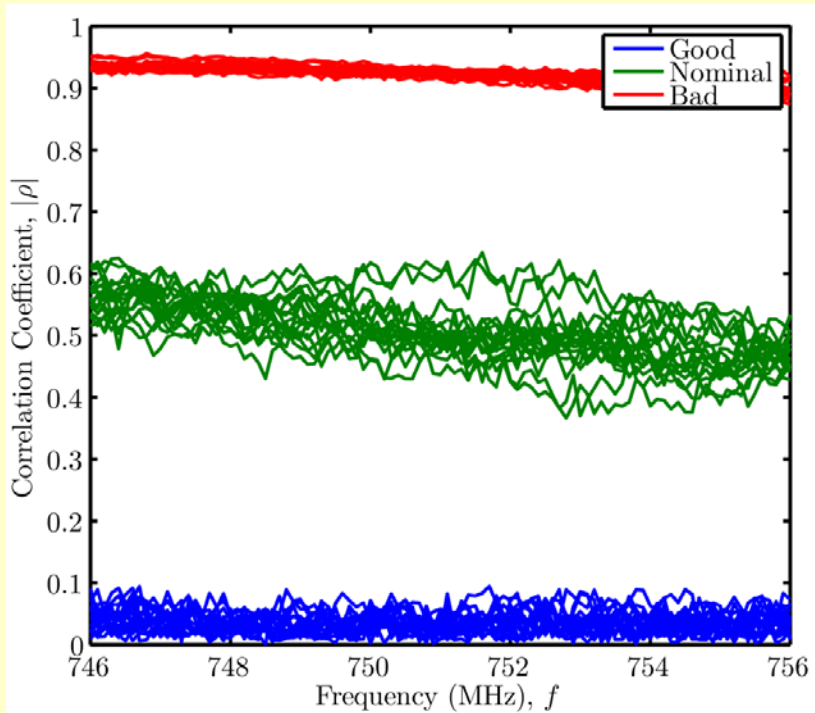


CTIA Antennas

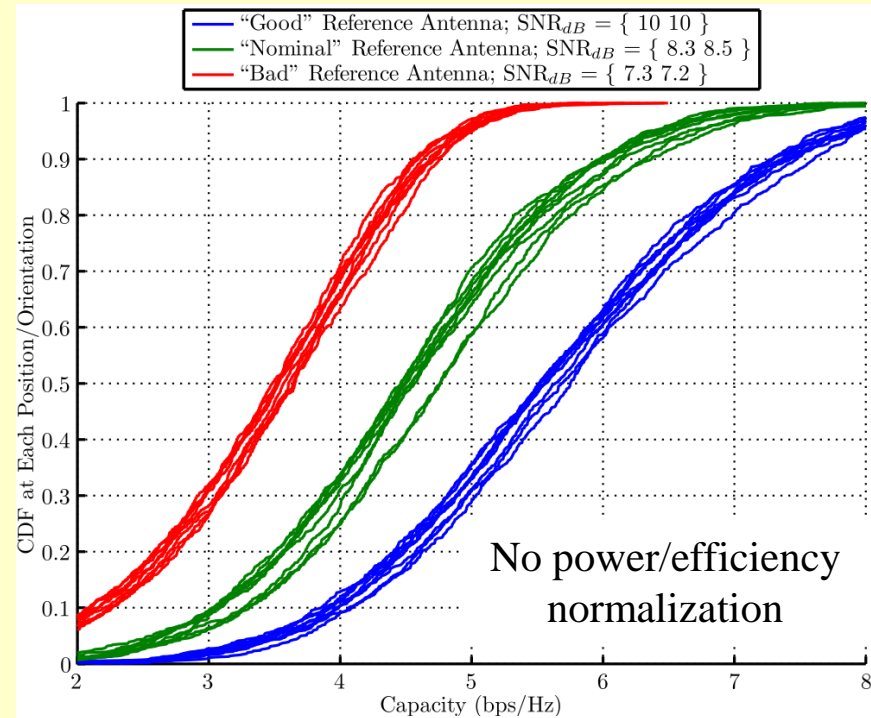


Measurement Set Up

# MIMO Antenna Correlation and Capacity



Correlation Coefficient Magnitudes for Different Positions/Orientations



Median capacity at 50<sup>th</sup> Percentile (bps/Hz):  
{ 3.5, 4.6, 5.6 }

- Capacity: Provides upper bound on throughput
- Distinction between antennas due to inclusion of antenna efficiencies.

# TRP: Machine-to-Machine Applications

## M2M: Automated wireless

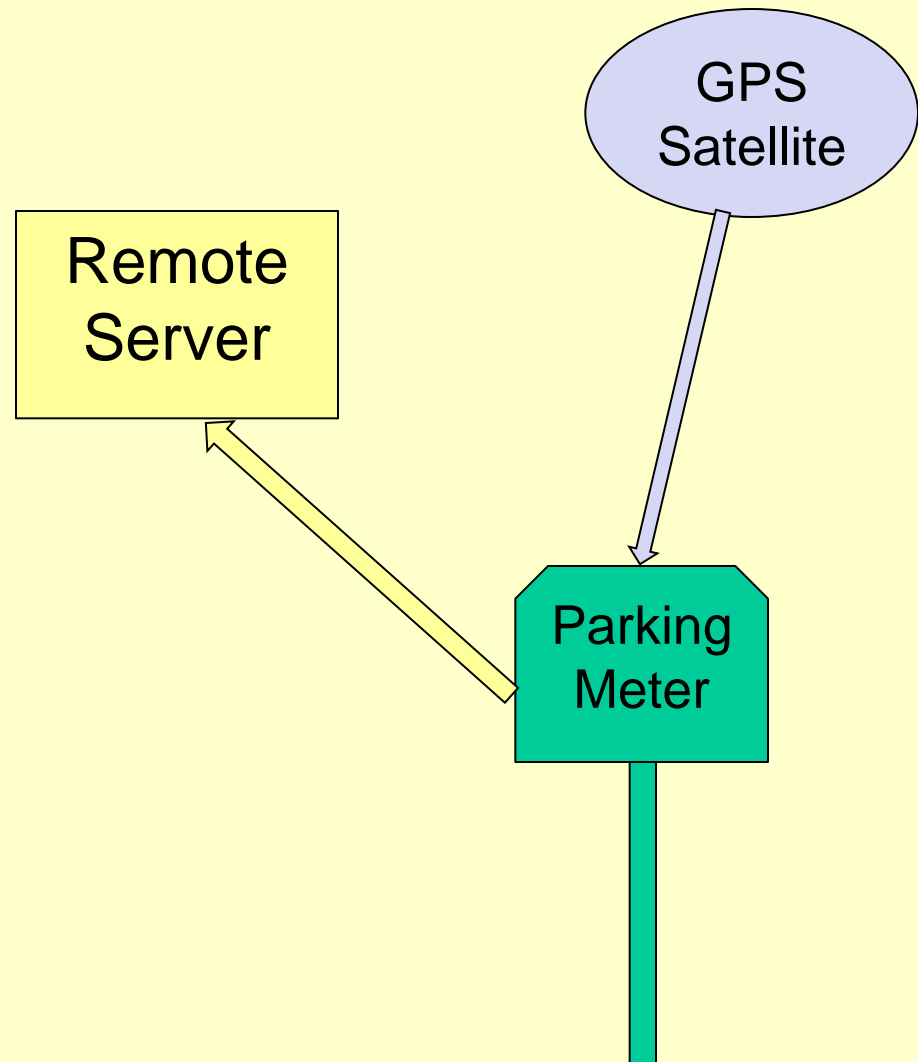
- ATMs, parking meters, home security systems, etc.
- Some are WiFi, GPS enabled:
  - Unlicensed: open to interference
  - Multiple radios/antennas
- Coexistence

## OTA Measurement Challenges

- Device dimensions often a significant fraction of working volume of test chamber
- Calibrations affected by antenna and device placement

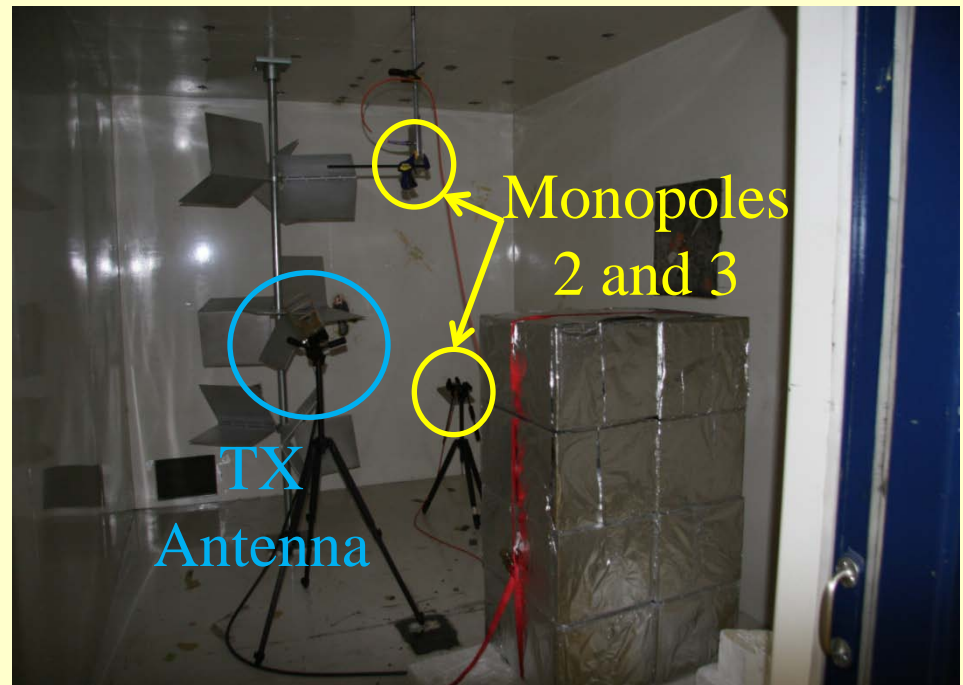
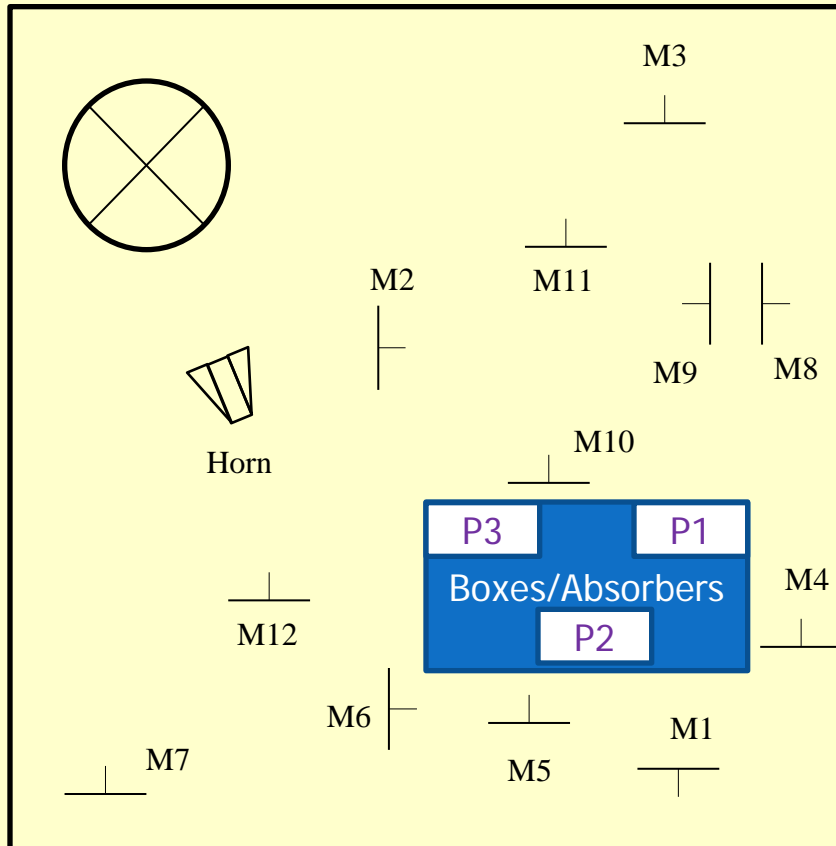
## Goal of NIST work

- Guidelines for use of reverberation chambers for large-form-factor device testing



# TRP: M2M Experimental Set-up

Large form factor devices will load the chamber, affect calibrations



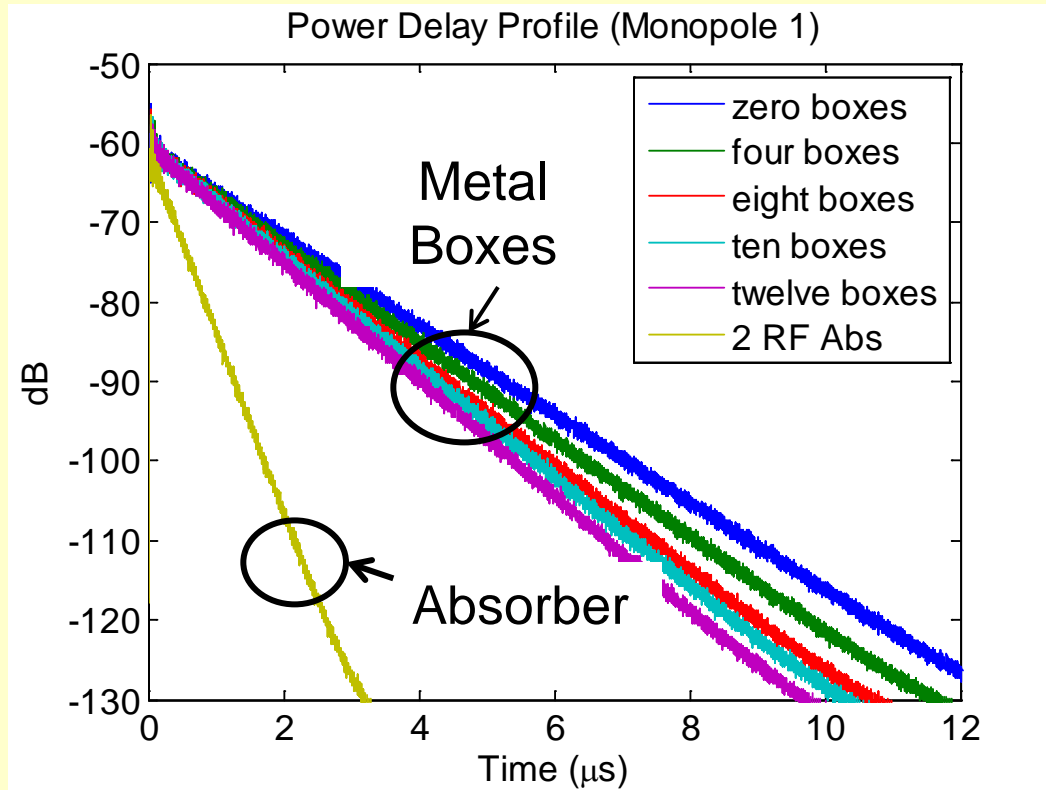
## Experiment:

- 12 omnidirectional receive antennas tuned to 1.9 GHz
- Absorbing and reflective objects of various sizes

# M2M: Metallic and Absorbing Objects

**Absorber:** damps out reflections when compared to metallic boxes

**Metallic boxes:** minor but measurable loading effects



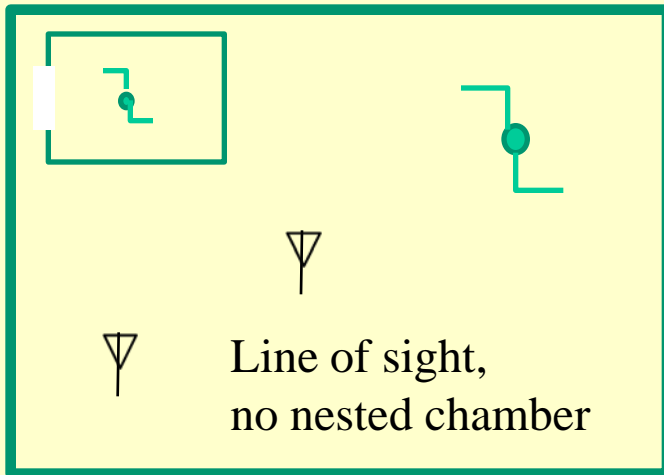
Loading	$T_{rms}$ (ns)
0	775
4	708
8	650
10	623
12	590
2 RF Abs	192

- Calibration and measurement guidelines must consider large-form-factor, absorbing devices
- Multiple-antenna M2M:

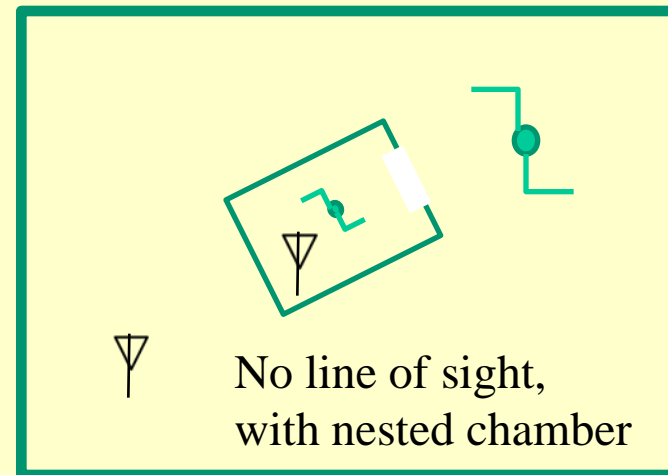
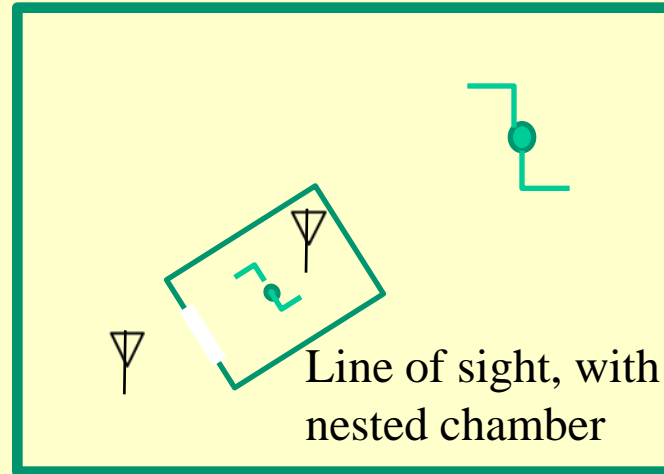
# Realistic MIMO Environments

## Non-line-of-sight: Nested Reverberation Chamber

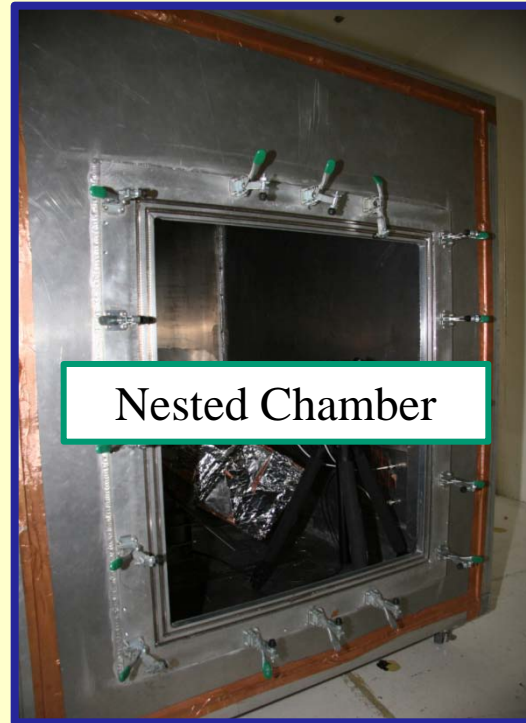
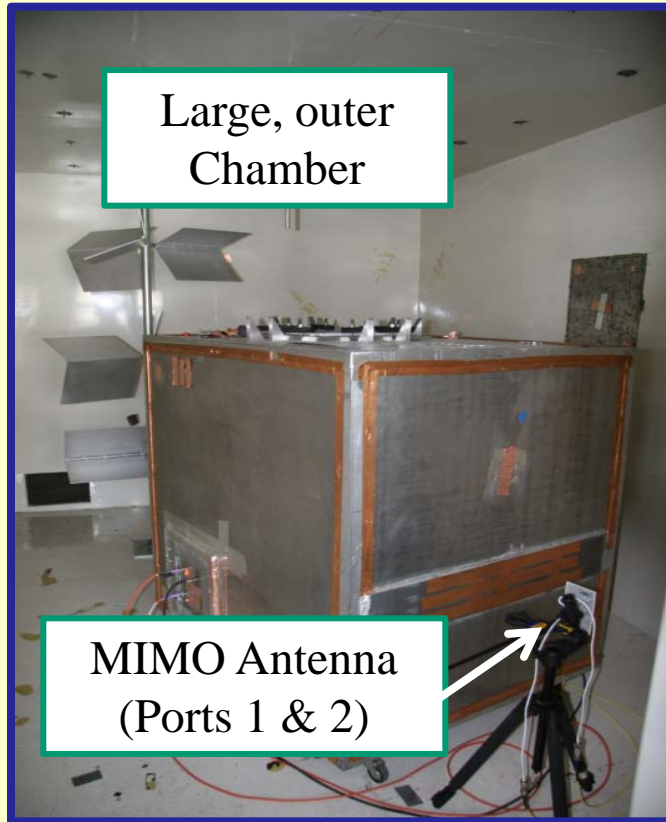
Replicate room-to-room or indoor-to-outdoor types of environments



1. The paddle in the outer chamber is turned through 100 positions, over  $360^{\circ}$ .
2. Paddle in the nested chamber is turned continuously.

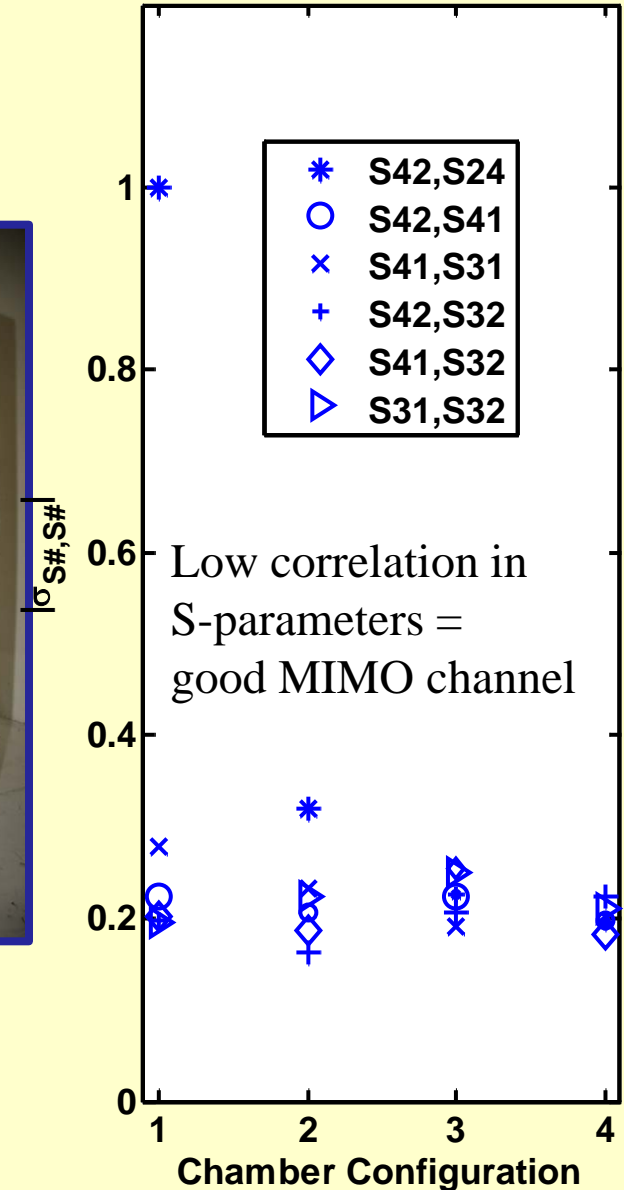


# Measuring MIMO Channel Correlation using a Nested Reverberation Chamber

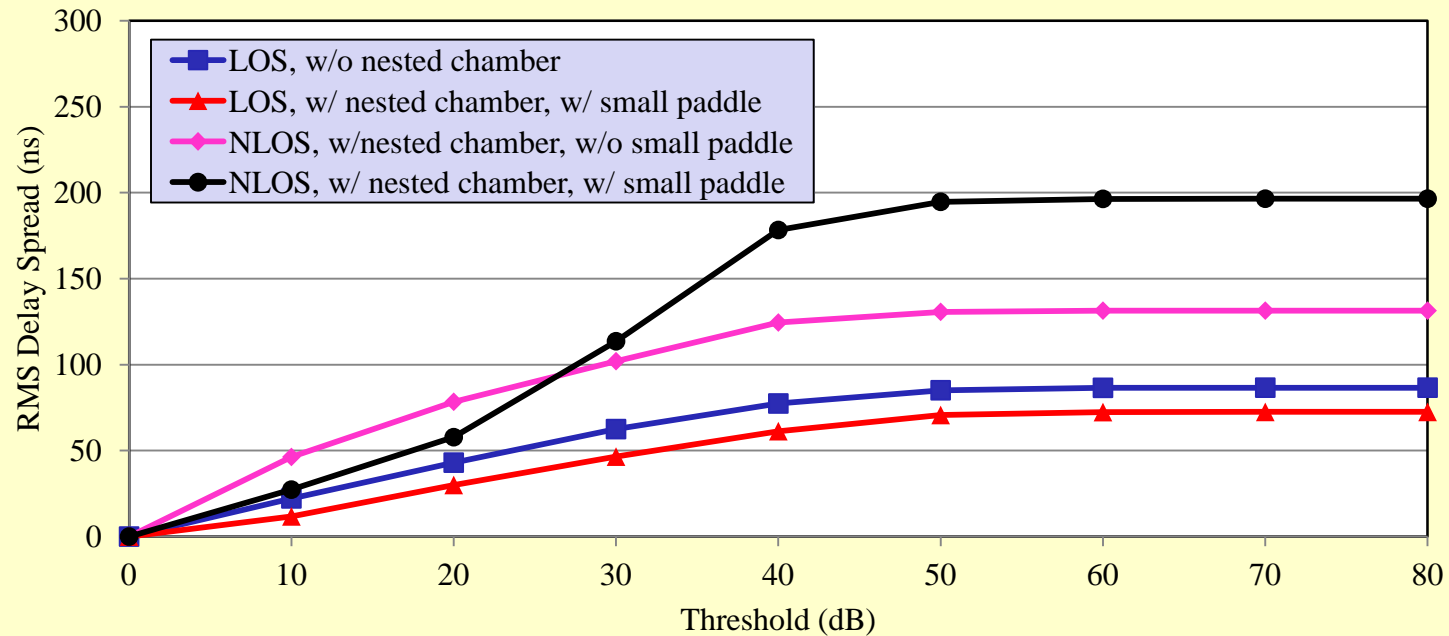


Chamber Configurations (2.4 GHz):

- 1) No stirring in small chamber
- 2) Stirring in both; no RF absorbers
- 3) Stirring in both, one RF absorber
- 4) Stirring in both, two RF absorbers



# Nested Chamber Wireless Environment



“Tune” power delay profile (RMS delay spread) with

- nested chamber orientation to TX antenna
- various stirring algorithms



# Reverberation Chambers for Wireless Device Testing

**Reverberation chambers represent reliable and repeatable test facilities that have the capability of simulating multipath environments for the testing of wireless communications devices.**

Ongoing research:

- Direct path with omnidirectional antennas
- Tuning decay times = field non-uniformity
- How to test devices with repeaters
- Creating complicated PDPs for wireless device test
- Automating PDP development
- Advanced transmission, multiple antenna systems
  - Test methods (CTIA, 3GPP groups)
  - Angle of arrival measurements
- Uncertainties

# Reverberation Chamber Standards Proposed Testing Methods

## Standards

- **International Standard IEC 61000-4-21:** Testing and measurement techniques – Reverberation chamber test methods
- **IEEE 299.1:** Testing shielded enclosures
- **3rd Generation Partnership Project (3GPP) RAN4**
  - R4-111690, “TP for 37.976: LTE MIMO OTA Test Plan for Reverberation Chamber Based Methodologies”

## Testing Methods

- **CTIA Certification Program Working Group Contribution**
  - RCSG090101, P.-S. Kildal and C. Orlenius, “TRP and TIS/AFS Measurements of Mobile Stations in Reverberation Chambers (RC)”
- “Utilizing a channel emulator with a reverberation chamber to create the optimal MIMO OTA test methodology”
  - C. Wright, S. Basuki, [8]

# *Summary*

- Reverberation chamber measurements are thorough and robust.
- Proper sampling techniques reduce measurement uncertainties
- Statistical models help minimize the number of samples required

# *Summary*

- Reverberation chambers capture radiated.
- Results are insensitive to EUT placement in the chamber
- Results are independent of EUT or antenna radiation pattern
- Enclosed system free from external interference
- **Relatively inexpensive**
- **Relatively fast**

# References from NIST on Wireless Measurements in Reverberation Chambers

- [1] C.L. Holloway, D.A. Hill, J.M. Ladbury, P. Wilson, G. Koepke, and J. Coder, “On the Use of Reverberation Chambers to Simulate a Controllable Rician Radio Environment for the Testing of Wireless Devices”, *IEEE Transactions on Antennas and Propagation, Special Issue on Wireless Communications*, vol. 54, no. 11, pp. 3167-3177, Nov., 2006.
- [2] E. Genender, C.L. Holloway, K.A. Remley, J.M. Ladbury, G. Koepke, and H. H., “Simulating the Multipath Channel with a Reverberation Chamber: Application to Bit Error Rate Measurements,” *IEEE Transactions on EMC*, vol. 52, no 4, pp. 766 – 777, Nov. 2010.
- [3] E. Genender, C.L. Holloway, K.A. Remley, J. Ladbury, G. Koepke and H. Garbe, “Using Reverberation Chamber to Simulate the Power Delay Profile of a Wireless Environment”, *EMC Europe 2008*, Sept, 2008, Hamburg, Germany.
- [4] H. Fielitz, K.A. Remley, C.L. Holloway, Q. Zhang, Q. Wu, and D. W. Matolak, “Reverberation-Chamber Test Environment for Outdoor Urban Wireless Propagation Studies”, *IEEE Antennas and Wireless Propag. Lett.*, 2009.
- [5] K.A. Remley, H. Fielitz, and C.L. Holloway, Q. Zhang, Q. Wu, and D. W. Matolak, “Simulation of a MIMO system in a reverberation chamber”, *IEEE EMC Symp.* August 2011
- [6] K.A. Remley, S.J. Floris, and C.L. Holloway, “Static and Dynamic Propagation-Channel Impairments in Reverberation Chambers,” submitted to *IEEE Transactions on EMC*, 2010.
- [7] D. Hill, “Electromagnetic Fields in Cavities: Deterministic and Statistical Theories” , IEEE Press, Copyright © 2009.

# Other References on Wireless Measurements in Reverberation Chambers

- [8] C. Wright, S. Basuki, "Utilizing a channel emulator with a reverberation chamber to create the optimal MIMO OTA test methodology," *Mobile Congress (GMC), 2010 Global*, vol., no., pp.1-5, 18-19 Oct. 2010.
- [9] N. Serafimov, P.-S. Kildal, and T. Bolin, "Comparison between radiation efficiencies of phone antennas and radiated power of mobile phones measured in anechoic chambers and reverberation chambers," in *Proc. IEEE Antennas Propag. Int. Symp. 2002, Jun. 2002, vol. 2, pp.478–481*.
- [10] P.-S. Kildal, K. Rosengren, J. Byun, and J. Lee, "Definition of effective diversity gain and how to measure it in a reverberation chamber," *Microwave Opt. Technol. Lett.*, vol. 34, no. 1, pp. 56–59, Jul. 2002.
- [11] K. Rosengren and P.-S. Kildal, "Radiation efficiency, correlation, diversity gain, and capacity of a six monopole antenna array for a MIMO system: Theory, simulation and measurement in reverberation chamber," *Proc. Inst. Elect. Eng. Microwave, Antennas, Propag.*, vol. 152, no. 1, pp. 7–16, Feb. 2005.
- [12] M. Lienard and P. Degauque, "Simulation of dual array multipath channels using mode-stirred reverberation chambers," *Electron. Lett.*, vol. 40, no. 10, pp. 578–5790, May 2004.
- [13] P.-S. Kildal and K. Rosengren, "Electromagnetic analysis of effective and apparent diversity gain of two parallel dipoles," *IEEE Antennas Wireless Propag. Lett.*, vol. 2, pp. 9–13, 2003.